RUTHENIUM(III) AQUA-CHLORO

COMPLEX CHEMISTRY:

The Interconversion of the Hexachlororuthenate(III)

and Aquapentachlororuthenate(III) Species.

Karen Viljoen

Thesis submitted in fulfilment of the requirements for the degree of

Master of Science

in Chemistry at the

University of Stellenbosch

Supervisor: Prof. K.R. Koch

Stellenbosch

December 2003

I the undersigned hereby declare that the work contained in this thesis is my own original work and that I have not previously in its entirety or in part submitted it at any university for a degree.

_____
Karen Viljoen

Date: December 2003

ABSTRACT

Ruthenium, as one of the platinum group metals, was investigated to determine the aquation rate constant of $[RuCl_6]^{3-}$ and the anation rate constant of $[RuCl_5(H_2O)]^{2-}$.   This two reactions represent the equilibrium reaction $[RuCl_6]^{3-} + H_2O \rightleftarrows [RuCl_5(H_2O)]^{2-} + Cl^-$. The reactions were followed, using stopped-flow injection and UV/Visible spectroscopy, at different temperatures.   The aquation and anation rate constants were determined with good precision and thermodynamic values for the reactions were calculated.

The pseudo first order aquation rate constant, k_{65}, was determined by calculation from the regression line as k_{65} = 52.1 ($\pm$3.7) x10^{-3} s^{-1} at 25$°$C.   The activation energy, E_a, is 90.1 ($\pm$1.2) kJ.mol^{-1} and the enthalpy and entropy of activation is 87.7 ($\pm$1.2) kJ.mol^{-1} and 24.7 ($\pm$4.3) J.K^{-1}.mol^{-1}, respectively.   The aquation rate constant was found to be dependent on the hydrochloric acid concentration, decreasing with increasing hydrochloric acid concentration.

From the regression line at 25$°$C the second order anation rate constant, k_{56}, was calculated as 1.62 ($\pm$0.11) x10^{-3} $M^{-1}s^{-1}$.   The activation energy is 88.0 ($\pm$1.4) kJ.mol^{-1}, with the enthalpy and entropy of activation 85.6 ($\pm$1.4) kJ.mol^{-1} and $-$11.2 ($\pm$4.7) J.K^{-1}.mol^{-1}, respectively.   The influence of the hydrochloric acid concentration of the solution on the anation rate constant was not investigated.

The equilibrium constant for the reaction studied was calculated from the rate constants for the aquation and anation reactions.   The equilibrium constant, K_6, was calculated as 0.0311 M^{-1} at 25$°$C.   The equilibrium constant, when compared to literature, was found to be dependent on the hydrochloric acid concentration.   It was then used, in conjunction with data from the literature, to construct two distribution diagrams.   Distribution diagrams for the Ru(III) aquachloro species

show between 79.9% to 72.3% $[RuCl_6]^{3-}$ present in 12M HCl. The two distribution diagrams were very similar and it is not possible to resolve the issue of a final distribution diagram for the aqua-chloro Ru(III) system without further investigation into the all the other rate constants of the Ru(III) aqua-chloro species.

The rate constants and thermodynamic values for the Ru(III) reaction were compared to corresponding data (from literature) for Rh(III) and Ir(III) because several comparisons between these platinum group metals have been noted. It was found that for both the aquation and anation rate constants, the following trend was observed: Ru(III) > Rh(III) > Ir(III). These differences are in certain cases exploited in the refining of these platinum group metals.

Crystals of diethylenetriamine hexachlororuthenate(III) was prepared and characterised by x-ray crystallography and CHN analysis. The average Cl-Ru bond length for the crystal was 2.371 Å. The crystal structure was compared to hexaaquaaluminium hexachlororuthenate(III) tetrahydrate and diethylenetriamine hexachlororhodate(III). The metal-chloride bond lengths of all the crystals were found to be similar (2.350 Å – 2.375 Å). The diethylenetriamine crystal structures compared well. The conclusion was that the crystals prepared were diethylenetriamine hexachlororuthenate(III).

OORSIG

Ruthenium(III), een van die platinum groep metaal-ione, is in hierdie studie ondersoek om die akwasie tempo konstante van $[RuCl_6]^{3-}$ en die anasie tempo konstante van $[RuCl_5(H_2O)]^{2-}$ te bepaal. Dié twee reaksies verteenwoordig die ewewigsreaksie $[RuCl_6]^{3-} + H_2O \rightleftarrows [RuCl_5(H_2O)]^{2-} + Cl^-$. Die verloop van die reaksies is met behulp van UV/Sigbare spektroskopie by verskillende temperature gevolg. Die akwasie en anasie tempo konstantes is bepaal met goeie presisie en die termodinamiese konstantes van die reaksies is bereken.

Die pseudo-eerste orde akwasie tempo konstante, k_{65}, is bepaal deur middel van regressie, as 52.1 ($\pm$3.7) $\times 10^{-3}$ s^{-1} by 25°C. Die aktiverings energie, E_a, is bereken as 90.1 ($\pm$1.2) kJ.mol^{-1} en die entalpie en entropie van aktivering is onderskeidelik 87.7 ($\pm$1.2) kJ.mol^{-1} en 24.7 ($\pm$4.3) J.K^{-1}.mol^{-1}. Daar is gevind dat die akwasie reaksie konstante afhanklik was van die soutsuur konsentrasie: dit neem af soos die soutsuur konsentrasie toeneem.

Met behulp van die regressie lyn is die anasie tempo konstante bepaal by 25°C as 1.62 ($\pm$0.11) $\times 10^{-3}$ M^{-1}s^{-1}. Die aktiveringsenergie is bepaal as 88.0 ($\pm$1.4) kJ.mol^{-1} en die entalpie en entropie van aktivering, onderskeidelik as 85.6 ($\pm$1.4) kJ.mol^{-1} en –11.2 ($\pm$4.7) J.K^{-1}.mol^{-1}. Die invloed van die soutsuur konsentrasie op die anasie tempo konstante is nie bepaal nie.

Die ewewigskonstante vir die reaksie wat ondersoek is, is bereken met die tempo konstantes vir die akwasie en anasie reaksies. Die ewewigskonstante, K_6, is bereken as 0.0311 M^{-1} by 25°C. Toe die ewewigskonstante vergelyk is met die literatuur waardes, is gevind dat die ewewigskonstante afhanklik is van die soutsuur konsentrasie. Saam met die waardes wat in die literatuur gevind is, is die ewewigskonstante gebruik om twee distribusie diagramme te bereken.

Die distribusie diagramme vir die Ru(III) spesies toon onderskeidelik 79.9% en 72.3% $[RuCl_6]^{3-}$ in 12M HCl. Die twee distribusie diagramme is baie eenders en dit is nie moontlik om 'n finale distribusie diagram op te trek totdat die uitstaande tempo konstantes tussen die akwachloro Ru(III) spesies bepaal word nie.

Die tempo konstantes en termodinamiese waardes wat bepaal is vir die Ru(III) reaksie is vergelyk met gelyksoortige waardes in die literatuur van Rh(III) en Ir(III) omdat daar ooreenkomste tussen die platinum groep metale opgemerk is. Daar is bevind dat die akwasie én anasie reaksies die volgende patroon volg: Ru(III) > Rh(III) > Ir(III). Die verskille word in sekere gevalle benut in die raffinering van hierdie metale.

Kristalle van dietileentriamien heksachlororuthenaat(III) is berei en gekarakteriseer met behulp van CHN analise en x-straal kristallografie. Die gemiddelde Cl-Ru bindingsafstand vir die kristal was 2.371 Å. Die kristalstruktuur is vergelyk met dié van heksaäkwaäluminium hexachlororuthenaat(III) tetrahidraat en diëtileentriamien heksachlororhodaat(III). Die chloried-metaal bindingsafstand vir die kristalle was soortgelyk (2.350 Å – 2.375 Å). Die diëtileentriamien kristalstrukture stem goed ooreen. Die gevolgtrekking was dat die kristalle wat voorberei is wel diëtileentriamien heksachlororuthenaat(III) was.

ACKNOWLEDGEMENTS

TABLE OF CONTENTS

TABLE OF FIGURES

TABLE OF TABLES

TABLE OF EQUATIONS

ABBREVIATIONS

$k_{(6-n)(5-n)}$	Rate constant for the reaction $[MCl_{6-n}(H_2O)_n]^{n-3} + H_2O \rightleftarrows [MCl_{5-n}(H_2O)_{n+1}]^{n-2} + Cl^-$
$k_{(5-n)(6-n)}$	Rate constant for the reaction $[MCl_{5-n}(H_2O)_{n-1}]^{n-2} + Cl^- \rightleftarrows [MCl_{6-n}(H_2O)_n]^{n-3} + H_2O$
K_6	Equilibrium constant for the aquation and anation reactions involving k_{65} and k_{56}, defined as: $$K_6 = \frac{\left[[RuCl_6]^{3-}\right]}{\left[[RuCl_5(H_2O)]^{2-}\right] \bullet \left[Cl^-\right]} = \frac{k_{56}}{k_{65}}$$
k_{54}	Aquation rate constant for the reaction $[MCl_5(H_2O)]^{2-} + H_2O \rightleftarrows [MCl_4(H_2O)_2]^- + Cl^-$
k_{45}	Anation rate constant for the reaction $[MCl_4(H_2O)_2]^- + Cl^- \rightleftarrows [MCl_5(H_2O)]^{2-} + H_2O$
K_5	Equilibrium constant for the aquation and anation reactions involving k_{54} and k_{45}.
k_{43T}	Aquation rate constant for the reaction *trans*-$[MCl_4(H_2O)_2]^- + H_2O \rightleftarrows$ *mer*-$[MCl_3(H_2O)_3] + Cl^-$
k_{34T}	Anation rate constant for the reaction *mer*-$[MCl_3(H_2O)_3] + Cl^- \rightleftarrows$ *trans*-$[MCl_4(H_2O)_2]^- + H_2O$
K^C_4	Equilibrium constant for the aquation and anation reactions involving k_{43C} and k_{34C}
mer	Meridional configuration
fac	Facial configuration
deta	diethylenetriamine
μ	Ionic strength (M)

1   INTRODUCTION

South Africa, with Anglo Platinum as the country's leading producer, produces the majority of the world's platinum group metals (platinum, palladium, rhodium, iridium, ruthenium and osmium).   To assist in future processes for refining the platinum group metals, there is a need for Anglo Platinum to understand the fundamental chemistry of the platinum group metals relevant to its current processes.

1.1   AIM OF THE STUDY

Ruthenium has by far the most extensive chemistry of the platinum group metals due to the numerous oxidation states it can achieve and of all the oxidation states, the chemistry of ruthenium(III) is the most varied.   There are cationic, neutral, anionic and several mixed oxidation state polynuclear species known.   Refining of the platinum group metals take place in aqueous hydrochloric acid medium.   It was therefore decided to limit this study to the chemistry of Ru(III) in aqueous hydrochloric acid media.   The literature suggest that the chemistry of ruthenium(III) in acidic chloride media is relatively simple with close similarity to that of rhodium(III) and iridium(III). Ruthenium(III) forms the hexachlororuthenate(III) anion at high chloride concentrations.   All of these aqua-chloro metal species undergo aquation as the chloride concentration decreases, with stepwise replacement of a chloride ligand by water giving complexes with the general formula of $[MCl_{6-n}(H_2O)_n]^{n-3}$.   There have been very few studies of the aqua-chloro species of Ru(III) with incomplete equilibrium and kinetic data[1].   The aim of this study was to investigate the speciation of ruthenium(III) in aqueous hydrochloric acid media and to thus add to the fundamental knowledge of the platinum group metals in order to assist in the future refining of these metals.

1.2 THE PLATINUM GROUP METALS

1.2.1 Discovery of the platinum group metals [2, 3]

The group of metals consisting of platinum, palladium, rhodium, iridium, osmium and ruthenium are known as the platinum group metals, or pgm. They are the second and third triads of group VIII of the transition group metals of the periodic table.

Platinum was used in ancient Egypt in the seventh century BC, although the Egyptians probably thought it was silver. De Ulloa, a Spanish naval officer and scientist, made the first definite reference to platinum in Colombia in 1736. Platinum means "little silver" in Spanish and points to the fact that it was thought to be unworkable silver. Wollaston discovered palladium (named after a newly discovered asteroid, Pallas, itself named after the Greek goddess of wisdom) in 1803 in the motherliquor left after the precipitation of chloroplatinate salt and, in 1804, he isolated another element from platinum ore, which he called rhodium (rose, after the colour of its chloro complexes). Osmium (Greek for odour) and iridium (Greek goddess Iris) were discovered by Tennant in 1803 in the insoluble black residue left after the dissolution of platinum in aqua regia. In 1827 Osann announced the discovery of three new metals: pluran, ruthen and polin however, he withdrew his claim when Berzelius inspected samples of these new metals, and concluded that they were mixtures of SiO_2, TiO_2, ZrO_2, Fe_2O_3 and iridium oxides. In the 1840's Klaus started examining the residues from a platinum refinery that were left after treatment with aqua regia. He isolated a new metal from these residues which he named ruthenium out of respect for Osann's work and in honour of his native Russia.

1.2.2 Occurrence and Distribution

The pgm are rare metals, with platinum the most common with an abundance[3] of 10^{-2} g.ton^{-1} (ppm) in the earth's crust. Palladium has an abundance of 10^{-2} to 10^{-3} g.ton^{-1}, osmium and iridium 10^{-3} g.ton^{-1} and rhodium and ruthenium 10^{-4} g.ton^{-1}.

The pgm are associated together in alloys and are mined together with silver, gold, nickel and copper in four main areas of the world, namely South Africa, Russia, Canada and USA. The greatest concentration of these metals occur in the Bushveld complex in South Africa and in Noril'sk in Russia. Together these two countries produce 90% of the world's pgm, with Russia as the principal source of palladium and South Africa as the major source of platinum and rhodium[4].

1.2.3 Physical Properties

The platinum group metals are typical of most metals in that they are silvery-white, lustrous, malleable and ductile but are harder than most other metals. Platinum's coefficient of expansion is the same as that of soda-glass, so it can be fused into the glass to give a permanent seal. Platinum and palladium are both dense refractory metals, but less so than iridium and rhodium. Palladium has the lowest density and melting point of any pgm, while iridium has the highest density. Densities and melting points decrease with increasing atomic number across this region of the periodic table. [2, 3] Table 1-1 provides a summary of the physical properties of the pgm.

Table 1-1: Physical properties of the pgm. [2]

Property	Atomic no	Atomic weight	Electronic configuration	Metal radius (pm)	Electro-negativity	Density 20ºC (g.cm^{-3})
Ru	44	101.07	[Kr] 4d^{7}5s^1	134	2.2	12.41
Os	76	190.2	[Xe]4f^{14} 5d^{6}6s^2	135	2.2	22.57
Rh	45	102.9055	[Kr]4d^{8}5s^1	134	2.2	12.39
Ir	77	192.22	[Xe]4f^{14} 5d^{7}6s^2	135.5	2.2	22.61
Pd	46	106.42	[Kr]4d^{10}	137	2.2	11.9
Pt	78	195.08	[Xe]4f^{14} 5d^{9}6s^1	138.5	2.2	21.41

1.2.4 Extraction and Purification [4, 5, 6]

The pgm occur in minute quantities in deposits of copper-nickel sulphide ore. The low abundance of the pgm in the earth's crust, and even in ores, means that 7-12 tonnes of ore must be processed to obtain a single ounce of platinum. Extracting pgm from ore requires a series of concentration stages. The mined ore (pgm content: 4-7 g/tonne)[*] is crushed, milled and mixed with water and reagents. Air is pumped through this mixture to form bubbles to which the base metal sulphides, associated with pgm, with the help of the reagents, adhere. The froth, or flotation concentrate (pgm content of 100-1000g/tonne), is removed and is smelted at about 1500°C during which the metals are concentrated in a matte while the unwanted material forms a slag, which is discarded. Air is bubbled through the molten matte to remove

---

[*] Pgm concentrations for Merensky Reef.

iron as its oxide and sulphur as SO_2.   The matte consisits of the pgm, gold, silver, copper, nickel and other base metals.   The next step is the refining of the matte (pgm content: >1400g/tonne) where the base metals (Ni, Cu, Co) are removed by sulphuric acid leaching leaving a concentrate containing the pgm.

The pgm concentrate, after removal of the base metals, contain the six pgm, gold, silver and smaller quantities of base metals.   Pgm refineries generally use hydrochloric acid and chlorine gas to dissolve the pgm concentrate.   The most effective way of separating osmium and ruthenium from other pgm's and from each other is distillation.   Anion exchange exploits the differences between the different anionic chloro complexes to achieve separation.   Solvent extraction has replaced anion exchange in recent years.
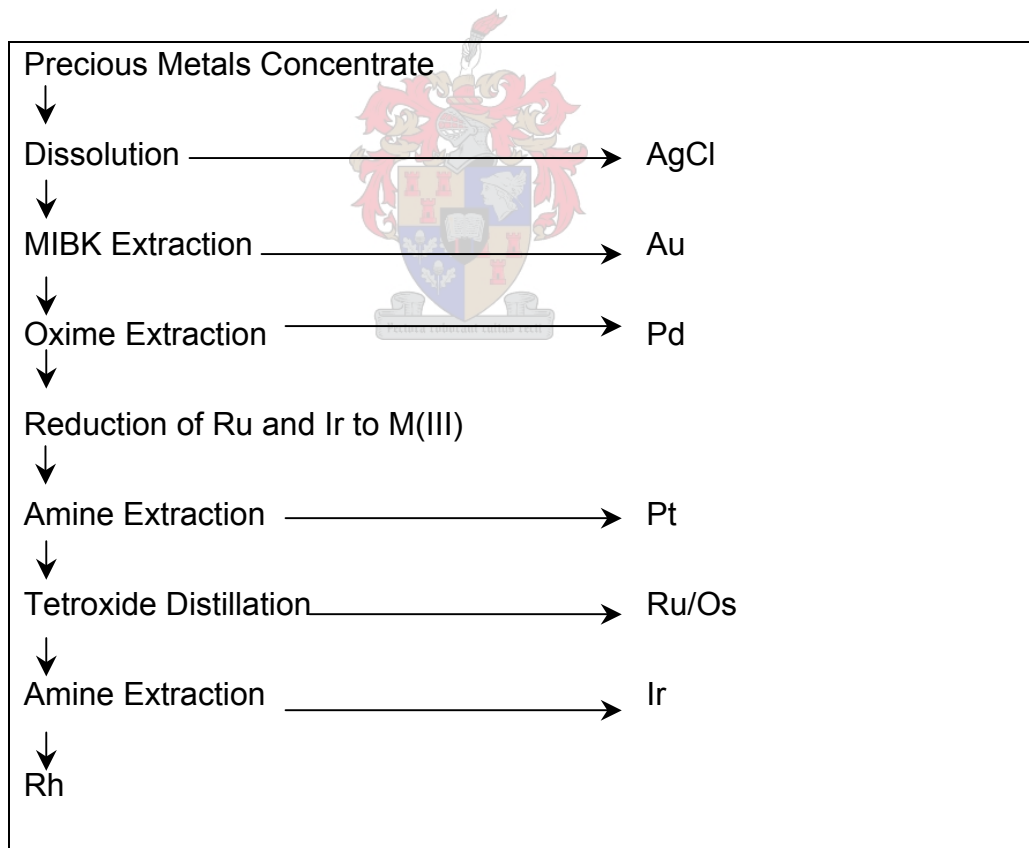
Figure 1-1: Matthey Rustenburg Refiners pgm extraction flowsheet. [5]

The Matthey Rustenburg Refiners flowsheet in figure 1.1 is explained in more detail.   Gold is removed by MIBK (methyl iso-butyl ketone)

solvent extraction as the $[AuCl_4]^-$ anion with the added advantage of removing several impurities like tellurium and arsenic. Organic reagents having hydroxy-oxime functionality are used to extract palladium but suffer from slow kinetics which is overcome by addition of accelerating additives. Oximes are commercially available and used particularly for copper extraction which, when present, co-extracts with palladium. The copper, when present, can be washed out prior to stripping of palladium from the organic with acid. After the removal of gold and palladium, platinum is removed using amine, if the iridium is in the Ir(III) oxidation state. The stripping of Pt from the loaded organic requires a strong acid to break the ion pair bond between the extractant and platinum. The osmium and ruthenium are then distilled as their tetroxides. The iridium is oxidised to Ir(IV) and then extracted using an amine. The control over the oxidation state of iridium is of great advantage in its separation from the other pgm, especially platinum that is also extracted with an amine. The rhodium is recovered from the resulting solution by precipitation or cation exchange removal.

1.2.5 Uses

The pgm's unique properties make them useful for a wide range of applications which are outlined in table 1-2.

Table 1-2: Uses of the platinum group metals. [4]

Autocatalysts	Control of vehicle pollution	Pt, Pd, Rh
Chemical	Catalysts for chemical synthesis.	Pt, Pd, Rh, Ru
	Electrode coatings.	Ir, Ru
Dental	Alloys for dental restorations.	Pt, Pd
Electronics	Computer hard disks.	Pt
	Multi-layer ceramic capacitors.	Pd
	Crucibles to grow single crystals.	Ir
Fuel cells	Catalysts for power generation.	Pt
Glass	Glass making equipment.	Pt, Rh
Investment	Coins and bars.	Pt

Jewellery	Wedding rings, fashion jewellery.	Pt
Medical	Anti-cancer drugs, implants.	Pt
Petroleum	Catalysts for gasoline refining.	Pt
Sensors	Temperature and gas sensing.	Pt, Rh
Others	Spark plugs, pollution control.	Pt, Ir

1.3   General Chemistry of the Individual Platinum Group Metals

The unique properties of the pgm are due to their binding and ionisation energies.   The ionisation energies depend on the energies of the valence electrons.   In the case of the pgm, these valence electrons are shared between the ns and $(n-1)$d orbitals, with the s orbitals being of higher energy.   Electrons expected in the ns orbitals are found in the $(n-1)$d orbitals which are more difficult to remove.   The ionisation energies are thus higher than expected because of the shift to lower orbitals.   The decrease in binding energies with increase in atomic number across each triad is the result of the added d electrons going into a spin-paired state in the orbitals and thus not being available for bonding.   The binding energies and ionisation potentials are greater for the second triad because of the greater nuclear charge operating at essentially fixed distances. [3]

The stability of the higher oxidation states of the elements has a tendency to decrease moving from left to right across the periodic table and has a tendency to increase from the second to the third row of the transition metal series.   This is seen by the fact that silver usually only forms monovalent complexes while ruthenium and osmium form stable octavalent tetroxides under highly oxidising conditions.   Furthermore, rhodium(IV) and palladium(IV) are only formed in highly oxidising conditions while platinum(IV) and iridium(IV) are stable in the presence of oxidant. [5]

1.3.1 Ruthenium and Osmium

Ruthenium and osmium are virtually unaffected by non-oxidising acids, even aqua regia. Except for oxidising agents, non-metals react only with difficulty with these metals, even at high temperatures. Both metals can be dissolved in molten alkali in the presence of air and the aqueous extracts of these fusions can be treated with chlorine and heated to distill off the tetroxides. They are stable to atmospheric attack although finely divided osmium gives off a distinctive OsO_4 smell.

The metals are the last group to attain the +8 oxidation state and osmium(VIII) is more stable than ruthenium(VIII), which decomposes violently to RuO_2 when heated above 100ºC. The most common oxidation state for ruthenium is +3 and for osmium it is +4. Ruthenium has an extensive aqueous cationic chemistry but not osmium[2]. Ruthenium and osmium both form volatile tetroxides under oxidising conditions and in refining this property allows these metals to be separated from the other pgm by distillation. Ruthenium tetroxide has a melting point of 25°C and a boiling point of 40°C, osmium tetroxide melts at 40°C and boils at 130°C, the formation of ruthenium tetroxide requiring a stronger oxidising agent than osmium. Ruthenium tetroxide is an unstable molecule and decomposes explosively, making distillation a potentially dangerous process. Osmium tetroxide dissolves in aqueous alkali solutions. Ruthenium tetroxide will oxidise dilute and concentrated hydrochloric acid and the process was investigated by Woodhead and Fletcher[7] who proposed the scheme in figure 1.2. Both metals form only disulfides and forms complexes with all halides. [2]

1.3.2 Rhodium and Iridium [2]

Rhodium and iridium react slowly with oxygen and halogens at red-hot temperature but are extremely inert to acids, even aqua regia. Both

metals can be fused with alkali's before dissolution in mineral acids. The range of oxidation states that the elements in this group can reach has diminished relative to the oxidation states reached by the preceding pgm. This is due to the increased stability of the *(n-1)*d electrons that are more strongly attracted to the nucleus. Rhodium and iridium have no oxidation states above +6. There are significant differences between the oxidation states of iridium and rhodium, more so than between the series 2 and 3 metals of the preceding groups. For example, the +4 oxidation state occurs to an appreciable extent in iridium but not in rhodium. The +3 oxidation state is the most important for iridium and rhodium while the +2 state is relatively unimportant. The +1 oxidation state is known with π-acceptor ligands, of which Wilkinson's catalyst [Rh(PPh$_3$)$_3$Cl] is an example.

Oxo anions are not formed by iridium and rhodium, the first heavy transition elements not to form them. This is presumably because their formation requires the donation of π electrons from the O to the metal and these metals become less able to act as π-acceptors as their d-orbitals are filled.
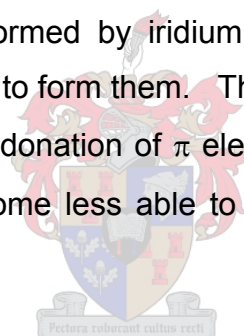
Rhodium and iridium form less oxides than the previous group. Their sulfides are very inert, especially toward acids and most are used as semi-conductors. The most stable halides of these two metals are the trihalides, the hexa- and pentahalides are reactive and unstable while the lower halides need further substantiation.

The chemistry of the oxidation states for rhodium and iridium above +4 is sparse.

$RuO_4 + HCl$ (in excess)

$\boxed{1}$ $> 0.5M\ HCl$

$[RuO_2Cl_4]^{2-}$

$\boxed{3}$ $>3MHCl$ $\boxed{2}$ 0.5 to $3M$ HCl

$[RuCl_6]^{2-}$ $Ru_2O_2Cl_4$

$> 6M\ HCl$ $\boxed{4}$ HCl H_2O

$[RuCl_5(H_2O)]^{2-}$ $[Ru_2OCl_8]^{2-}$

1. $RuO_4 + 4\ H^+ + 6\ Cl^- \rightleftharpoons [RuO_2Cl_4]^{2-} + Cl_2 + 2\ H_2O$

2. $2[RuO_2Cl_4]^{2-} + 4\ H^+ \rightleftharpoons Ru_2O_2Cl_4 + 2\ Cl_2 + 2\ H_2O$

3. $[RuO_2Cl_4]^{2-} + 4\ HCl \rightleftharpoons [RuCl_6]^{2-} + Cl_2 + 2\ H_2O$

4. $2\ [RuCl_6]^{2-} + 2\ H_2O \rightleftharpoons 2\ [RuCl_5(H_2O)]^{2-} + Cl_2$
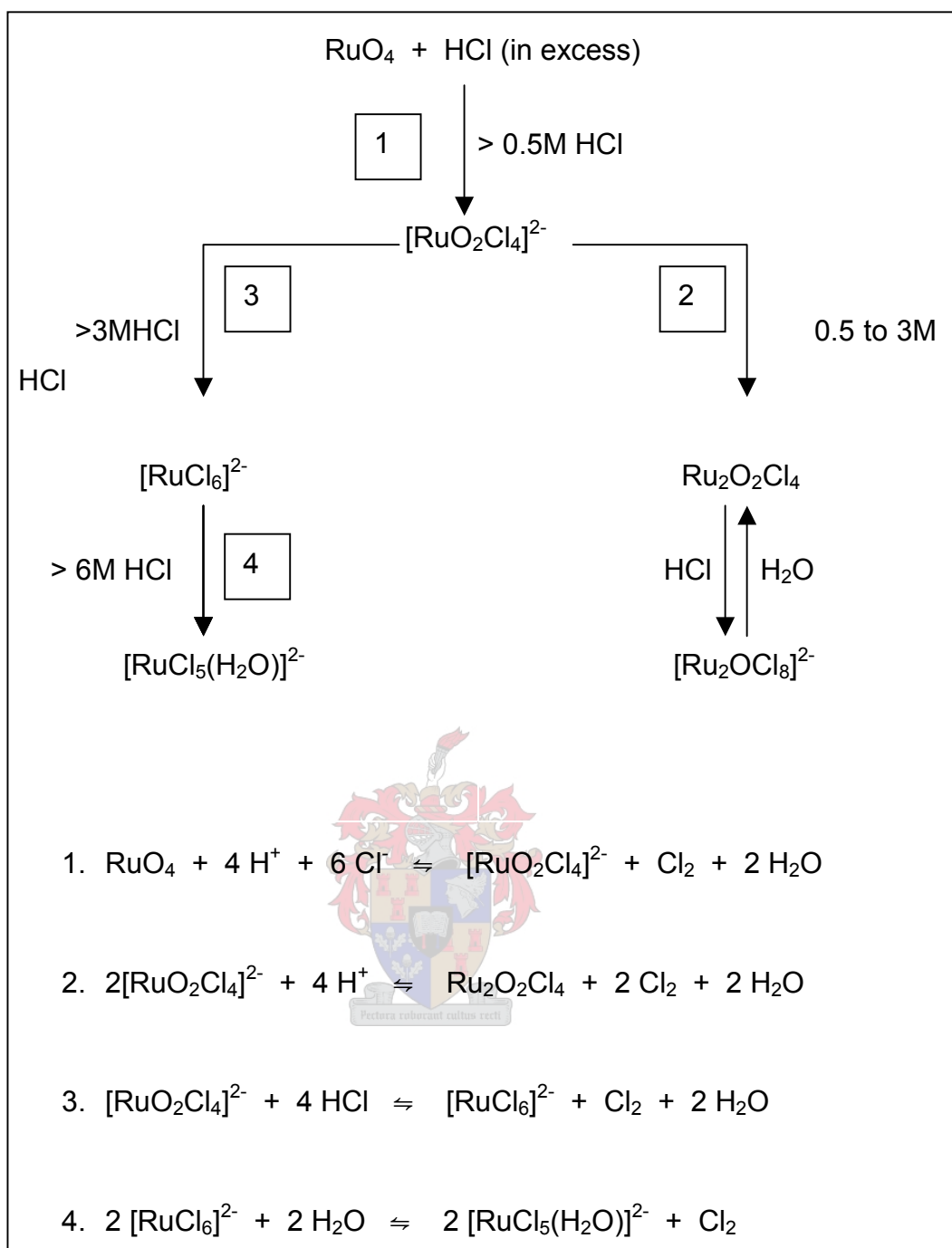
Figure 1-2: Scheme for the dissolution of RuO_4 in HCl. [7]

1.3.3 Platinum and Palladium [2]

In the massive state, these metals are very resistant to atmospheric corrosion at normal temperatures. Palladium is oxidised by oxygen, fluorine and chlorine at red heat and dissolves slowly in mineral acids. Platinum is more resistant to chemical attack than palladium and is

10

barely affected by mineral acids, except aqua regia.   Both metals dissolve in fused alkali metal oxides and peroxides.   Both metals absorb molecular hydrogen, palladium up to 800 times its own volume, when being cooled down from red-hot in an atmosphere of H_2.

The range of oxidation states that these two metals can achieve is smaller than those of the preceding pgm.   The differences between the two metals are also becoming increasingly evident.   The maximum oxidation state achieved is +6 and is only reached by platinum as PtF_6, which is one of the strongest oxidising agents known, and is very volatile.   Palladium only reaches oxidation state +4.   The most common oxidation state is +2 for palladium and +2 and +4 for platinum; there are no oxidation states below 0.   Square planar geometry is preferred in the +2 oxidation state and the kinetically inert platinum(II) complexes have been widely used in kinetic studies.

In the divalent state, platinum and palladium show class-b (Lewis soft acid) characteristics, preferring CN^- and ligands with nitrogen or heavy donor atoms rather than O or F ligands.   Platinum(IV) shows class-a behaviour and is reduced to platinum(II) by P and As donor ligands.

Each metal forms only one oxide (PdO and PtO_2) and mono- and disulfides (PdS, PtS, PdS_2 and PtS_2).   In the +2 oxidation state the metals readily form complexes with the halides.

1.4   The Aquation and Chloride Anation Kinetics of $[MCl_{6-n}(H_2O)_n]^{n-3}$ where M=Ru, Ir or Rh[8]

The equilibrium between a pair of complexes is determined by the rate of aquation of the complex containing the higher number of chloride ligands and the rate of anation of the complex containing the higher number of aqua ligands.   Using the Ru(III) complexes as an example the calculation of the rate constants and equilibrium constants are explained.   Using the convention used in this study, the rate constant's

subscript refers to the number of chloride ligands on the reagent and in the product ($k_{(reagent)(product)}$); e.g. the rate constant k_{56} would refer to the chloride anation reaction $[RuCl_5(H_2O)]^{2-} + Cl^- \rightarrow [RuCl_6]^{3-} + H_2O$. The equilibrium constant subscript will correspond to the amount of chloride ligands on the product complex. Isomers of *cis* and *trans* are also denoted in the rate constant (e.g. k_{43T}) and follows the same rules as the reagent and product; i.e. k_{43T} is the aquation reaction from the *trans* tetrachloro complex to the *mer*-trichloro complex. This follows the reaction: *trans*-$[RuCl_4(H_2O)_2]^- + H_2O \rightarrow$ *mer*-$[RuCl_3(H_2O)_3] + Cl^-$.

The aquation reaction of $[RuCl_6]^{3-}$ involves the loss of a chloride ion:

$$[RuCl_6]^{3-} + H_2O \underset{k_{56}}{\overset{k_{65}}{\rightleftarrows}} [RuCl_5(H_2O)]^{2-} + Cl^- \qquad \textbf{Equation 1-1}$$
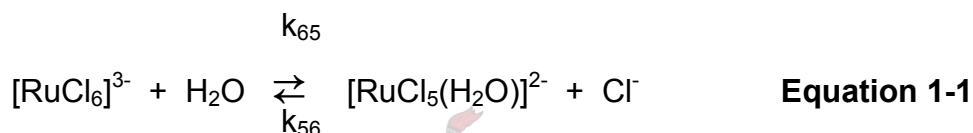
The equilibrium constant for this reaction, K_6, is defined as follows:

$$K_6 = \frac{\left[[RuCl_6]^{3-}\right]}{\left[[RuCl_5(H_2O)]^{2-}\right] \cdot \left[Cl^-\right]} \qquad \textbf{Equation 1-2}$$

The concentration of water is, in theory, so much greater than that of any other reagent in the reaction, that it remains constant. By convention, the concentration of water is therefore omitted from the equation.

The reaction rate is expressed as the change in the concentration of a reagent per time. The rate of decrease of $[RuCl_6]^{3-}$ by aquation to $[RuCl_5(H_2O)]^{2-}$ is given by:

$$\frac{-d\left[[RuCl_6]^{3-}\right]}{dt} = k_{65}\left[[RuCl_6]^{3-}\right] \qquad \textbf{Equation 1-3}$$

The rate of formation of $[RuCl_6]^{3-}$ by anation of $[RuCl_5(H_2O)]^{2-}$ is given by:

$$\frac{d\left[[RuCl_6]^{3-}\right]}{dt} = k_{56}\left[[RuCl_5(H_2O)]^{2-}\right]\cdot\left[Cl^-\right]$$ **Equation 1-4**

At equilibrium the rate of formation of $[RuCl_6]^{3-}$ from anation is equal to rate of loss of $[RuCl_6]^{3-}$ from aquation. Thus:

$$k_{65}\left[[RuCl_6]^{3-}\right] = k_{56}\left[[RuCl_5(H_2O)]^{2-}\right]\cdot\left[Cl^-\right]$$ **Equation 1-5**

Rearrangement gives:

$$\frac{\left[[RuCl_6]^{3-}\right]}{\left[[RuCl_5(H_2O)]^{2-}\right]\cdot\left[Cl^-\right]} = \frac{k_{56}}{k_{65}}$$ **Equation 1-6**

Thus, from equation 1-2 and 1-7:

$$K_6 = \frac{k_{56}}{k_{65}}$$ **Equation 1-7**

The larger the numerical value of the rate constant (k) of a reaction, the faster that reaction takes place. The aquation rate constants for the aquation of $[RuCl_6]^{3-}$ and $[RuCl_5(H_2O)]^{2-}$ are 6.7×10^{-2} s^{-1} and 2.8×10^{-4} s^{-1} respectively[8,9]. This means that 6.7% of $[RuCl_6]^{3-}$ will aquate to $[RuCl_5(H_2O)]^{2-}$ every second and 0.028% of $[RuCl_5(H_2O)]^{2-}$ per second will aquate to cis-$[RuCl_4(H_2O)_2]^-$. From these values it can be concluded that the aquation of $[RuCl_6]^{3-}$ to $[RuCl_5(H_2O)]^{2-}$ is about 250 times faster than the aquation of $[RuCl_5(H_2O)]^{2-}$ to cis-$[RuCl_4(H_2O)_2]^-$. The very fast kinetics of the aquation of $[RuCl_6]^{3-}$ to $[RuCl_5(H_2O)]^{2-}$ limits the methods that can be used to follow the kinetics and determine the rate constants. Ion exchange (separation of species at a given time after which the amount of each species is measured) and manual

methods of determination (manual mixing and measurement) cannot be used because they require slow or no change in equilibrium while the determination is taking place. A method such as stopped-flow analysis where the reagents are mixed in the viewing cell (in-situ) and measured with the minimum delay after mixing is more appropriate.

1.4.1 Fundamentals of Kinetics [11]

The order of a reaction is the sum of the exponents of the concentration factors in the rate law. For the aquation of $[RuCl_6]^{3-}$ (equation 1-3) the sum exponents of the concentration factors is 1 (there is only one concentration factor), the reaction rate is therefore first order. The chloride anation of $[RuCl_5(H_2O)]^{2-}$ (equation 1-4) is a second order reaction that can be approximated as a first order reaction as the chloride ion concentration will have to be very high to allow the reaction to be studied.

The first order reaction

$$A \rightarrow P \qquad\qquad \textbf{Equation 1-8}$$

follows the following rate law:

$$\frac{-d[A]}{dt} = \frac{d[P]}{dt} = k[A] \qquad\qquad \textbf{Equation 1-9}$$

integration between the limits $t_0=0, [A]_0$ and $t, [A]_t$ yields

$$[A]_t = [A]_0 e^{-kt} \qquad\qquad \textbf{Equation 1-10}$$

$$\ln[A]_t = \ln[A]_0 - kt \qquad\qquad \textbf{Equation 1-11}$$

Setting the concentration of other reagents that would influence the rate very high would ensure that they remain effectively constant during the reaction. Only [A] would change appreciably with time. The kinetic order with respect to time would equal the rate with respect to [A]. Pseudo first order kinetics would be followed if the dependence on [A] is first order. When all concentrations, except one, is set much

higher (so they can be treated as approximate constants) it is called "flooding" or "isolation" (the dependence on one reagent is isolated).

The concentration of A decreases exponentially with time when the reaction follows first order kinetics.   From equation 1-11 it follows that a plot of ln $[A]_t$ versus time would give a straight line with slope equal to –k.   This slope and rate constant are independent of $[A]_0$.   This means that a definite fraction of the reaction occurs over a given time interval, independent of $[A]_0$.   If this fraction is 50% of the reaction, substitution of $[A]_{1/2}=[A]_0/2$ into equation 1-11 yields:

$$t_{1/2} = \frac{\ln 2}{k} = \frac{0.693}{k}$$
<div style="text-align:right">Equation 1-12</div>

This is the half-life or half-time for the reaction and it is independent of $[A]_0$.

To be truly first order a plot of ln $[A]_t$ versus time must be linear.   This is a necessary condition but not sufficient proof unless accurate data are taken to at least two half-lives or 75% reaction.   Over shorter intervals curved functions may appear linear.

When a reactant, A, contributes to an instrument reading, Y, a fractional change in Y is proportional to that in A.   When that reaction goes to completion:

$$[A]_t = [A]_0 \left[\frac{Y_t - Y_\infty}{Y_0 - Y_\infty} \right]$$
<div style="text-align:right">Equation 1-13</div>

If the reaction does not go to completion and equilibrium is obtained, equation 1-13 changes to:

$$[A]_t = [A]_e + ([A]_0 - [A]_e) \left[\frac{(Y_t - Y_\infty)}{(Y_0 - Y_\infty)} \right]$$

Equation 1-14

The equation is valid for a single reaction that proceeds to completion with components that contribute linearly to Y.

It can be applied to different rate laws, in this case first order kinetics:

$$\ln\left(\frac{[A]_t}{[A]_0} \right) = \ln\left(\frac{Y_t - Y_\infty}{Y_0 - Y_\infty} \right) = -kt$$

Equation 1-15

$$Y_t = Y_\infty + (Y_0 - Y_\infty)e^{-kt}$$

Equation 1-16

Thus linear plots of $\ln|Y_t - Y_\infty|$ versus time characterises first order reactions.

1.4.2 Influence of temperature on reaction rate [11]

Reaction rates increase with increasing temperature. There are two forms to express the rate constant as a function of temperature.

The first is the Arrhenius equation:

$$k = Ae^{(-E_a/RT)}$$

Equation 1-17

with   A the pre-exponential factor

E_a the Arrhenius activation energy

T the temperature (K)

R the gas constant (8.314 J.K^{-1}.mol^{-1})

The second uses transition state theory

$$k = K(k_B T/h) e^{(\Delta S^{\ddagger}/R)} e^{(-\Delta H^{\ddagger}/RT)}$$ **Equation 1-18**

with k_B Boltzmann's constant (1.381×10^{-23} J.K^{-1})

h Planck's constant (6.626×10^{-34} J.s)

$\Delta S^{\ddagger}$ the standard entropy of activation

$\Delta H^{\ddagger}$ the standard enthalphy of activation

K the transmission factor (in nearly all reactions in solution $K=1$)

Fitting data in the logarithmic form for both the equations results in:

$$\ln k = \ln A - (E_a/RT)$$ **Equation 1-19**

A plot of ln k versus 1/T will give A as the intercept and E_a as the slope.

$$\ln(k/T) = \ln(k_B/h) + (\Delta S^{\ddagger}/R) - (\Delta H^{\ddagger}/RT)$$ **Equation 1-20**

Plotting ln (k/T) versus 1/T means that $\Delta S^{\ddagger}$ can be calculated from the intercept ($\ln(k_B/h) = 23.760$) and $\Delta H^{\ddagger}$ can be obtained from the slope.

The activation energy and activation enthalpy for a reaction with very rapid kinetics are relatively small.

The Gibbs free energy of the reaction at a specific temperature can be calculated using equation 1-21:

$$\Delta G^{\ddagger} = \Delta H^{\ddagger} - T\Delta S^{\ddagger}$$ **Equation 1-21**

1.4.3 Influence of ionic strength on reaction rates [12]

The interactions between two reactants are considered in the kinetics of the reactants.   The interactions of the non-reactive ions in solution

around the reagent ions influence the rate of reaction.   The ionic strength is a measure of the effect the non-reactive electrolytes have on the reaction and can be defined as:

$$ionic \quad strength = \mu = \frac{1}{2}\left([A]Z_A^2 + [B]Z_B^2 + [C]Z_C^2 + ...\right)$$ **Equation 1-22**

where   [A], [B] and [C] represent the molar concentrations of all the ions A, B, C… in solution

Z_A, Z_B, Z_C, … represent the ions' charges

1.4.4 Isomers of Octahedral Compounds [12]

The arrangement of ligands around a central metal atom can vary and this results in different isomers of the same compound.   An isomer, according to the IUPAC definition, is "one of several species (or molecular entities) that have the same atomic composition (molecular formula) but different line formulae or different stereochemical formulae and hence different physical and/or chemical properties".   Two similar ligands can be arranged on "the same side" (*cis*) or "across" (*trans*) the central atom in an octahedral configuration (figure 1-3 and 1-4).
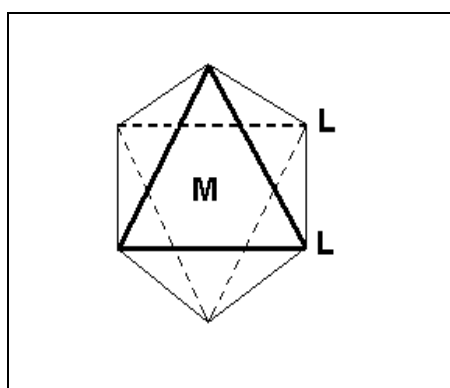
Figure 1-3: *cis*-[ML$_2$]
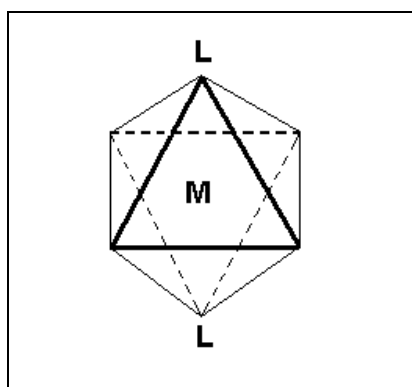
Figure 1-4: *trans*-[ML$_2$]

Three similar ligands may be arranged on an octahedron in a *cis* fasion giving the facial (*fac*) isomer (figure 1-5) or with one pair of ligands in a *trans* position, giving the meridional (*mer*) isomer (figure 1-6).
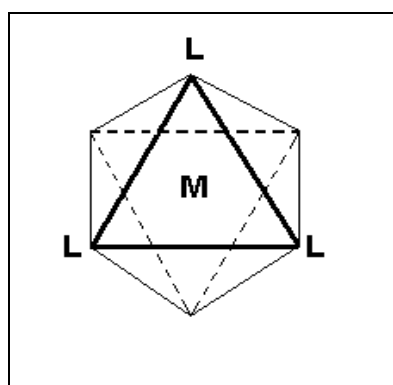
Figure 1-5: *fac*-[ML$_3$]
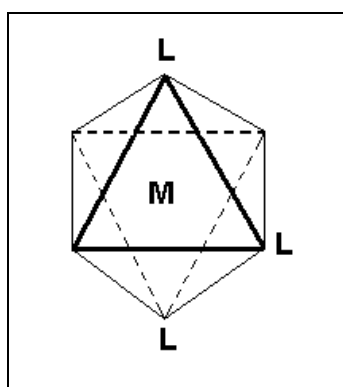
Figure 1-6: *mer*-[ML$_3$]

Certain ligands have the ability to labilise ligands *trans* to themselves. This is called the trans effect and will be explained in more detail in paragraph 1.4.6. The ligands can be arranged in an order indicating their ability to do so:

F^-, OH^-, H_2O, NH_3, py < Cl^- < Br^- < I^-, SCN^-, NO_2^-, $C_6H_5^-$ < $S=C(NH_2)_2$, CH_3^-, H^-, PR_3, AsR_3 < CN^-, CO, C_2H_4
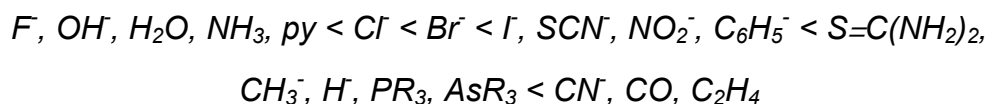
1.4.5 Kinetics of Aquation and Chloride Anation of Iridium(III) Aqua-Chloro Species

Poulsen and Garner[14] reported the aquation rate constant, $k_{65}=9.4(\pm 0.60)\times 10^{-6}$ s^{-1}, for the $[IrCl_6]^{3-}$ species at 15.05°C with the activation energy, $E_a=127.3(\pm 8)$ kJ. The anation rate constant, k_{56}, for $[IrCl_5(H_2O)]^{2-}$ was determined as 5×10^{-5} $M^{-1}s^{-1}$. The activation energy could not be determined as the data was not accurate enough and the ionic strength too high to justify extrapolation to infinite dilution. Grant[13] reported a value of 2.0×10^{-6} $M^{-1}.s^{-1}$ for k_{56} at 25°C.

The reaction:

$$[IrCl_5(H_2O)]^{2-} + H_2O \underset{k_{45}}{\overset{k_{54}}{\rightleftarrows}} [IrCl_4(H_2O)_2]^- + Cl^-$$
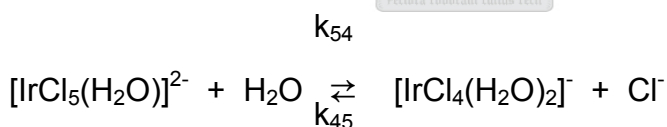
was researched by Chang and Garner[15] who reported the rate constants at 50°C as $k_{54}=1.26$ (± 0.05) $\times 10^{-5}$ s^{-1}, $E_a=123.1$ (± 3) kJ and $k_{45}=6.7$ (± 0.4) $\times 10^{-5}$ $M^{-1}s^{-1}$, $E_a=116.4$ (± 3) kJ. They also estimated a value for the aquation of $[IrCl_4(H_2O)_2]^-$, $k_{43}=2.9$ (± 0.1) $\times 10^{-6}$ s^{-1} at 50°C.

A value of $k_{43T}=5.1$ (± 0.2) $\times 10^{-7}$ s^{-1} and $E_a=127.7$ (± 3) kJ was reported at 50°C by El-Awady[16], for the reaction:

$$trans\text{-}[IrCl_4(H_2O)_2]^- + H_2O \underset{k_{34T}}{\overset{k_{43T}}{\rightleftarrows}} mer\text{-}[IrCl_3(H_2O)_3] + Cl^-$$
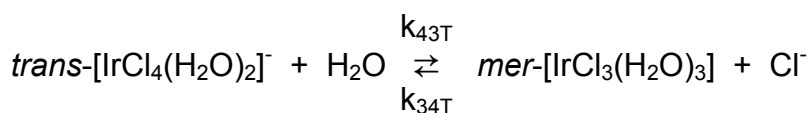
The opposing rate constant, k_{34T} was reported to have a value of 2.2 (±0.2) x10^{-5} M^{-1}s^{-1} with the activation energy E_a=120.5 (±3) kJ. The reaction of the *cis*-[IrCl$_4$(H$_2$O)$_2$]$^-$ isomer gave both the *mer*- and *fac*-[IrCl$_3$(H$_2$O)$_3$] in the ratio 40%:60%, respectively and k_{43}=2.56 (±0.07) x10^{-5} s^{-1}.

There is a ten times decrease in reaction rate from k_{65} (the aquation of [IrCl$_6$]$^{3-}$) to k_{54} (the aquation of [IrCl$_5$(H$_2$O)]$^{2-}$). The rate of aquation of the iridium aqua-chloro species decreases as the number of chloride ligands on the central metal atom decrease. The chloride anation rate constants for the aqua-chloro species do not follow a similar trend and do not decrease significantly as the number of chloride ligands decreases on each complex.

1.4.6 Kinetics of Aquation and Chloride Anation of Rhodium(III) Aqua-Chloro Species

The reaction scheme for rhodium(III) (figure 1.7) was drawn up by Palmer and Harris[17]. The steric course of the reactions is dictated only by the trans-effect of the chloride ligands in each species. The aquation of [RhCl$_6$]$^{3-}$ and its subsequent aquated species proceeds only by loss of a chloride *trans* to another chloride (*trans* effect, figure 1-8), to produce only *cis* species and the sequence stops at the very stable *fac*-[RhCl$_3$(H$_2$O)$_3$] (figure 1-7). There is only a short equilibrium series in the whole Rh(III) scheme (figure 1.7), namely the aquation of [RhCl$_6$]$^{3-}$ to [RhCl$_5$(H$_2$O)]$^{2-}$ from where aquation produces *only* the *cis*-[RhCl$_4$(H$_2$O)$_2$]$^-$, the aquation of which *only* produces the *fac*-[RhCl$_3$(H$_2$O)$_3$] (figure 1-7). The equilibrium series is set out below:

$$[RhCl_6]^{3-} \xleftrightarrow{\;K_6\;} [RhCl_5(H_2O)]^{2-} \xleftrightarrow{\;K_5^C\;} cis-[RhCl_4(H_2O)_2]^- \xleftrightarrow{\;K_4^C\;} fac-[RhCl_3(H_2O)_3]$$
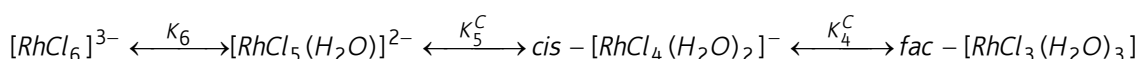
The values K_4^c=6.3 M^{-1}, K_5^c=5.3 M^{-1} and K_6=0.039 M^{-1} were obtained by Palmer and Harris[17]. This explains why no *trans* isomers were

observed in the studies of chloroaquarhodium(III) complexes when the starting material was $[RhCl_6]^{3-}$ anion[18].   The aquation rate constants (k_{65}, k^c_{54}, k^c_{43}) in the equilibrium series (figure 1-7) decrease by approximately a factor of 10 each time a chloride is exchanged for a water molecule.   This means that the loss of a chloride is slower when there are fewer chloride ligands on the complex.   The chloride anation rate constants (k_{56}, k^c_{45}, k^c_{34}) in the equilibrium series do not decrease as rapidly as the corresponding aquation rate constants (k_{65}, k^c_{54}, k^c_{43}).

trans isomers $[Rh(H_2O)_6]^{3+}$ *cis* isomers

$k_{01} = 3.3 \times 10^{-7}\ M^{-1}s^{-1}$

$[RhCl(H_2O)_5]^{2+}$

$k^t_{12} = 3.1 \times 10^{-5}\ M^{-1}s^{-1}$

trans-$[RhCl_2(H_2O)_4]^+$ *cis*-$[RhCl_2(H_2O)_4]^+$

$k^{tc}_{32} = 5.4 \times 10^{-6}\ s^{-1}$

$k^{ct}_{23} = 1.9 \times 10^{-4}\ M^{-1}s^{-1}$

$k^t_{23} = 3.6 \times 10^{-8}\ M^{-1}s^{-1}$

mer-$[RhCl_3(H_2O)_3]$ *fac*-$[RhCl_3(H_2O)_3]$

$k^t_{34} = 5.2 \times 10^{-4}\ M^{-1}s^{-1}$ $k^t_{43} = 2.1 \times 10^{-4}\ s^{-1}$ $k^c_{43} = 1.5 \times 10^{-4}\ s^{-1}$ $k^c_{34} = 9.3 \times 10^{-4}\ M^{-1}s^{-1}$

trans-$[RhCl_4(H_2O)_2]^-$ *cis*-$[RhCl_4(H_2O)_2]^-$

$k^c_{54} = 1.1 \times 10^{-3}\ s^{-1}$

$k^c_{45} = 5.9 \times 10^{-3}\ M^{-1}s^{-1}$

$k^t_{45} = 1.8 \times 10^{-7}\ M^{-1}s^{-1}$

$[RhCl_5(H_2O)]^{2-}$

$k_{65} = 4.9 \times 10^{-2}\ s^{-1}$ $k_{56} = 1.9 \times 10^{-3}\ M^{-1}s^{-1}$

$[RhCl_6]^{3-}$ All constants at 50°C
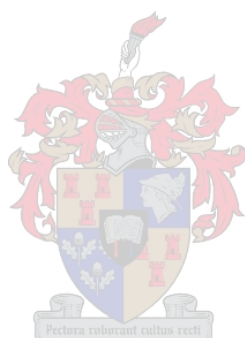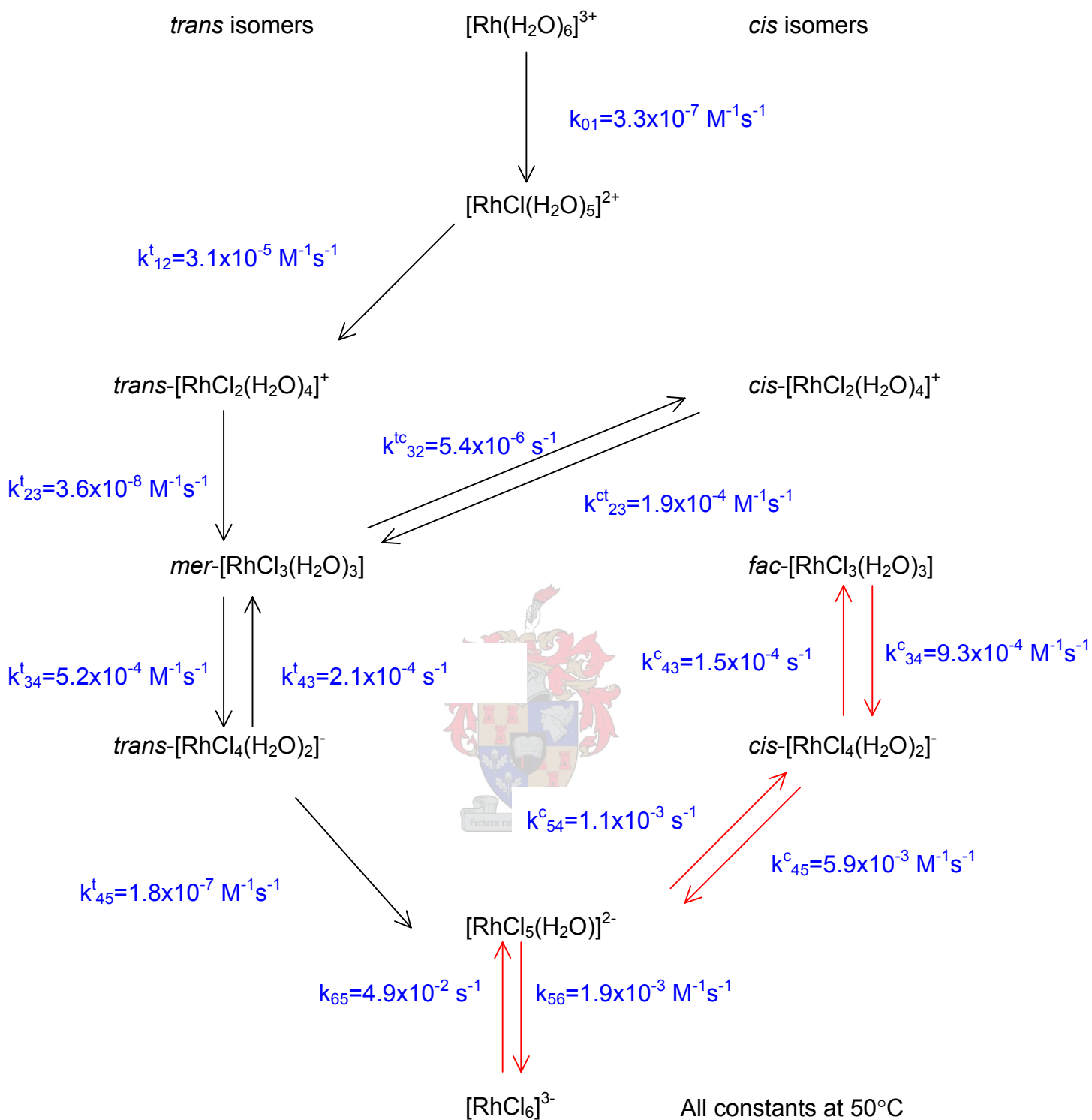
Figure 1-7: Scheme of the reaction kinetics of Rh(III), redrawn from Palmer and Harris. [17]
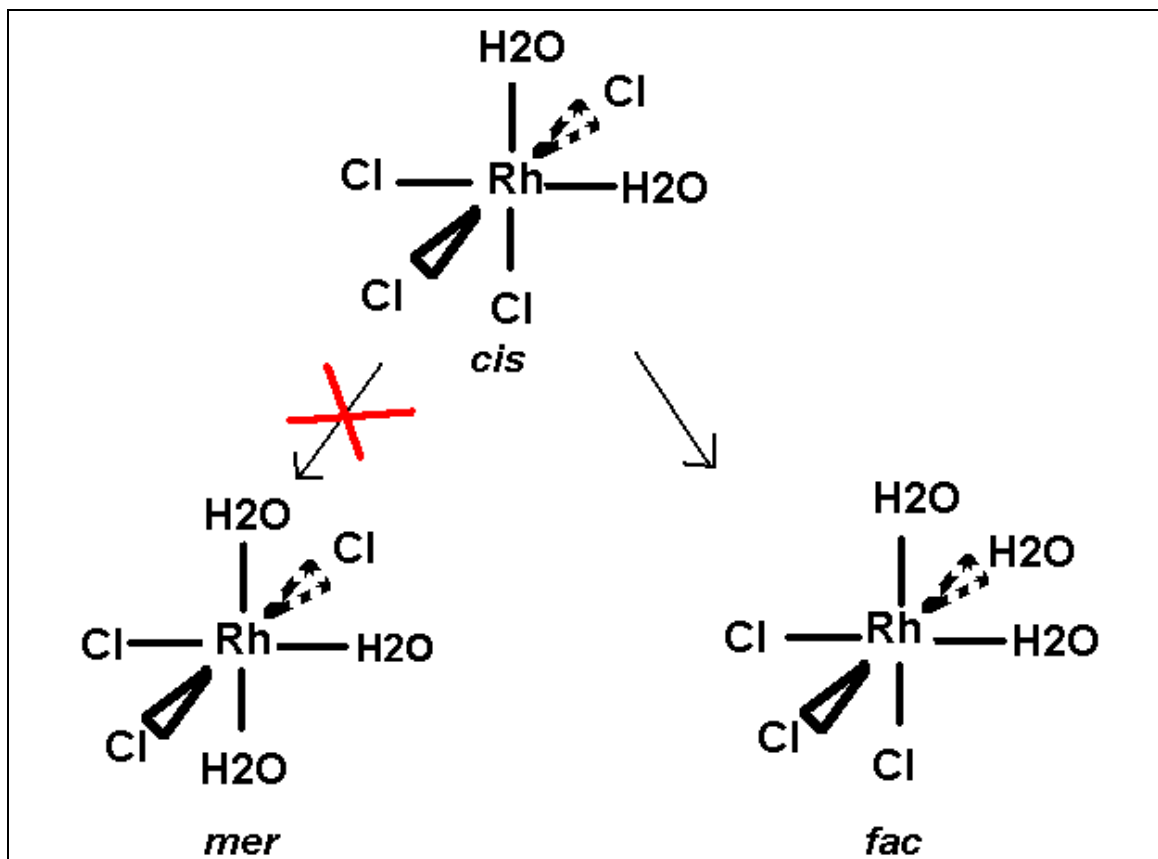
Figure 1-8: The *trans* effect.

The selective precipitation of rhodium in the presence of iridium with polyamines is described as an improvement in pgm refining[19]. The rhodium is precipitated as the $[RhCl_6]^{3-}$ anion. The rhodium is in the +3 oxidation state while iridium is oxidised to Ir(IV) and ruthenium is converted to a chloro-nitrosyl complex in the +2 oxidation state. This method of precipitation can be used to selectively precipitate ruthenium, iridium or rhodium in the +3 oxidation state.

Dark red single crystals of diethylenetriammonium hexachlororhodate(III), $[H_3N(CH_2)_2NH_2(CH_2)_2NH_3][RhCl_6]$, were prepared by Frank[20]. X-Ray crystallography determined the space group as C2/c with a=30.956(4) Å, b=7.371(2) Å, c=12.9736(15) Å, β=113.787(11)° and Z=8 (figures 1-9 and 1-10). The average rhodium-chloride bond length was 3.35 Å.
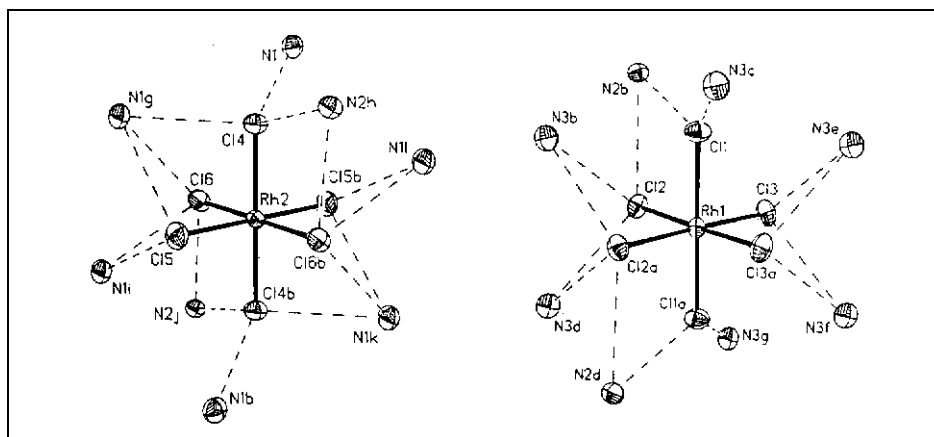
Figure 1-9: Configuration of the [RhCl$_6$]$^{3-}$ anion in the crystal structure. [20]
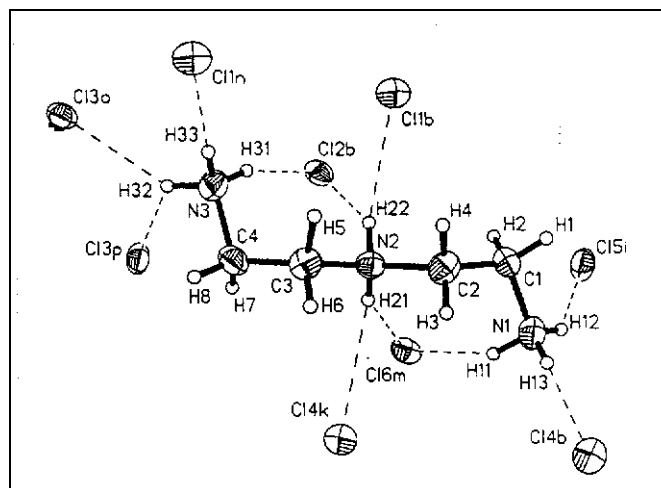
Figure 1-10: Configuration of the diethylenetriammine cation. [20]

1.4.7 Characterisation and Kinetics of Aquation and Chloride Anation of Ruthenium(III) Aqua-Chloro Species

All the rate constants collected from the literature for the aquachlororuthenate(III) species were compiled in figure 1-11 to present an overall view of what data was available from the literature. The rate constants in red are from Adamson's unpublished literature[9, 10] and refer to the higher chloro species (hexa-, penta- and tetrachloro species). The data in green are from Connick[21] and are focused around the dichloro- and trichloro species.

The aquation rate constants (k_{65}, k_{54}) decrease by approximately a factor of 100 from $[RuCl_6]^{3-}$ to $[RuCl_5(H_2O)]^{2-}$ to $[RuCl_4(H_2O)_2]^-$. Connick[21] commented on this and approximated a time of greater than one year for the loss of a chloride from $[RuCl(H_2O)_5]^{2+}$ while the loss of a chloride from $[RuCl_6]^{3-}$ happens in less than a few seconds at room temperature.

1.4.7.1 Characterisation of Ruthenium(III) Aqua-Chloro Species

From the literature it is evident that the bulk of research on ruthenium and especially ruthenium(III) was done in the 1950's and 60's. This was due to the fact that ruthenium was a by-product of nuclear processes and needed to be removed. Its chemistry needed to be understood before efficient removal could be achieved. Renewed interest in ruthenium was generated by its use in catalysis in the 1980's.

The series of ruthenium(III) species in aqueous hydrochloric acid medium can be summarised as $[RuCl_{6-n}(H_2O)_n]^{n-3}$ and was first separated and characterised by various people before research could be done on the kinetics of the series. The focus was on the separation and characterisation in the early stages.
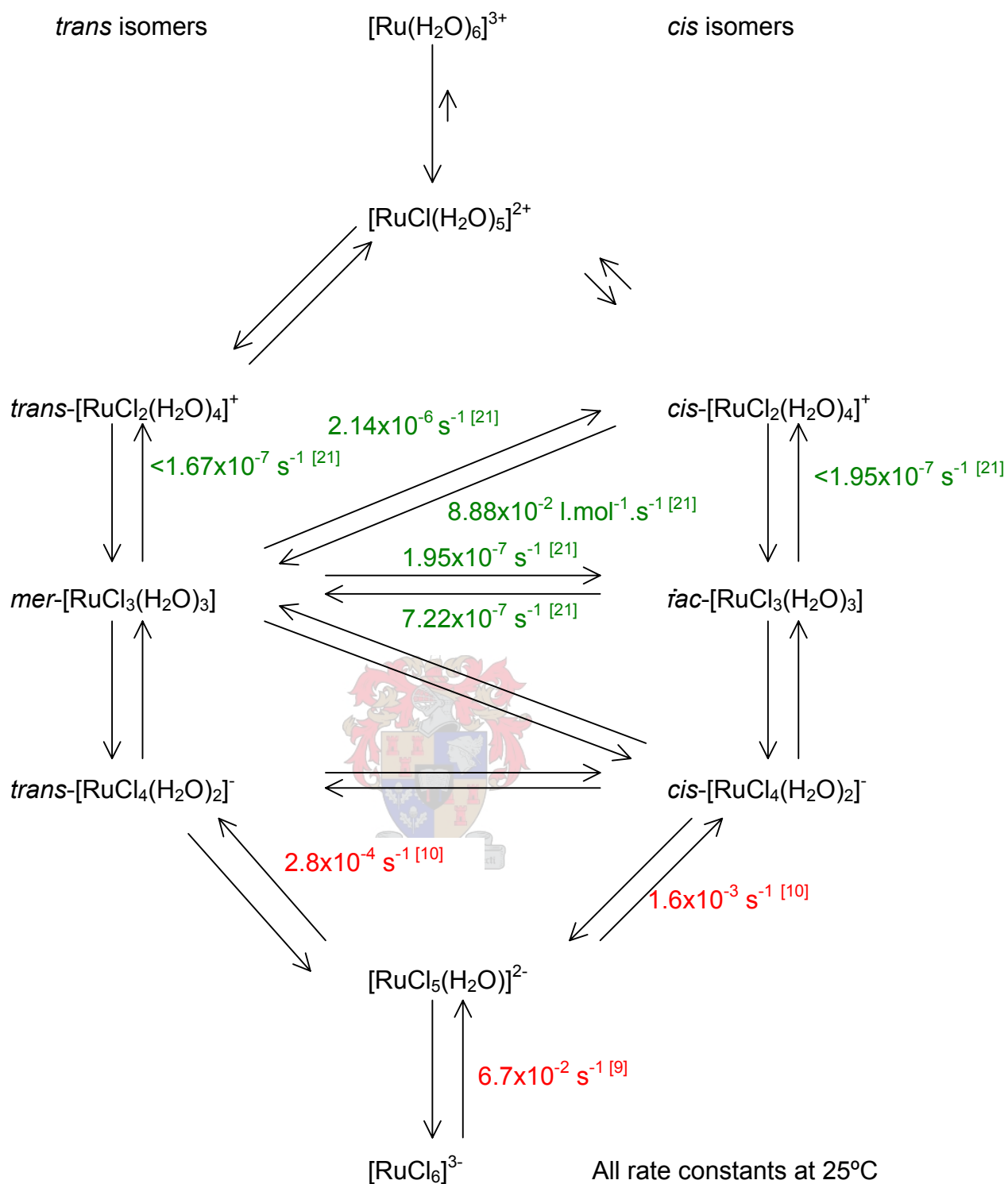
Figure 1-11: Scheme for the reaction kinetics of ruthenium(III). Compiled from Adamson[9, 10] (data in red) and Connick[21] (data in green).

The cationic species: $[Ru(H_2O)_6]^{3+}$ (figure 1-12) and $[RuCl(H_2O)_5]^{2+}$ (figure 1-13) were first successfully separated and characterised by Cady and Connick[22] in 1957. A third species was tentatively identified as $[RuCl_2(H_2O)_4]^+$. These complexes are slow to equilibrate and this characteristic was exploited to characterise the complexes. Ion exchange was used to determine the charge per metal atom and the charge per species. With this known, the formula of the complex could be deduced as there was only one known charged ligand available, namely chloride.

There are some considerations before using ion exchange as a method for separating species. The kinetics of interconversion or equilibrium between species has to be slow such that minimum interconversion between species occurs in the time the separation is completed.
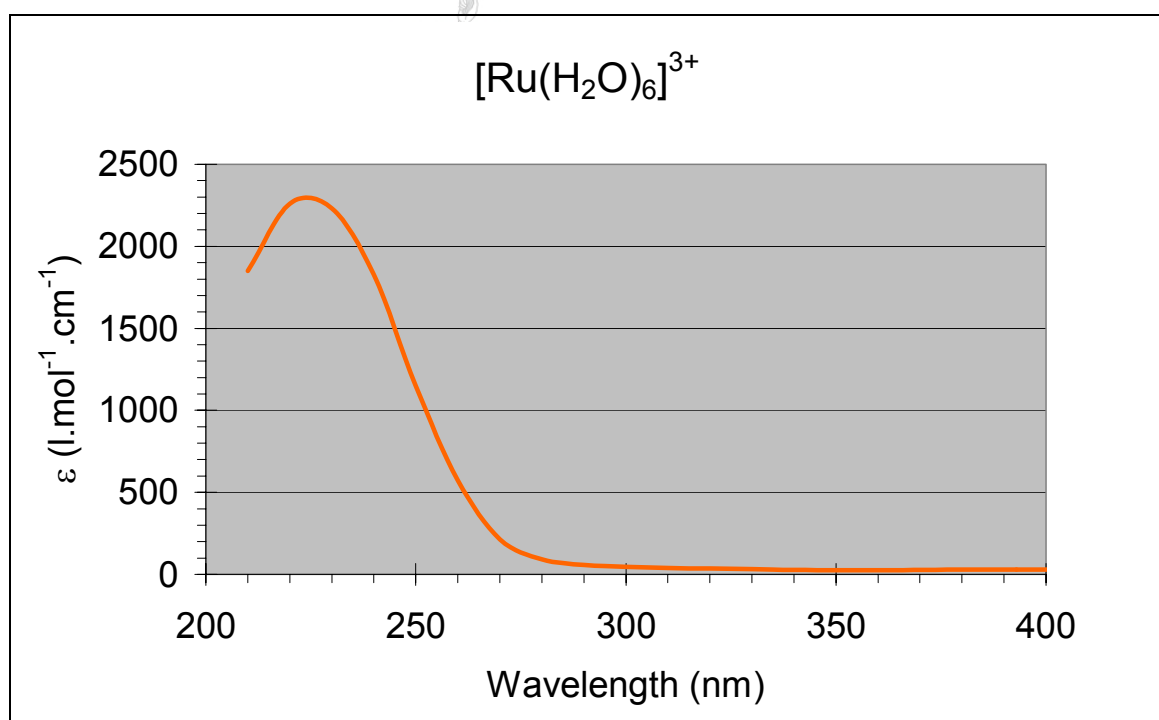
Figure 1-12: UV/Vis spectrum of $[Ru(H_2O)_6]^{3+}$, redrawn from Cady and Connick. [22]
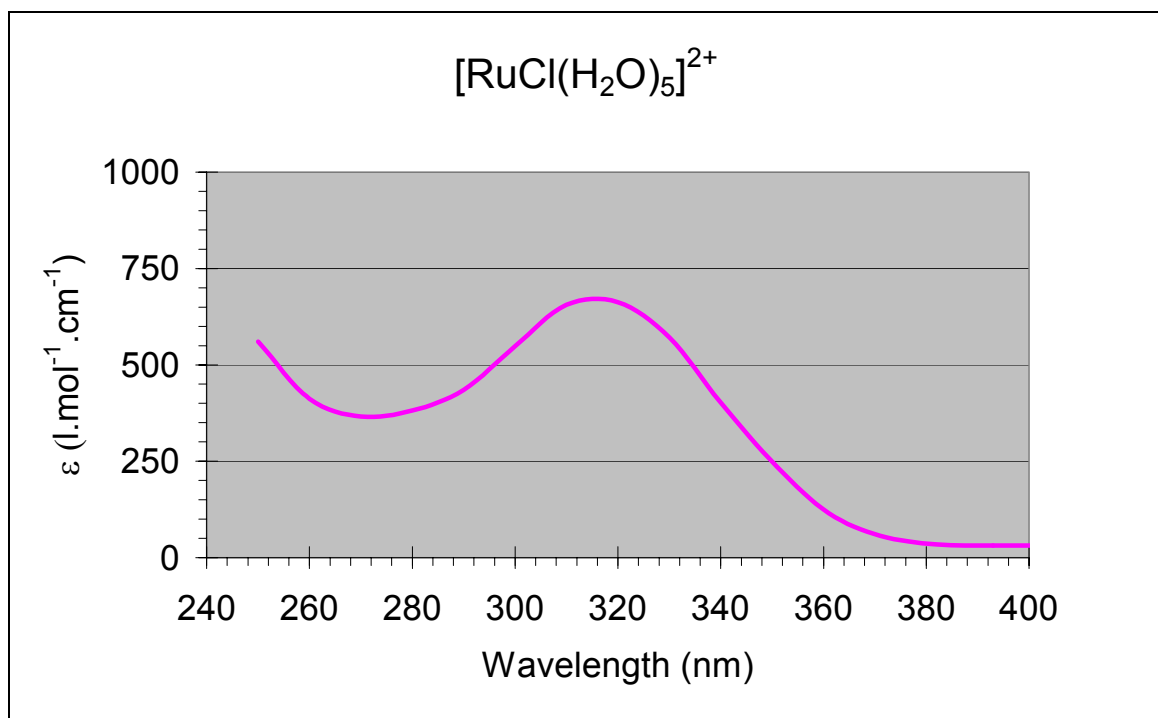
Figure 1-13: UV/Vis spectrum of $[RuCl(H_2O)_5]^{2+}$, redrawn from Cady and Connick. [22]
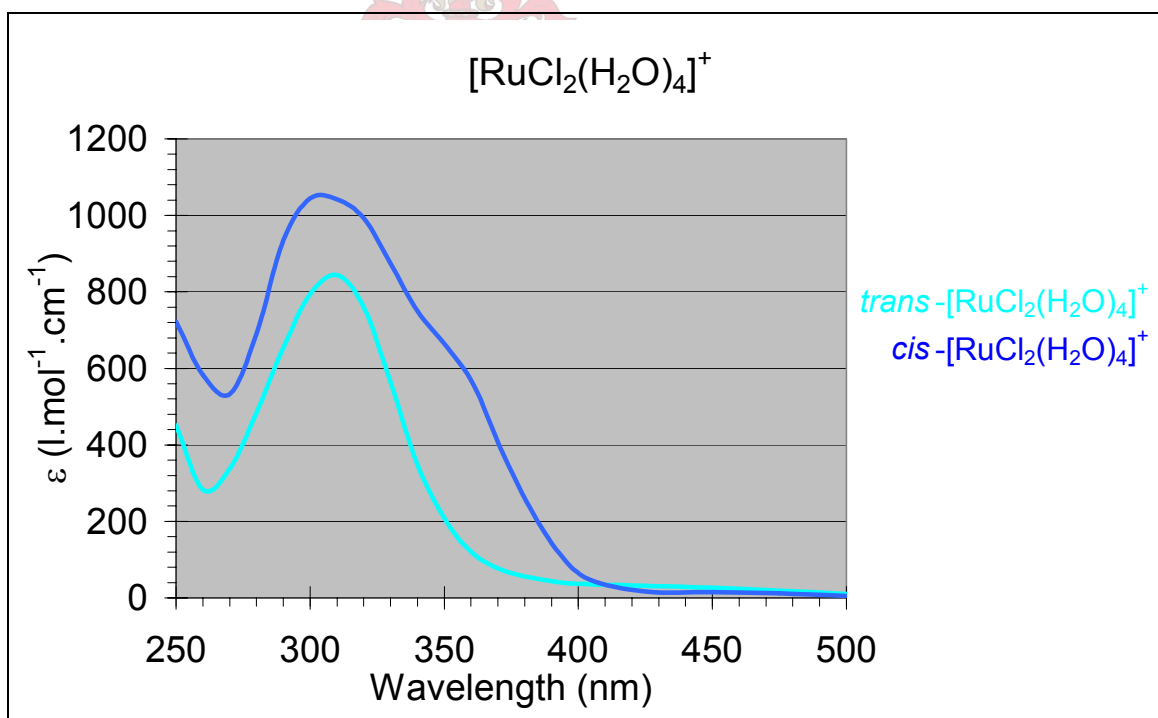
Figure 1-14: UV/Vis spectrum of $[RuCl_2(H_2O)_4]^+$, redrawn from Fine. [24]

Connick and Fine[23, 24] adapted the method, reported by Cady and Connick, to identify $[RuCl_2(H_2O)_4]^+$ (figure 1-14) as its *cis* and *trans* isomers, by using a buffered eluent to elute the species.

Fine, in his thesis[24], encountered problems with the identification of the neutral species, $[RuCl_3(H_2O)_3]$. He employed the method of freezing-point lowering to identify this species. The main method to separate the species of ruthenium(III) up to this point was based on ion exchange and its properties. The anionic and cationic species in a solution containing ruthenium(III) were separated from the neutral species by passing the solution through a cation and anion exchange column. The spectra of the two isomers obtained in separation are distinct (figure 1-15) and the assignment of the isomers were proven by Mercer and MacAllister[25] by the measurement their dipole moments.
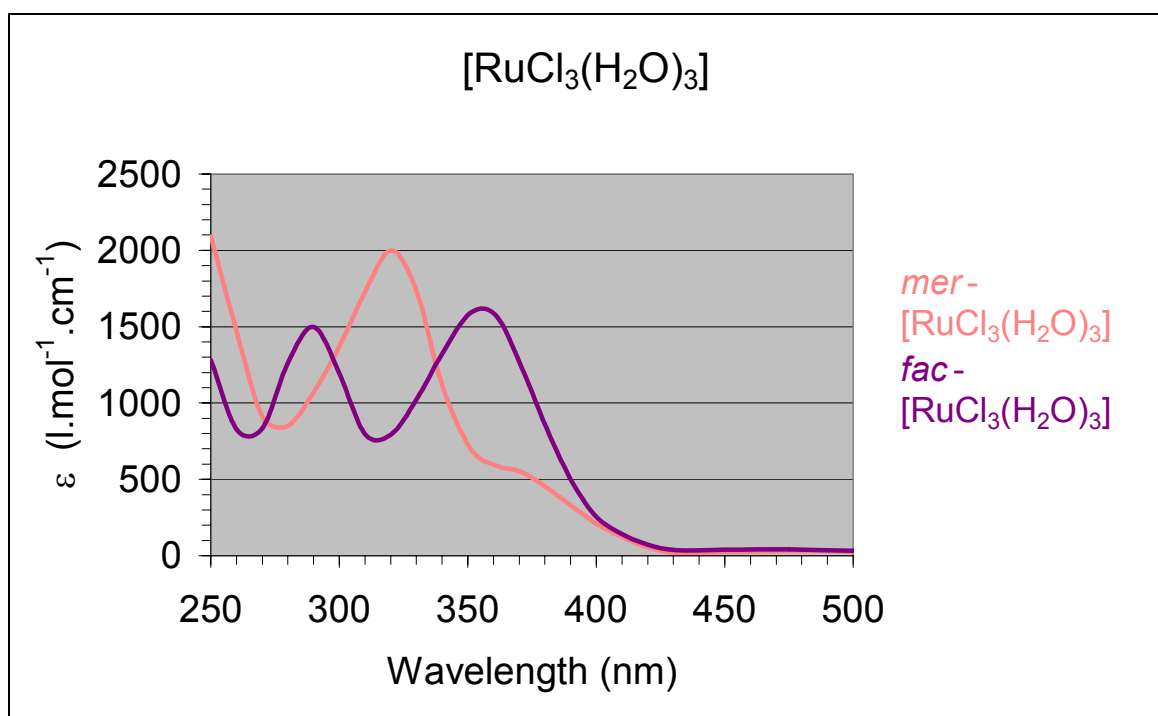
Figure 1-15: UV/Vis spectrum of the isomers of $[RuCl_3(H_2O)_3]$, redrawn from Fine. [24]

Fine[24] found that the anionic species of the group presented a problem in that the kinetics of these species is faster than that of the cationic species. The effect of the chloride ion concentration in the eluant and during separation was also a problem as the formation of the anionic species is very dependent on this. These problems increase as the number of chloride ligands on the complex increases, and the

equilibrium time between the anionic species decreases. The ion exchange separation was attempted on $[RuCl_4(H_2O)]^{2-}$ and two isomers were separated, the UV/Vis spectra of which are shown in figure 1-16.
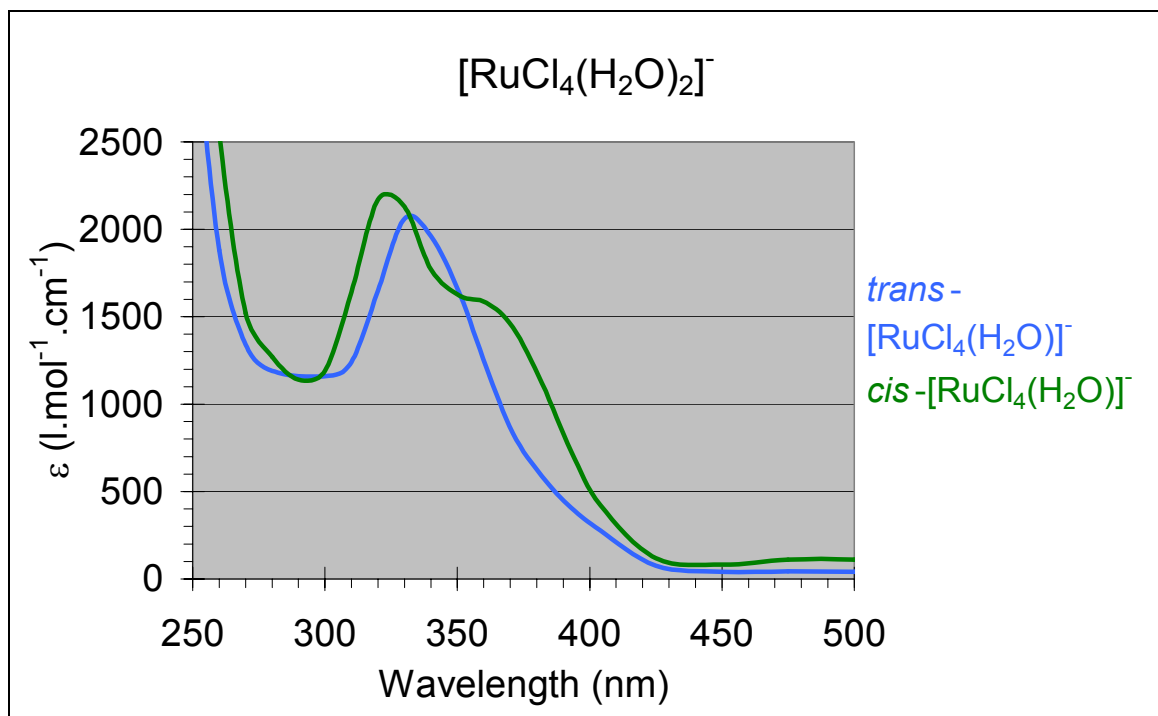
Figure 1-16: UV/Vis spectrum of the isomers of $[RuCl_4(H_2O)_2]^{2-}$, redrawn from Fine. [24]

Adamson, Connick and Fine[26], in an unpublished report, assigned the *cis* and *trans* configuration to the two isomers by crystallisation of one of the isomers of $[RuCl_4(H_2O)_2]^{2-}$. The isomer that eluted last was crystallised and the crystal structure of tetraphenylarsonium *cis*-diaquatetrachlororuthenate monohydrate was reported by Hopkins[27]. This confirms the observations made by several investigators[22, 24] that the *trans* isomer is more readily eluted than the *cis* isomer.

For the reaction:

$[RuCl_4(H_2O)_2]^- + H_2O \rightleftarrows [RuCl_3(H_2O)_3] + Cl^-$
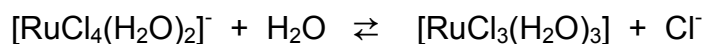
Fine[24] reports a value of 0.833 M^{-1} for the equilibrium constant K_4, having used ion exchange to separate the species. Ohyoshi[28] reports values of 0.7 M^{-1} (at $\mu=0.21$) and 0.6 M^{-1} at ($\mu=0.46$) using paper

electrophoresis for the separation of the species. Taqui-Khan[29] used polarography to determine the rate constants k_{34} (1.30×10^4 $M^{-1}.s^{-1}$) and k_{43} (0.43×10^4 s^{-1}) which yields $K_4 = 0.33$ M^{-1}. Given the different techniques and conditions used, these results are in good agreement.

The spectrum of $[RuCl_5(H_2O)]^{2-}$ was reported by Fine[24] and Adamson[10] (figure 1-17). The spectra have their maxima at 330 nm but the molar extinction coefficients vary due to solution and solid state spectra having been obtained, respectively. The molar extinction coefficient is a characteristic of the conditions under which the spectrum was determined.

Adamson[10] prepared cesium aquapentachlororuthenate crystals that were characterised by Hopkins[30]. The solute concentrations in the solution that yielded the crystals were [Ru(III)]=0.05M, [Cs$^+$]=0.25M and [Cl$^-$]$\approx$2M. The crystals were dissolved in 1M HCl at 4°C to obtain the solution spectrum, while the solid spectrum was obtained by pressing of the crystals into a KBr disk.
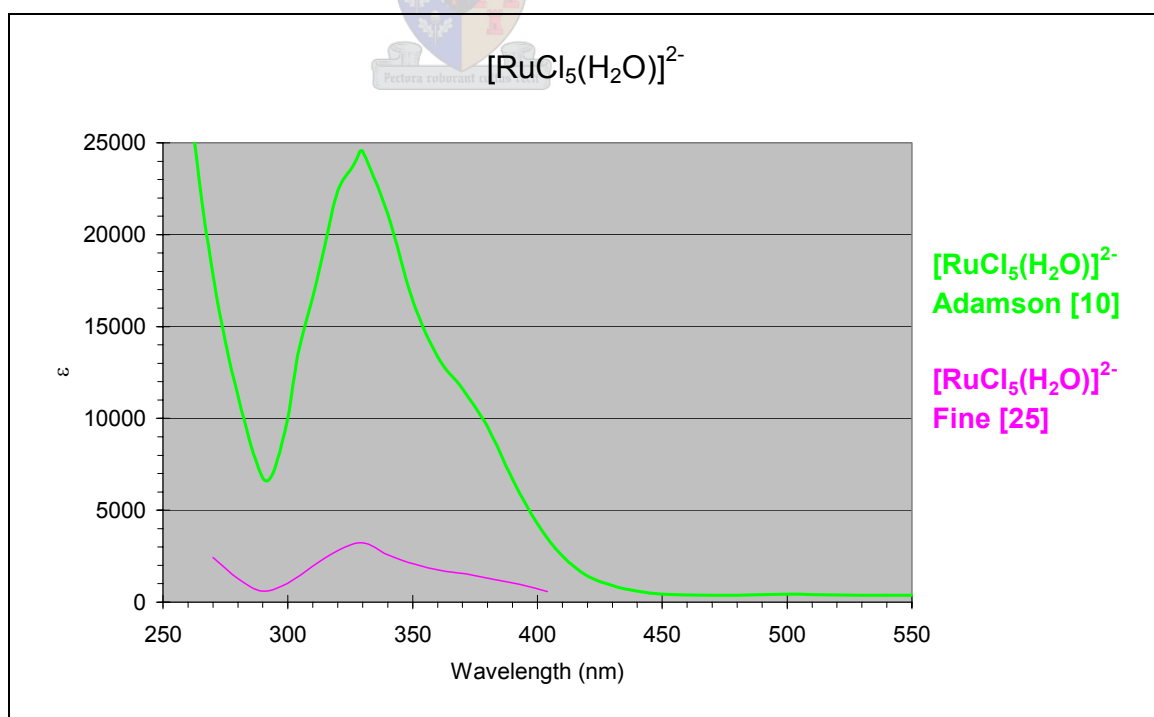
Figure 1-17: UV/Vis spectrum of $[RuCl_5(H_2O)]^{2-}$, redrawn from Adamson and Fine. [10, 24]

The rate constants for the aquation of $[RuCl_5(H_2O)]^{2-}$ were determined by dissolution of crystals in 0.1M HCl[10]. The *cis↔trans* isomerisation reaction of the $[RuCl_4(H_2O)_2]^-$ product of the aquation of $[RuCl_5(H_2O)]^{2-}$ was followed using ion exchange. The first order rate constant for the overall reaction (k_{54}):

$$[RuCl_5(H_2O)]^{2-} + H_2O \rightarrow [RuCl_4(H_2O)_2]^- + Cl^-$$
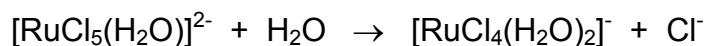
was determined as 1.9 ($\pm$0.07) x10^{-3} s^{-1} at 25°C and unit ionic strength. The corresponding enthalpy was calculated as 89.6 ($\pm$3) kJ.mol^{-1}. The aquation products of this reaction, the *cis* and *trans* isomers of $[RuCl_4(H_2O)_2]^-$, are formed simultaneously in the ratio k_{54C}:k_{54T} = 5.70($\pm$0.45):1. This equates to k_{54C}=1.6 ($\pm$0.07) x10^{-3} s^{-1} and k_{54T}=2.8 ($\pm$0.7) x10^{-4} s^{-1}.

$$[RuCl_5(H_2O)]^{2-} + H_2O \quad\nearrow\searrow\quad \begin{array}{l} cis\text{-}[RuCl_4(H_2O)_2]^- + Cl^- \\ trans\text{-}[RuCl_4(H_2O)_2]^- + Cl^- \end{array}$$
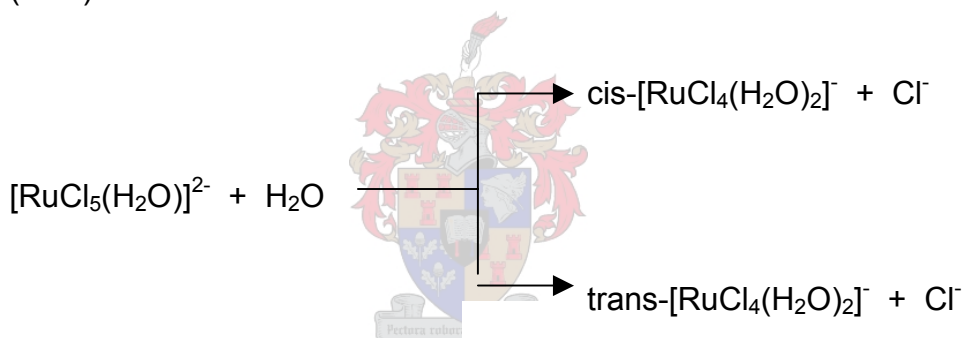
Unpublished papers of Adamson[9] report the structure, spectrum (figure 1-19) and kinetics of the aquation of the hexachlororuthenate(III) anion (table 1-3 and figure 1-18) and the pentachloroaquaruthenate(III) anion[9]. In the study of the hexachlororuthenate(III) anion, crystals of hexaaquoaluminium hexachlororuthenate tetrahydrate were prepared and characterised. The crystal and molecular structure of this crystal were published by Hopkins[31] and confirm an octahedrally coordinated $[RuCl_6]^{3-}$ anion. The crystals were found to be stable in air but very soluble in water. The study of the monoclinic $Al(H_2O)_6RuCl_6\cdot4H_2O$ crystal determined a=10.492 (5) Å, b=11.415 (5) Å, c=7.069 (5) Å, β=92.69 (2)°, Z=2 and D_x=2.045 g.cm^{-3}. The space group of the crystals is $P2_1/n$. Comparisons between the UV/Vis spectrum of the crystal $Al(H_2O)_6RuCl_6\cdot4H_2O$ and the spectrum of ruthenium(III) in 12M

HCl shows evidence that $[RuCl_6]^{3-}$ exists in solution. Determining[9] the proportion of $[RuCl_6]^{3-}$ present in 12M HCl proved unsuccessful but results suggest that 95% of Ru is present as $[RuCl_6]^{3-}$ with a small amount of $[RuCl_5(H_2O)]^{2-}$ and traces of $[RuCl_4(H_2O)_2]^{-}$.

James[32] described a method for the preparation of crystals of $K_3[RuCl_6]$ from ruthenium trichloride. Ruthenium trichloride is known to be a mixture of oxy and hydroxychloro species with ruthenium in the +3 and +4 oxidation states. In this report, ruthenium trichloride is dissolved in methanol and reduced with hydrogen while boiling under reflux. After about 5 hours, during which the solution turns green, potassium chloride is added and the mixture is boiled under reflux in an atmosphere of air. A brown precipitate is formed and separated from the colourless supernatant liquid by filtration and washed with methanol. The crude product was recrystallised from 12M HCl. The product was analysed by chemical analysis, UV/Vis and IR.

The kinetics of the aquation of $[RuCl_6]^{3-}$ to $[RuCl_5(H_2O)]^{2-}$ was analysed and found to be first order[9]. The rate constant, k_{65} at 25°C, was determined by extrapolation as 6.7 ($\pm$1) x10^{-2} s^{-1}, with an enthalpy of 113 ($\pm$6) kJ/mol and entropy of activation of +117 ($\pm$21) J.deg^{-1}.mol^{-1}. The influence of the total ruthenium concentration, chloride concentration and proton concentration was briefly investigated. It was found that the rate of aquation is possibly dependent on ionic strength, increasing with decreasing ionic strength. The rate of aquation was found to be independent of both the total ruthenium concentration and proton concentration over the small concentration range studied. The aquation product of $[RuCl_5(H_2O)]^{2-}$, from the aquation of $[RuCl_6]^{3-}$, was found to be mainly *cis*-$[RuCl_4(H_2O)_2]^{-}$. This is due to the *trans* labilising effect of the chloride ligand. Further rate constant data for the aquation of $[RuCl_6]^{3-}$ from Adamson[33] are shown in table 1-4.

Table 1-3: Rate constant data of the aquation of $[RuCl_6]^{3-}$ to $[RuCl_5(H_2O)]^{2-}$. [9]

Temp	[Ru]x10^{-4} (M)	[H$^+$] (M)	[Cl$^-$] (M)	μ (M)	k$_{65}$ x10^{-3} (s^{-1})
1.0°C	1.99	1.00	1.00	1.00	1.2 (±0.08)
	1.99	1.00	0.38	1.00	1.3
	1.99	0.38	0.38	0.38	1.7
6.6°C	1.00	1.00	1.00	1.00	3 (±0.3)
	1.99	1.00	1.00	1.00	3.2 (±0.3)
	1.99	0.38	1.00	1.00	3.5
	1.99	0.19	1.00	1.00	3.3
11.9°C	1.99	1.00	1.00	1.00	7.8 (±0.7)
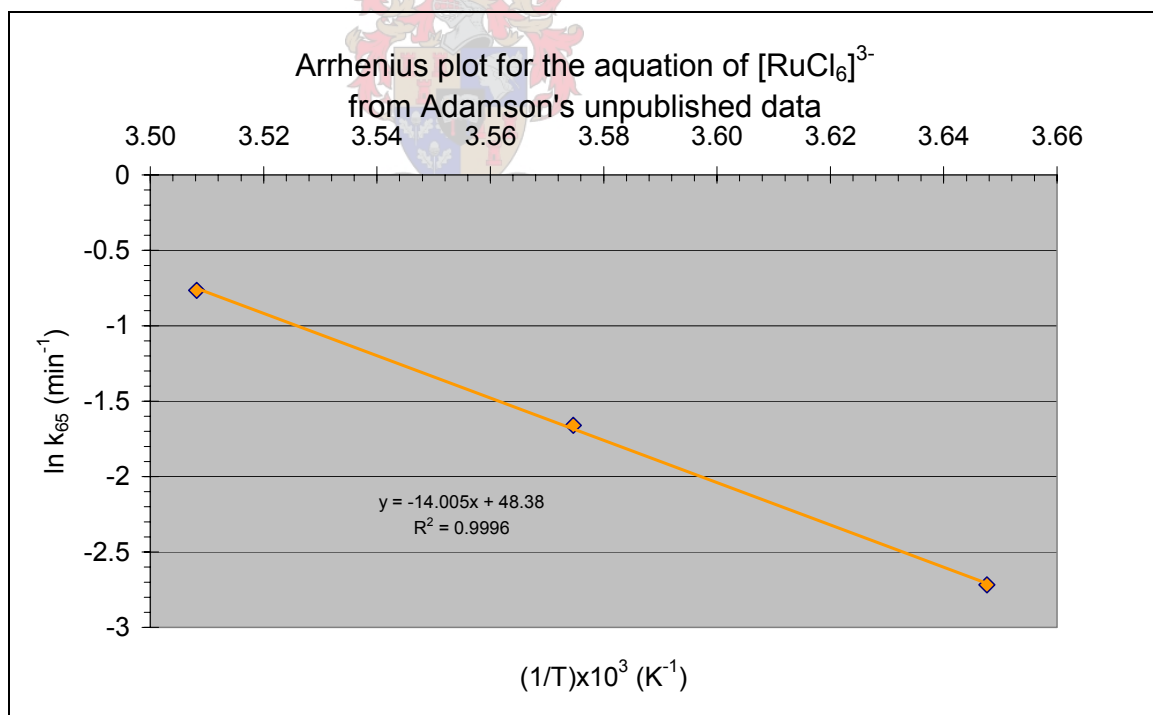
Figure 1-18: Arrhenius plot for the aquation of $[RuCl_6]^{3-}$, compiled from Adamson. [9]
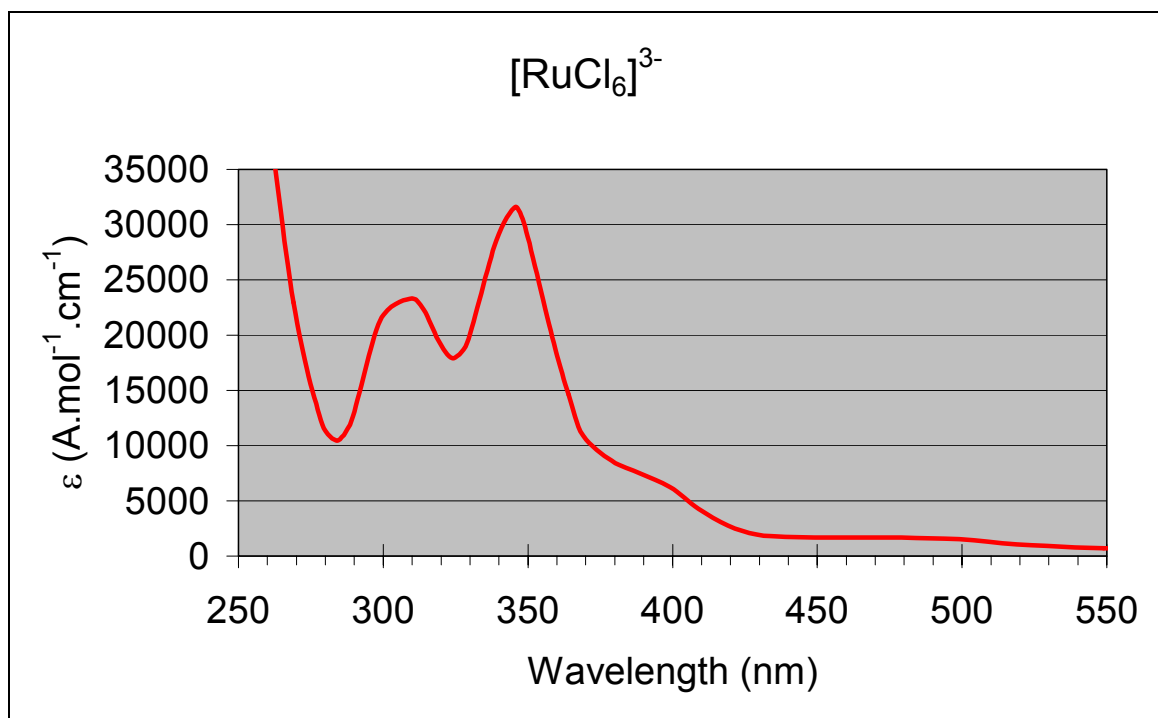
Figure 1-19: UV/Vis spectrum of $[RuCl_6]^{3-}$, redrawn from Adamson. [9]

Adamson[33] reported values for k_{65}, the aquation rate constant for $[RuCl_6]^{3-}$, calculated from isotopic exchange data, at different HCl concentrations.

Table 1-4: Reported values for the aquation rate constant for $[RuCl_6]^{3-}$, k_{65}, at 25°C. [33]

HCl (M)	k_{65} (s^{-1})
11.75	1.7×10^{-3}
11.3	1.8×10^{-3}
9.25	2.2×10^{-3}
7.8	2.9×10^{-3}
6.0	4.6×10^{-3}
1.0	6.7×10^{-2}

The rate constant shows a decrease in rate of aquation with increasing HCl concentration, which concurs with Fine's data[24] that shows an increase in the equilibrium constant, K_6, above 6M HCl. The equilibrium constant K_6 is defined as k_{56}/k_{65}.

For the aquation/anation of ruthenium(III) in chloride media Fine[24] reported the equilibrium constants (table 1-5) in his thesis. There is a significant increase in K_5 at 6M HCl strength and there are no values for K_5 and K_6 at HCl concentrations below 4M HCl nor are there values for K_5 above 6M HCl. The speciation diagram (figure 1-20) thus shows the concentrations of $[RuCl_6]^{3-}$ and $[RuCl_5(H_2O)]^{2-}$ below 4M and of $[RuCl_4(H_2O)_2]^-$ above 6M as 0%. The concentration of $[RuCl_3(H_2O)_3]$ above 3M is also shown as 0%. Fine concluded that the concentration of $[RuCl_6]^{3-}$ in 11 and 12M HCl is 100%.

Table 1-5: Equilibrium constant values. [24]

HCl (mol.l^{-1})	K_2 (M^{-1})	K_3 (M^{-1})	K_4 (M^{-1})	K_5 (M^{-1})	K_6 (M^{-1})
0.05	32.26	26.32			
0.1	2.78	2.63			
1			0.87		
2			0.9		
3			0.76		
4				0.116	0.172
5				0.154	0.145
6				1.111	0.185
7				-	0.435
8				-	0.5
9				-	0.625
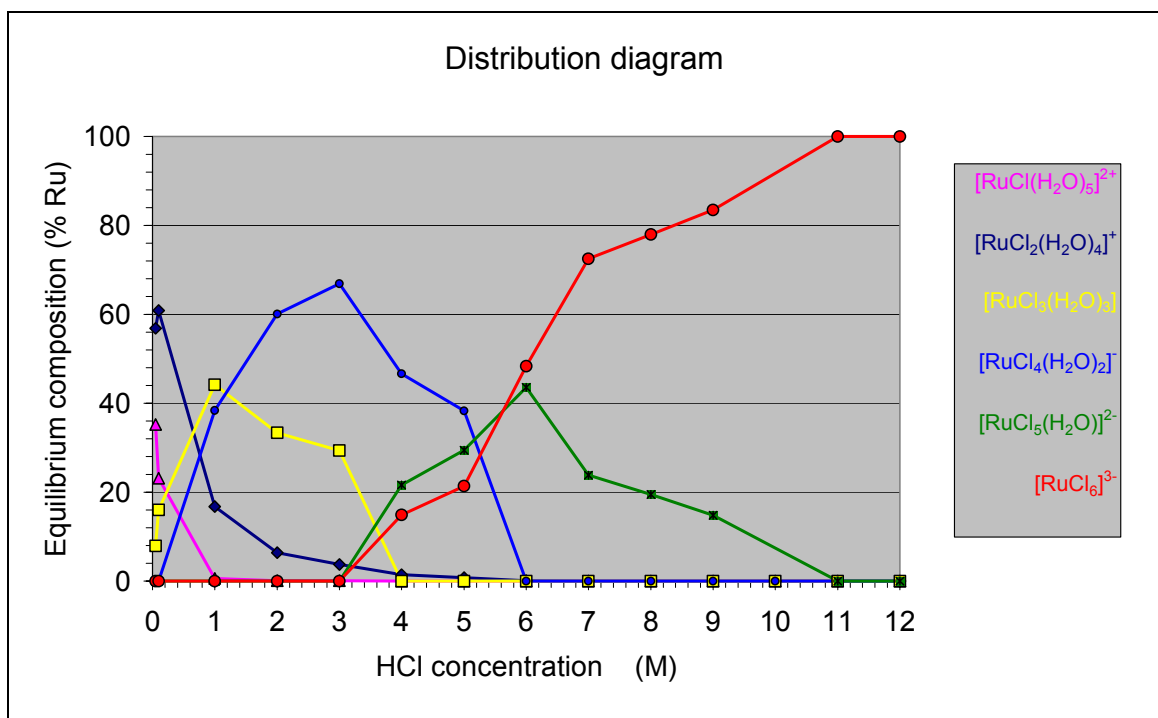
Figure 1-20: Distribution diagram, redrawn from Fine. [24]

Connick[21] reported the equilibrium constants for the $[RuCl_{6-n}(H_2O)_n]^{n-3}$ series:

Table 1-6: Equilibrium constant data. [21]

Reaction	K (M^{-1})	Ionic strength (M)
$[RuCl(H_2O)_5]^{2+} + Cl^- \rightleftharpoons [RuCl_2(H_2O)_4]^+ + H_2O$	~30	0.1
$[RuCl_2(H_2O)_4]^+ + Cl^- \rightleftharpoons [RuCl_3(H_2O)_3] + H_2O$	2.7	0.1
$[RuCl_3(H_2O)_3] + Cl^- \rightleftharpoons [RuCl_4(H_2O)_2]^- + H_2O$	0.8	3
$[RuCl_4(H_2O)_2]^- + Cl^- \rightleftharpoons [RuCl_5(H_2O)]^{2-} + H_2O$	~0.14	5
$[RuCl_5(H_2O)]^{2-} + Cl^- \rightleftharpoons [RuCl_6]^{3-} + H_2O$	~0.1	5

These equilibrium constants were used to construct a distribution diagram for the series (figure 1-21). In 12M hydrochloric acid the $[RuCl_6]^{3-}$ species account for 41.97% of the total ruthenium present while $[RuCl_5(H_2O)]^{2-}$ and $[RuCl_4(H_2O)_2]^-$ accounts for 34.98% and

20.82% respectively.   The balance is made up by $[RuCl_3(H_2O)_3]$ (2.17%) and $[RuCl_2(H_2O)]^+$ (0.07%).

This distribution diagram differs from that of Fine[24] in that the concentration of $[RuCl_6]^{3-}$ in 12M HCl is 41.97%.   Fine does note, however, that due to the high electrolyte concentrations of the solutions, the activities of the solutions could cause the values of the constants above 4M HCl to be inaccurate.   Connick does not discuss how the problems with the activity of chloride were overcome in the determination of equilibrium values he reports.   Fine's thesis was published in 1958 and Connick's paper, published in 1961, credits Fine and Mercer with the results presented on Ru(III) kinetics.   From this information it is clear that Fine, with Mercer and Connick, continued his research into the kinetics of Ru(III) aqua-chloro species.   Fine's distribution diagram looks uneven because of the large increases in the values of the equilibrium constant values with increasing chloride concentration.
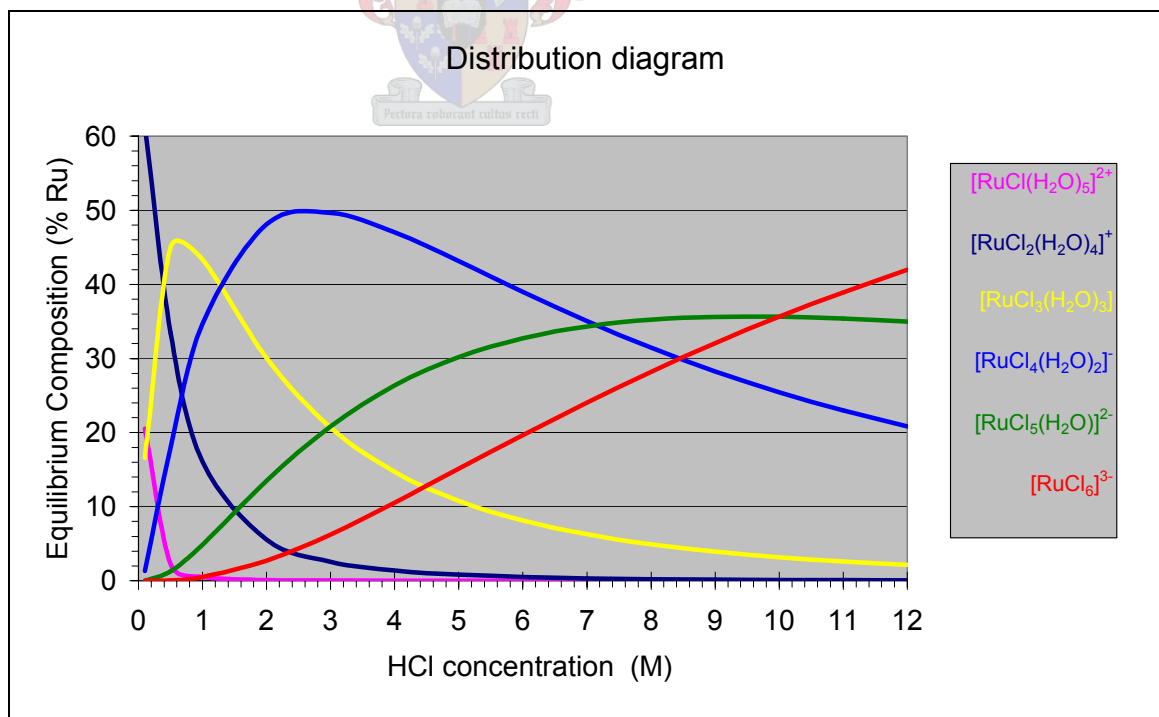
Figure 1-21: Distribution diagram for $[RuCl_{6-n}(H_2O)_n]^{n-3}$, compiled from Connick.[20]

1.5 PROBLEM INVESTIGATED

The more aquated species of the series have been studied by Connick[21] and others[22, 23, 25, 34, 35, 36].   From Connick's[21] distribution diagram it can be seen that the concentration of the cationic complexes is very low in solutions higher than 1 M HCl.   PGM refining makes use of hydrochloric acid solutions in which the pgm are dissolved and then extracted.   These hydrochloric acid solutions are usually of high concentration and from the data available, it is unlikely that the higher aquated cationic species are present in refining solutions in significant concentration.   The discrepancies in the distribution diagrams reported, particularly at the higher HCl concentrations, confirm that an investigation into the speciation of Ru(III) in hydrochloric acid medium is overdue.

Fine[24] reported values for K_6 (as defined in equation 1.2) for the equilibrium between $[RuCl_6]^{3-}$ and $[RuCl_5(H_2O)]^{2-}$ at different hydrochloric acid concentrations.   Adamson quoted values for k_{65} (as defined in equation 1.1) from unpublished data[9] and also from isotopic exchange experiments[33].   There was no further data on the aquation rate constant (k_{65}, as defined in equation 1.1) and no data at all on the anation rate constant, k_{56}.

$$[RuCl_6]^{3-} + H_2O \underset{k_{56}}{\overset{k_{65}}{\rightleftarrows}} [RuCl_5(H_2O)]^{2-} + Cl^-$$ **Equation 1-1**
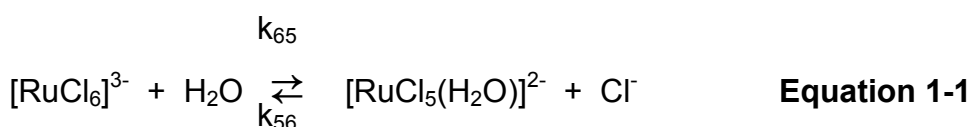
$$K_6 = \frac{\left[[RuCl_6]^{3-}\right]}{\left[[RuCl_5(H_2O)]^{2-}\right] \cdot \left[Cl^-\right]}$$ **Equation 1-2**

The papers from Adamson[9, 10, 26] were not published because Connick, his supervisor, accepted a position as vice-chancellor and presumably lost touch with the author.   The fact that crystal data from the studies were reported by Hopkins[27, 30, 31] adds substance to Adamson's

investigation.   There may have been papers on the anation of $[RuCl_5(H_2O)]^{2-}$ that have not been published but their existence could not be confirmed other than being mentioned in Adamson's unpublished papers.

Looking at figure 1-11 that details the known rate constants for the aqua-chloro ruthenate(III) series, the lack of known data between the anionic species is apparent.   In order to study the speciation, the species need to be separated.   The method of separation to be used depend on the speed with which the species equate.   At the start of this study it was known that the kinetics of the anionic species of ruthenium(III) were faster than that of the equivalent rhodium(III) and iridium(III) species.   The unpublished papers from Adamson[9, 10] were obtained but the data, such as the rate constants for the aquation of $[RuCl_6]^{3-}$ and the chloride anation rate for $[RuCl_5(H_2O)]^{2-}$, had to be verified.
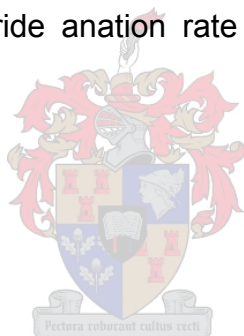
1.6 Background on Techniques Employed

1.6.1 UV/Visible Spectroscopy [12]

Light passing through a sample gets absorbed and the difference between the incident radiation (I_0) and the transmitted radiance (I) is the amount of light absorbed. The amount of light absorbed is expressed as transmittance (T) or absorbance (A). The transmittance is usually expressed as a percentage.

$$\%T = (I/I_0) \times 100 \qquad \textbf{Equation 1-23}$$

$$A = -\log T \qquad \textbf{Equation 1-24}$$

The relationship between the absorbance and both the concentration and path length is usually linear. The Beer-Lambert law shows the relationship between the absorbance of a substance and its concentration.

$$A = \varepsilon bc \qquad \textbf{Equation 1-25}$$

> where
>
> A is the absorbance
>
> ε is the molar absorption or extinction coefficient ($M^{-1}.cm^{-1}$)
>
> b is the path length (cm)
>
> c is the concentration of the substance ($mol.dm^{-3}$)

The extinction coefficient is characteristic of a substance in a precisely defined set of conditions, such as wavelength, solvent and temperature. The extinction coefficients also vary from instrument to instrument.

Beer's law states that the absorbance is proportional to the number of molecules that absorb radiation at the specified wavelength. This holds when more than one absorbing species is present. The absorbance at any wavelength in a mixture is equal to the sum of the absorbance of each component at that wavelength.

$$A_{total} = A_1 + A_2 + \ldots + A_n$$

$$= \varepsilon_1 bc_1 + \varepsilon_2 bc_2 + \ldots + \varepsilon_n bc_n \qquad \textbf{Equation 1-26}$$

To compensate for reflection losses, scattering due to inhomogeneities in the solvent and large molecules, the absorbance through a blank (solvent) is usually compared with the absorbance through the substance.

The kinetics of the reaction may be followed by collecting the absorbance at a chosen wavelength at chosen intervals over a period of time. The data collected can then be mathematically processed to calculate the rate constant for the reaction.
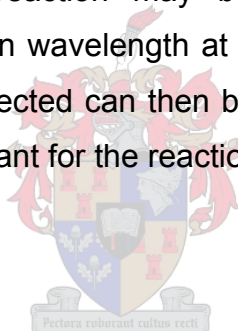
2 EXPERIMENTAL

2.1 CHEMICALS

1. Potassium aquapentachlororuthenate(III), Johnson Matthey, Britain.

2. Hydrochloric acid, 37%, Premium grade, Saarchem.

3. Lithium chloride (anhydrous), UnivAR grade, Saarchem.

4. Potassium chloride, AR Grade, PAL Chemicals.

5. Methanol, CP Grade, Holpro Analytics.

6. Diethylenetriamine, AR grade, Aldrich.

7. Perchloric acid, 70%, Puriss, Fluka.

The potassium aquapentachlororuthenate(III) was dissolved in a 3M hydrochloric acid solution and the UV/Vis spectrum determined. The concentration of the ruthenium in the solution was determined by ICP (Inductively Coupled Plasma) analysis. The diethylenetriamine was made up in a 6M HCl solution to the desired concentration before use.

2.2 PREPARATION OF HEXACHLORORUTHENATE(III) CRYSTALS

In the preparation of potassium hexachlororuthenate(III) James' method[32] was adapted by using $K_2[RuCl_5(H_2O)]$ (1g) as a starting material and 12M HCl (50ml) as the solvent. After KCl (0.9g) was added, crystals in the form of platelets were obtained. Excess KCl precipitated and was visible as white crystals between these platelets as well as conglomerations of KCl and darker material. The darker material might be unreacted $K_2[RuCl_5(H_2O)]$. The recrystallisation will also be influenced by the excess KCl present. The mother liquor was

not colourless, as reported by James, and the conclusion is that not all the ruthenium crystallised. Recrystallisation of the product was not successful.

For isolating hexachlororuthenate(III), the trivalent cation diethylenetriammonium is preferred as it is more selective at forming precipitates with trivalent anions, thus ensuring that no other aquachlororuthenate(III) species are precipitated[19]. Diethylenetriammonium hexachlororhodate(III) crystals were prepared by Frank[20] and this method was thought to be viable for precipitation of hexachlororuthenate(III) as the two pgm have certain similarities. The potassium hexachlororuthenate(III) (3.5634g) was dissolved in 12M HCl (100ml) and heated to 75°C while stirring. A 0.48 M diethylenetriamine solution in 6M HCl was added to the ruthenium solution over a period of 6 hours. The solution was allowed to cool to ambient temperature and then left for 12 hours before it was filtered. The crystalline material was washed with ethanol and weighed (3.9792g, yield 99.59%). The sample was investigated under a microscope and conglomerations of small red crystals and a small portion of black crystals were observed. The black crystals could be unreacted aquapentachlororuthenate(III).

2.3 UV/VISIBLE SPECTROSCOPY: EQUIPMENT AND TECHNIQUES USED

The fast rate of the aquation of $[RuCl_6]^{3-}$ (6.7×10^{-2} s^{-1})[9] required the use of stopped-flow equipment to facilitate the measurement of the absorbance over the period of reaction. The use of a spectrophotometer to rapidly acquire spectra was also necessary. The equipment used for the acquisition of the data is listed below:

1.   Selecta Frigiterm −10 waterbath (0°C −100°C, ±0.05°C; pumprate 12 l/min).

2.   Hi-Tech Scientific SFA-20 Rapid Kinetic Accessory[37].

3.   Varian Cary 50 UV/Visible Spectrophotometer.

A Hi-Tech Scientific SFA-20 for stopped-flow rapid kinetics (figure 2-1) was used to follow the reactions.   Features of the SFA-20 include a dead-time of less than 8 ms, temperature control, pneumatic drive injection and variable ratio mixing.   The system was set-up as standard and tested.

Reagents were loaded into reservoir syringes and the drive syringes were filled from these (figure 2-2).   The lines to the cell were loaded and left to reach the desired temperature in the water-cooled umbilical cord.   The pneumatic drive was activated and the cooled reagents in the lines were pushed into the mixing chamber and then into the cell. Mixing of the reagents occurs just before the viewing cell in a mixing chamber, flushing all reagents out of the cell.   When the pneumatic drive stops, automatic acquisition of the data starts.   The cell was placed in a water cooled cell holder that was cooled by the same bath that regulated the umbilical cord.   The path length used on the cell was 2 mm.

The data obtained using this standard set-up showed constant absorbance increases after 15 seconds.   The absorbance increased with every data acquisition.   It was established that bleeding of the reagents from the lines to the cell occurred after this time.   The problem was solved by moving the mixing point to just after the drive syringes (10 mm line length) by inserting a T-piece in the line.   The mixed reagent line was then lengthened (2 m), to improve mixing, before joining it to a reagent line going into the umbilical cord.   The second reagent line was blocked off.   The waste reagents line was disconnected from the waste syringe and led into a waste container.

Figure 2-1: The SFA-20†. [37]
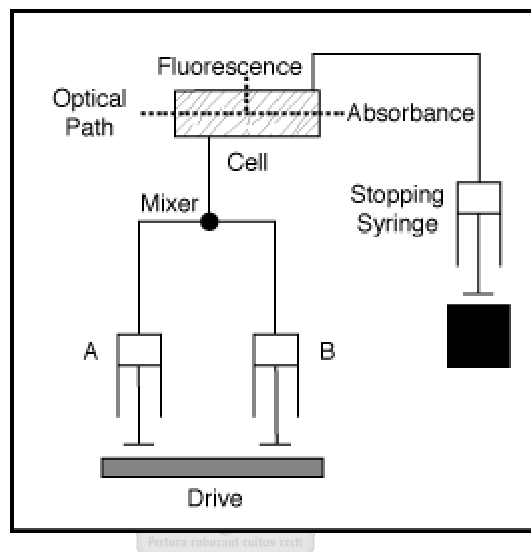
Figure 2-2: Graphical representation of the flow in the SFA-20†. [37]

After this set-up was tested at 21°C in a temperature controlled room, the temperature control of the reaction was addressed. The whole system was placed into a cooler box and the 2 m mixed reagent line was connected to copper tubing that was cooled by the same bath that cooled the umbilical cord. For measurements at low temperatures, ice bricks were placed in the cooler box to maintain the temperature prior to injection. Once the reaction was in progress, the thermostatted cell

---

† Reproduced with the permission of Hi-Tech Scientific, United Kingdom.

holder controlled the temperature of the cell and the reacting mixture. The reagents were kept in the water bath to equilibrate prior to loading the reservoir syringes.

In order to prevent condensation on the cell windows, the spectrophotometer chamber was purged with instrument grade nitrogen for the duration of runs.

Beer's law of additive absorptions was used to determine the spectrum of mixtures of $[RuCl_6]^{3-}$ and $[RuCl_5(H_2O)]^{2-}$ (figure 2-3), using molar extinction coefficients determined on the Cary 50 Spectrophotometer. The concentration values were calculated according to the theoretical percentage aquation that took place.

Figure 2-3: Predicted aquation spectra for $[RuCl_6]^{3-}$ using Beer's law of additive absorptions.

2.3.1.1 Manipulation of data

A full spectrum was collected over a wavelength range of 290 nm to 450 nm. The Cary 50 Spectrophotometer software is very versatile in how the data is collected. The time over which a signal is averaged can be selected and an increased average time will result in a smoother signal. The Cary 50 us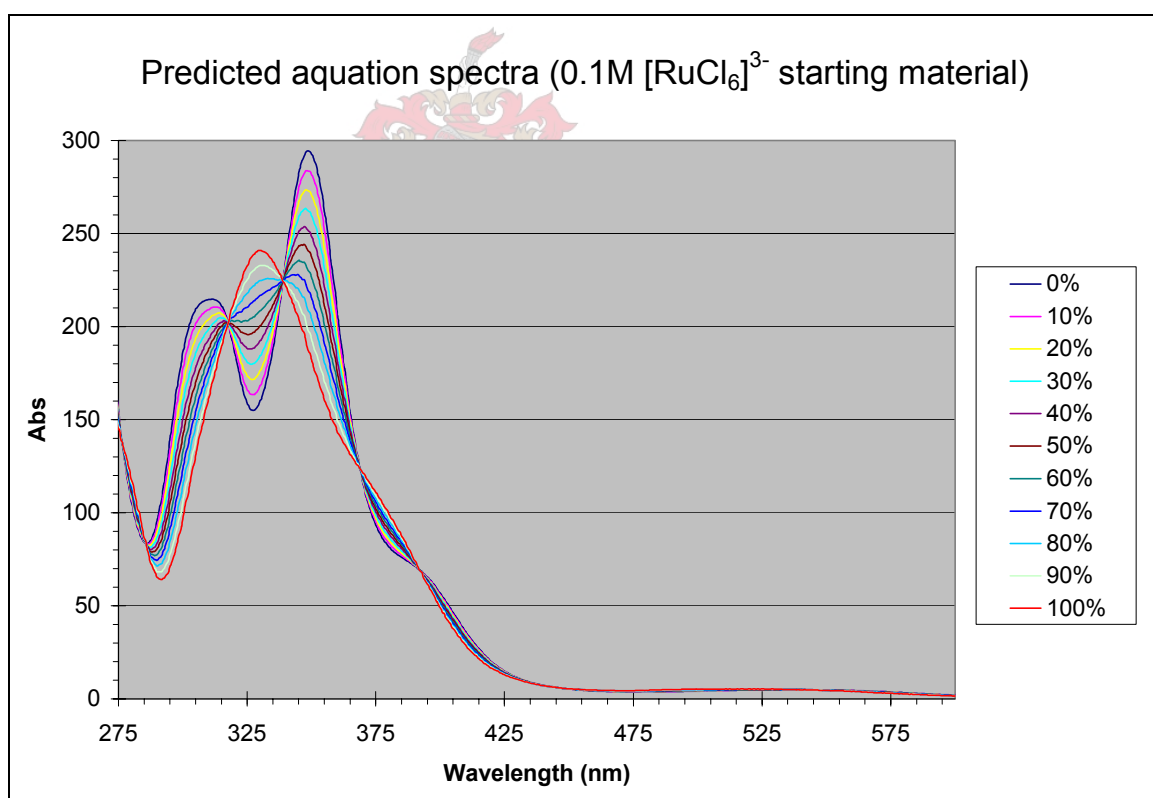es a Xenon flash lamp with an average flash time of 0.0125 seconds. The interval, which can be individually set, sets the number of measurements over a fixed wavelength range. For a scan to be completed more quickly, the interval needs to be increased. The "Advanced Collect" feature allows for different stages to be selected and this allows for variation in the data collection rates within one kinetic run (table 2-1). In these stages the cycle time can be selected. The cycle time, in minutes, is the rate at which the system will cycle the specified setup. The stop time, in minutes, is the amount of time an analysis will continue.

The various parameters for the Varian WinUV software for the runs done in this study were as follows: average time = 0.1 s, interval = 2 nm and scan rate = 1200 nm/min.

Table 2-1: Data collection periods.

Stage	Cycle (min)	Stop (min)
1	0.2	5.0
2	2.0	120.0
3	10.0	600.0

The absorbances of the spectra collected were then plotted against time, at a selected wavelength, using the Cary software. The wavelengths used in this study were 349 nm and 329nm, which correspond to the absorption maxima for $[RuCl_6]^{3-}$ and $[RuCl_5(H_2O)]^{2-}$, respectively. Following aquation of $[RuCl_6]^{3-}$ the product of the

aquation, $[RuCl_5(H_2O)]^{2-}$, itself aquates.   Plotting the absorbance at 329nm against time, the time (t) at which the formation of $[RuCl_5(H_2O)]^{2-}$ reaches a maximum can be determined.   Assuming 100% $[RuCl_6]^{3-}$ at time 0 s and 0% at the end time, the percentage $[RuCl_6]^{3-}$ remaining versus time was plotted.   A straight line was fitted to the plot of the log(%$[RuCl_6]^{3-}$ remaining) versus time.   Using this equation for the fitted straight line, the half life time ($t_{\frac{1}{2}}$) could be determined from which the aquation rate constant was calculated.   A similar approach was used to determine the anation rate constant.
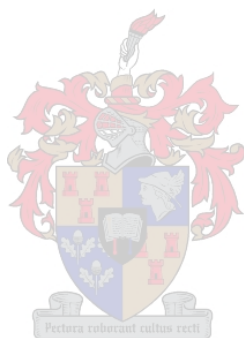
3 RESULTS AND DISCUSSION

3.1 DIETHYLENETRIAMINE HEXACHLORORUTHENATE(III) CRYSTALS

Diethylenetriammonium hexachlororuthenate(III) crystals were prepared (see paragraph 2.2) and investigated under a microscope and found to be conglomerates of small red crystals.   A small amount of black crystals was noted and is thought to be unreacted potassium aquapentachlororuthenate.   In order to characterise the compound that was crystallised, a sample was submitted for CHN analysis and x-ray crystallography[38].

Micro analysis on a sample of the crystals was performed and the amount of C, H and N were determined.   The analysis results are listed in table 3-1.

Table 3-1: Results of the CHN analysis on the diethylenetriamine hexachlororhuthenate(III) crystals ($C_4H_{16}Cl_6N_3Ru$).

	Calculated for $C_4H_{16}Cl_6N_3Ru$	Found
% C	11.44%	11.22%
% N	10.00%	9.46%
% H	3.84%	3.55%

The diethylenetriamine hexachlororuthenate(III) crystal used for x-ray crustallography was not of a high quality and thus the results from the analysis showed high variances, resulting in high final R indices.   The data from the characterisation is shown in table 3-2 and additional data is given in Appendix A.

Table 3-2: Crystal data and structure refinement for diethylenetriamine hexachlororuthenate(III) compared to diethylenetriamine hexachlororhodate(III)[20].

Empirical formula	$C_4H_{16}Cl_6N_3Ru$	$C_4H_{16}Cl_6N_3Rh$
Formula weight	419.97 g.mol^{-1}	421.81 g.mol^{-1}
Temperature	203(2) K	293(1) K
Wavelength	0.71073 Å	0.71073 Å
Crystal system, Space group	Monoclinic, Cc	C2/c
Unit cell dimensions	a = 31.015(6) Å	a = 30.956(4) Å
	b = 7.3506(15) Å	b = 7.371(2) Å
	c = 13.053(3) Å	c = 12.9736(15) Å
	β = 114.82(3)°	β = 113.787(11)°
Volume	2701.1(9) Å^3	2708.7(8) Å^3
Z	8	8
Calculated density	2.065 mg.m^{-3}	-
Absorption coefficient	2.317 mm^{-1}	-
Crystal size	0.10 x 0.10 x 0.05 mm	0.15 x 0.1 x 0.12 mm
Limiting indices	$-39 \leq h \leq 40$	$-1 < h < 37$
	$-9 \leq k \leq 9$	$-9 < k < 8$
	$-16 \leq l \leq 16$	$-15 < l < 14$
Final R indices	R1 = 0.1017	R1 = 0.0271
	wR2 = 0.2333	wR2 = 0.0279
R indices (all data)	R1 = 0.1265	
	wR2 = 0.2469	wR2 = 0.0301

The average Ru-Cl bond length for the diethylenetriamine hexachlororuthenate(III) crystal was 2.371 ($\pm$ 0.028) Å. The average bond length for Ru-Cl in the hexaaquaaluminium hexachlororuthenate(III) tetrahydrate[31] was 2.375 ($\pm$ 0.008) Å and in

diethylenetriamine hexachlororhodate(III)[20] the average bond length for Rh-Cl was 2.350 ($\pm$ 0.009) Å.

The final R-indices are high because of the poor crystal quality and there are two crystallographic independent molecules, A and B (figure 3-1) with poor crystallographic agreement between their chemically equivalent bond lengths due to poor structure resolution. The counter-ion, diethylenetriamine, suffered high thermal motions and is possibly disordered and the hexachlororuthenate(III) cation is in pseudo-octahedral. The cation bond angles are not 90° but are all slightly larger or smaller than 90°, meaning that the octahedron is slightly distorted and the Ru-Cl bond lengths between *trans* chloride ligands are not equal (see Appendix A, table A-2). The crystal packing along the b and c axes are shown in figures 3-2 and 3-3.
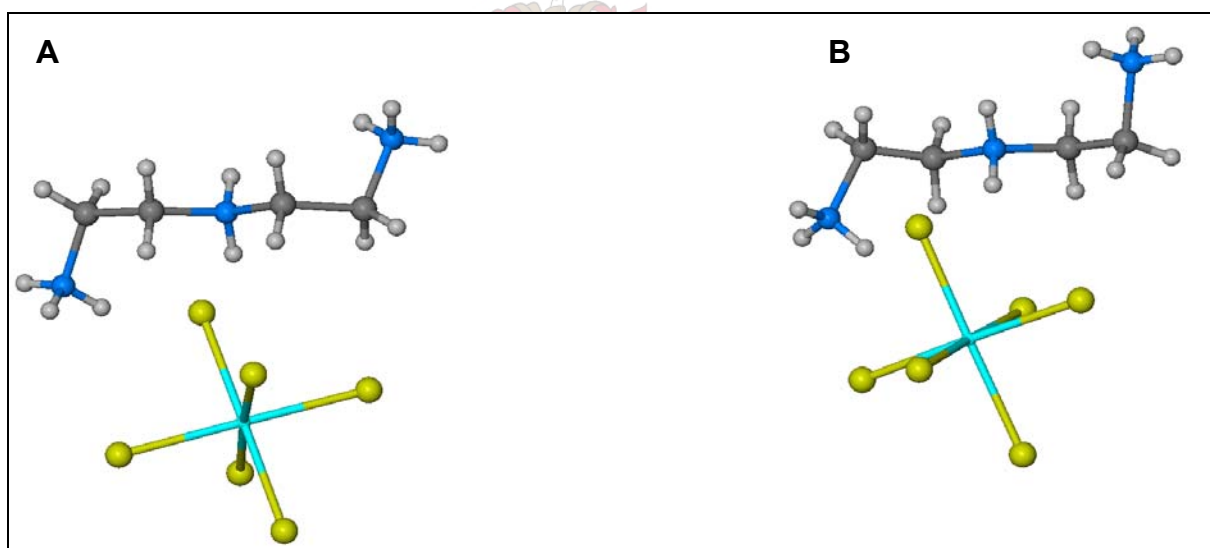

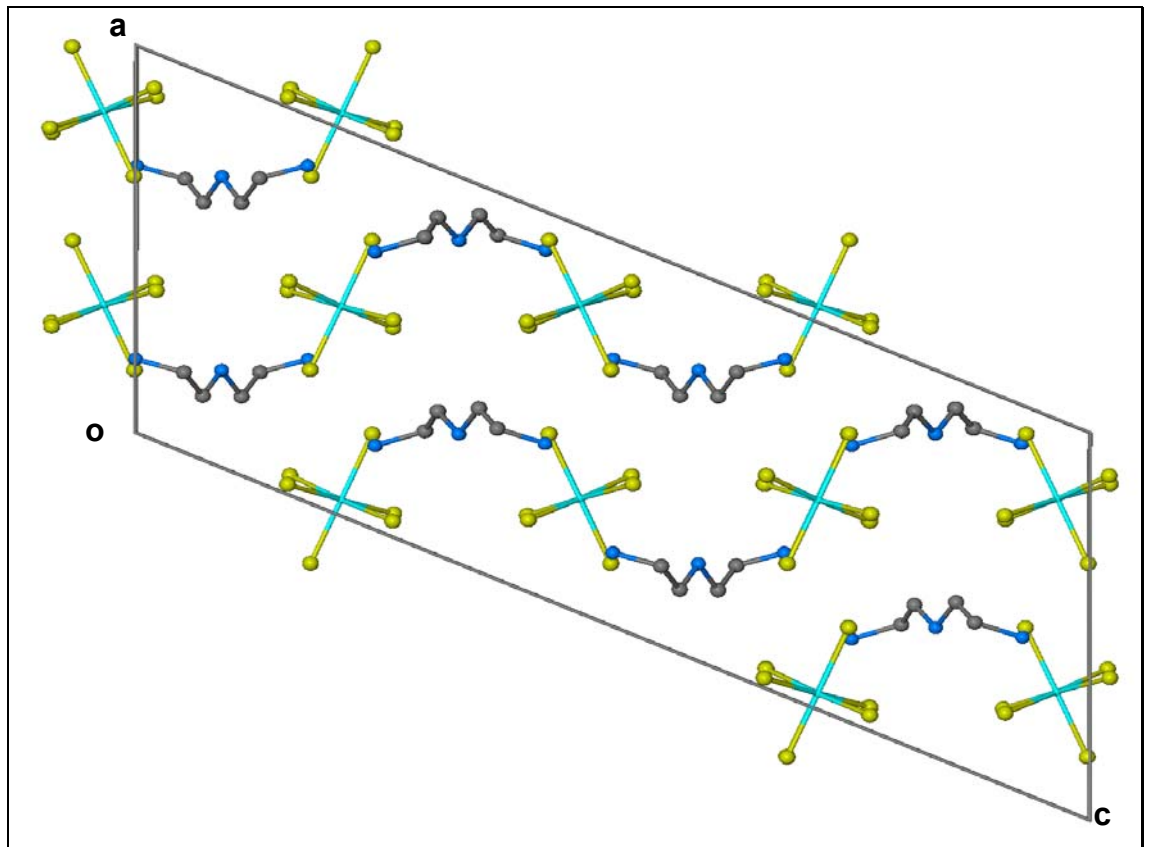**Figure 3-1:** The two crystallographic independent molecules.
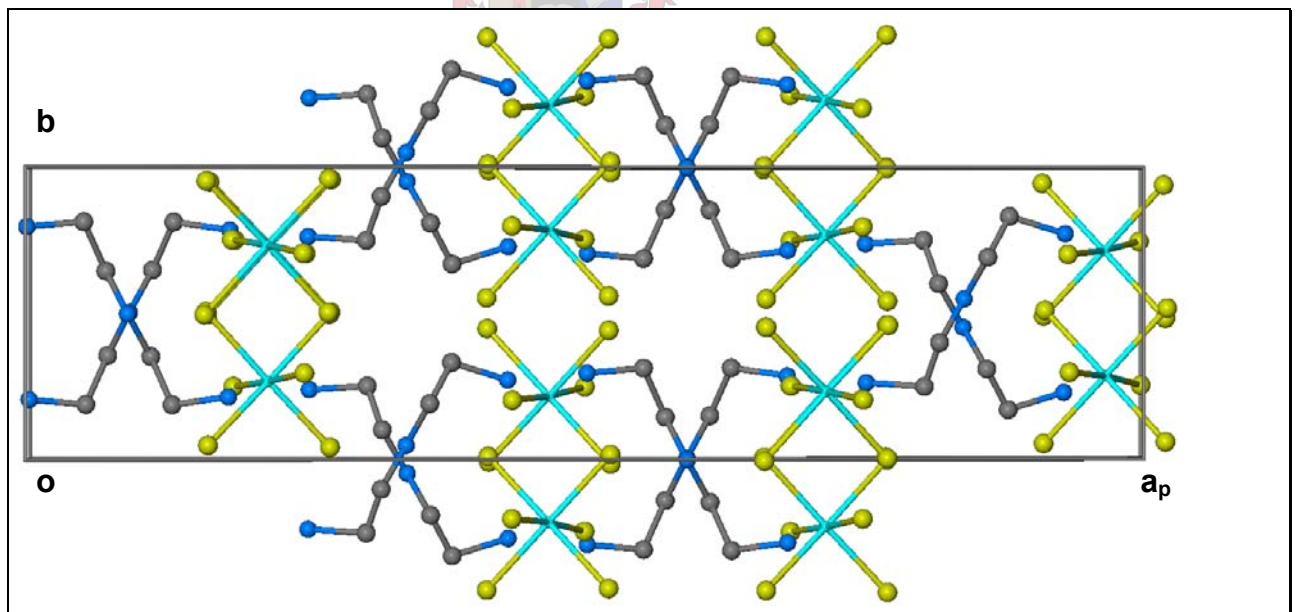
Figure 3-2: The crystal packing, viewed along the b-axis.

Figure 3-3: The crystal packing, viewed along the c-axis.

3.2   KINETICS, RATE CONSTANTS AND EQUILIBRIUM CONSTANTS

3.2.1   The effect of temperature on the rate constants of aquation of $[RuCl_6]^{3-}$ and of the anation of $[RuCl_5(H_2O)]^{2-}$

The aquation of $[RuCl_6]^{3-}$ and the chloride anation of $[RuCl_5(H_2O)]^{2-}$ was investigated at 25°C, 21°C, 10°C and 5°C.   The tables and graphs containing all the individual experimental information and information on the standard deviation calculations are available in Appendix B. The aquation (k_{65}) and chloride anation (k_{56}) rate constants determined are summarised in the table 3-3.

Table 3-3: Summary of the data collected for the aquation of $[RuCl_6]^{3-}$ (k_{65}) and the chloride anation of $[RuCl_5(H_2O)]^{2-}$ (k_{56}).

	Temp (°C)	5.0	10.0	21.0	25.0
	$(1/T) \times 10^3$ (K^{-1})	3.60	3.53	3.40	3.35
Aquation	$k_{65} \times 10^{-3}$ (s^{-1})	3.90 (±0.24)	7.37 (±0.48)	31.4 (±2.0)	53.0 (±3.7)
Anation	$k_{56} \times 10^{-3}$ (M^{-1}.s^{-1})	0.129 (±0.0087)	0.240 (±0.017)	1.03 (±0.069)	1.61 (±0.11)
K_6 (M^{-1})		0.0331 (±0.0030)	0.0326 (±0.0031)	0.0318 (±0.0029)	0.0311 (±0.0030)

From the regression lines, calculated using the rate constants in table 3-3, the values for k_{65}=52.1 (±3.7) x10^{-3} s^{-1} and k_{56}=1.62 (±0.11) x10^{-3} M^{-1}s^{-1} at 25°C are obtained.   The value of K_6 at 25°C can then be calculated from equation 1-7 as 0.0311 (± 0.0030) M^{-1}.
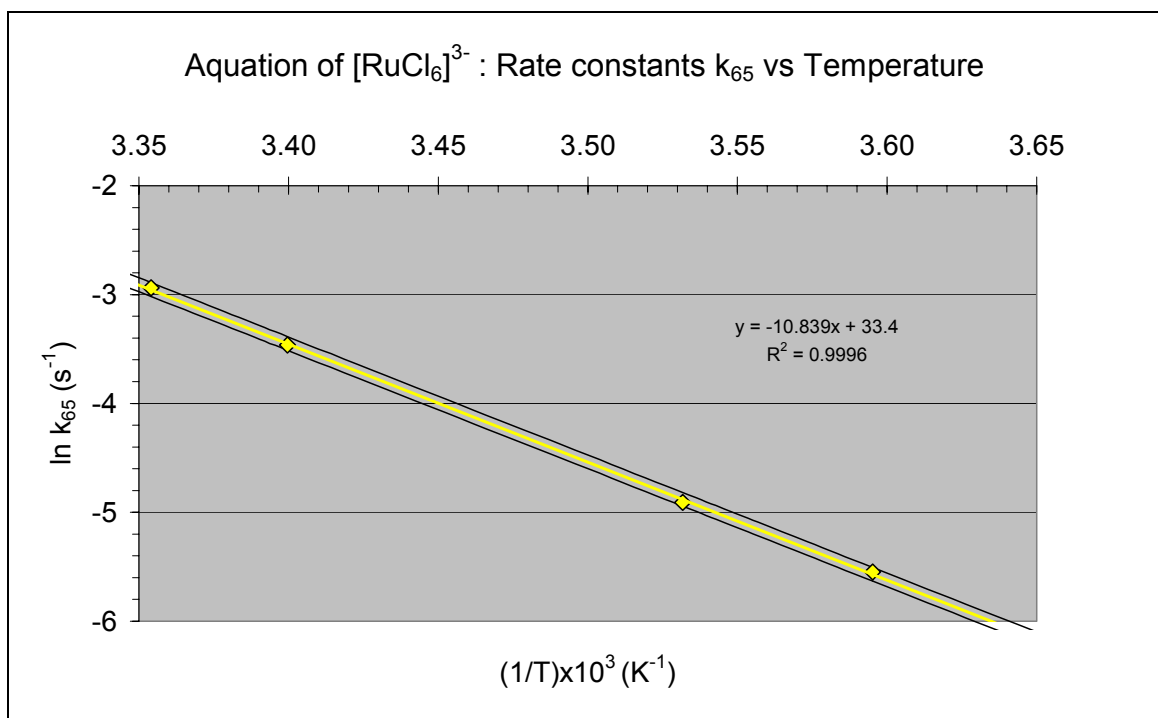
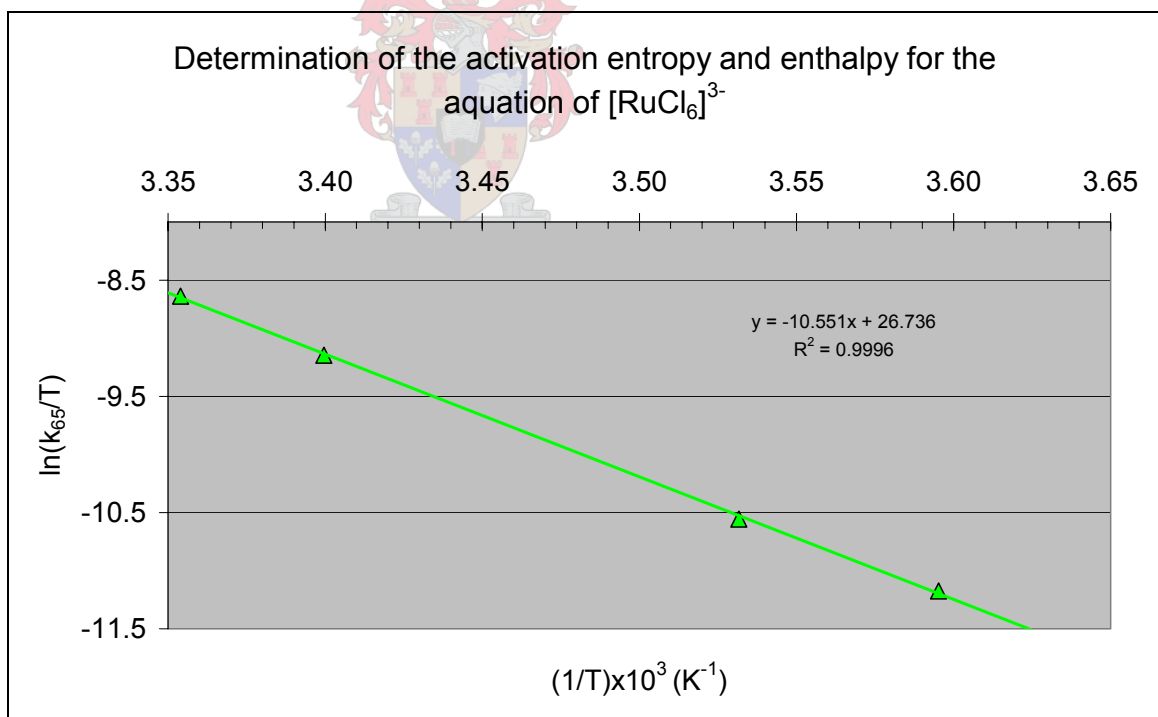**Figure 3-4:** Rate constants (k_{65}) versus temperature for the aquation of $[RuCl_6]^{3-}$.

Figure 3-5: Plot of $\ln(k_{65}/T)$ versus temperature for the aquation of $[RuCl_6]^{3-}$.

The thermodynamic values of the aquation and anation reactions under investigation were calculated (as discussed in paragraph 1.4.2) from the graphs in figures 3-4 to 3-7.

The thermodynamic data calculated for the aquation of $[RuCl_6]^{3-}$:

E_a = 90.1 ($\pm$1.2) kJ.mol^{-1}

A = 3.20 ($\pm$0.52) x10^{14} s^{-1}

$\Delta H^{\ddagger}$ = 87.7 ($\pm$1.2) kJ.mol^{-1}

$\Delta S^{\ddagger}$ = 24.7 ($\pm$4.3) J.K^{-1}.mol^{-1}

The standard free energy of activation can be calculated at a specific temperature as follows:

$\Delta G^{\ddagger}$ = $\Delta H^{\ddagger}$ - T($\Delta S^{\ddagger}$)
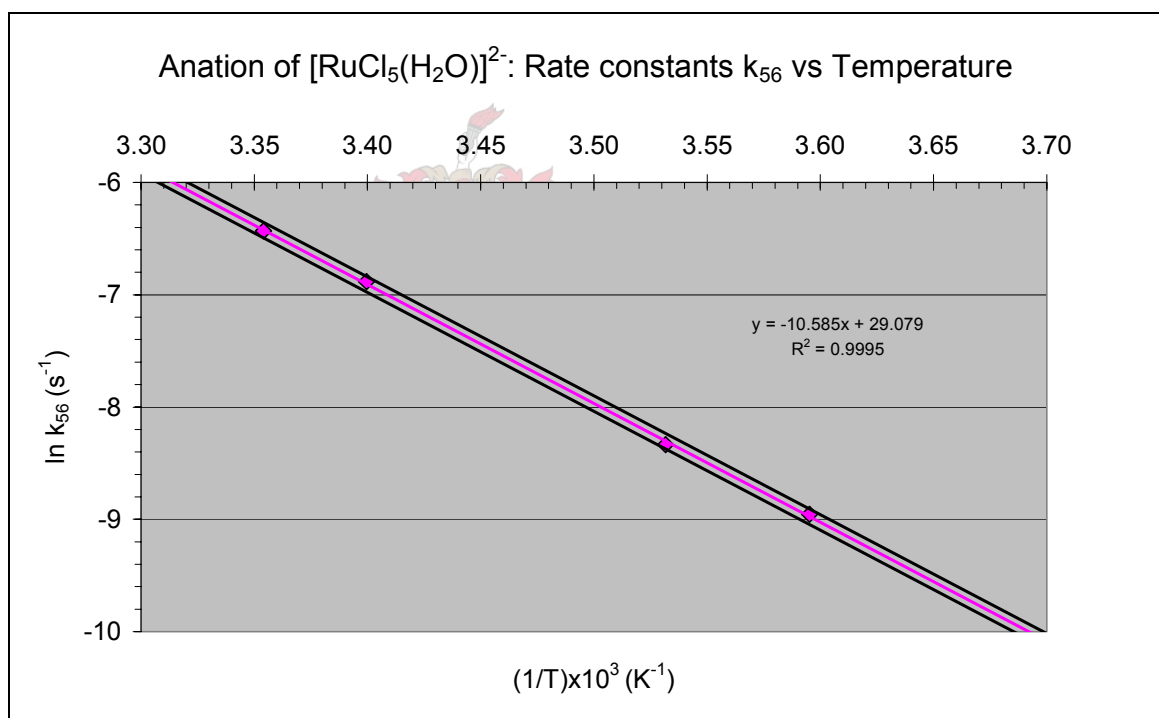
$\Delta G^{\ddagger}$ = 80.4 ($\pm$1.2) kJ.mol^{-1} at 25°C

Figure 3-6: Rate constants (k_{56}) versus temperature for the chloride anation of $[RuCl_5(H_2O)]^{2-}$.
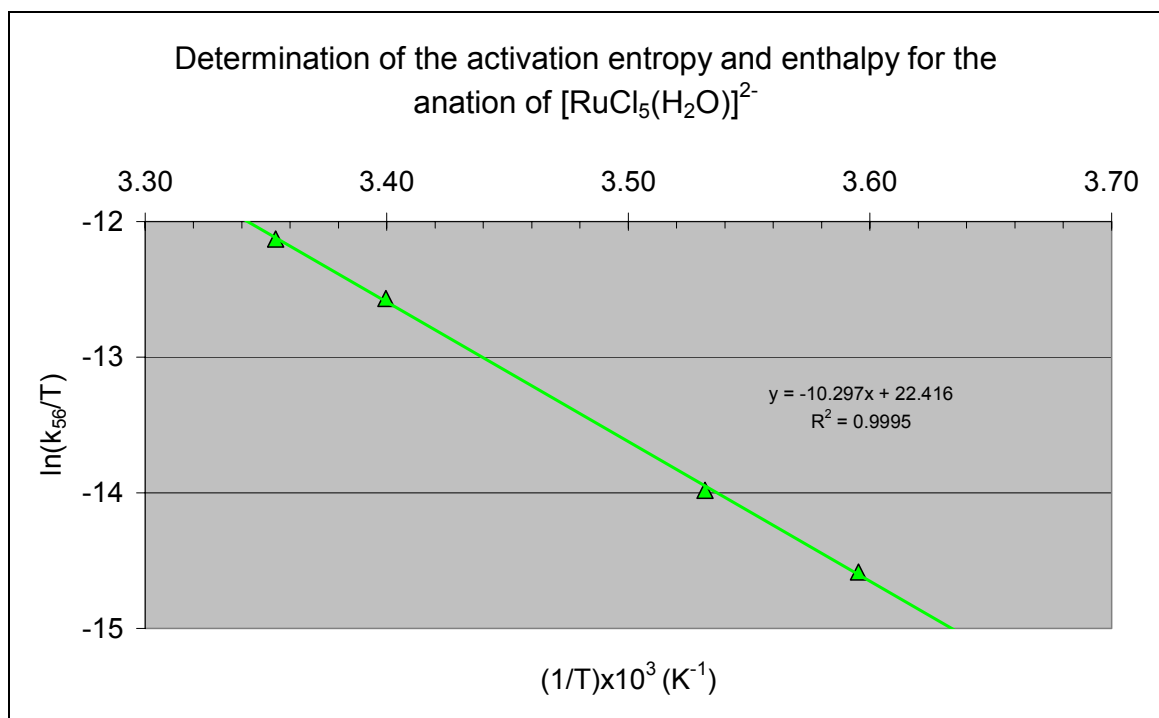
Figure 3-7: Plot of $\ln(k_{56}/T)$ versus temperature for the chloride anation of $[RuCl_5(H_2O)]^{2-}$.

The thermodynamic data calculated for the anation of $[RuCl_5(H_2O)]^{2-}$:

E_a = 88.0 ($\pm$1.4) kJ.mol^{-1}

A = 4.26 ($\pm$0.6) x10^{12} s^{-1}

$\Delta H^{\ddagger}$ = 85.6 ($\pm$1.4) kJ.mol^{-1}

$\Delta S^{\ddagger}$ = -11.2 ($\pm$4.7) J.K^{-1}.mol^{-1}

$\Delta G^{\ddagger}$ = 87.0 ($\pm$1.4) kJ.mol^{-1} at 25°C

From the thermodynamic values that were determined it is possible to compare the Gibbs energy values and see that it is more favourable to form the aquation reaction products than the anation reaction products.

3.2.1.1 Comparison of data from this study for the aquation of $[RuCl_6]^{3-}$ with Adamson

The aquation rate constant determined in this study was compared to the aquation rate constant in Adamson's unpublished papers because

there was no other value available in literature. A comparison between the data obtained in this study and that of Adamson[9] can be seen in figures 3-8 and 3-9.
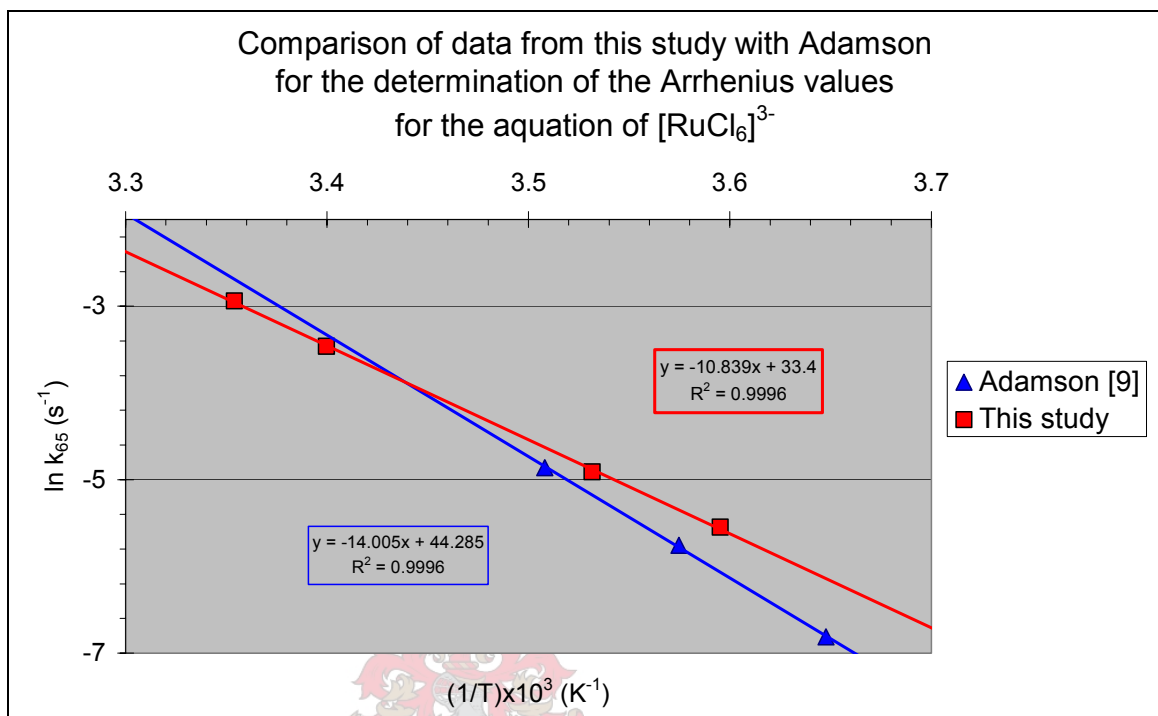

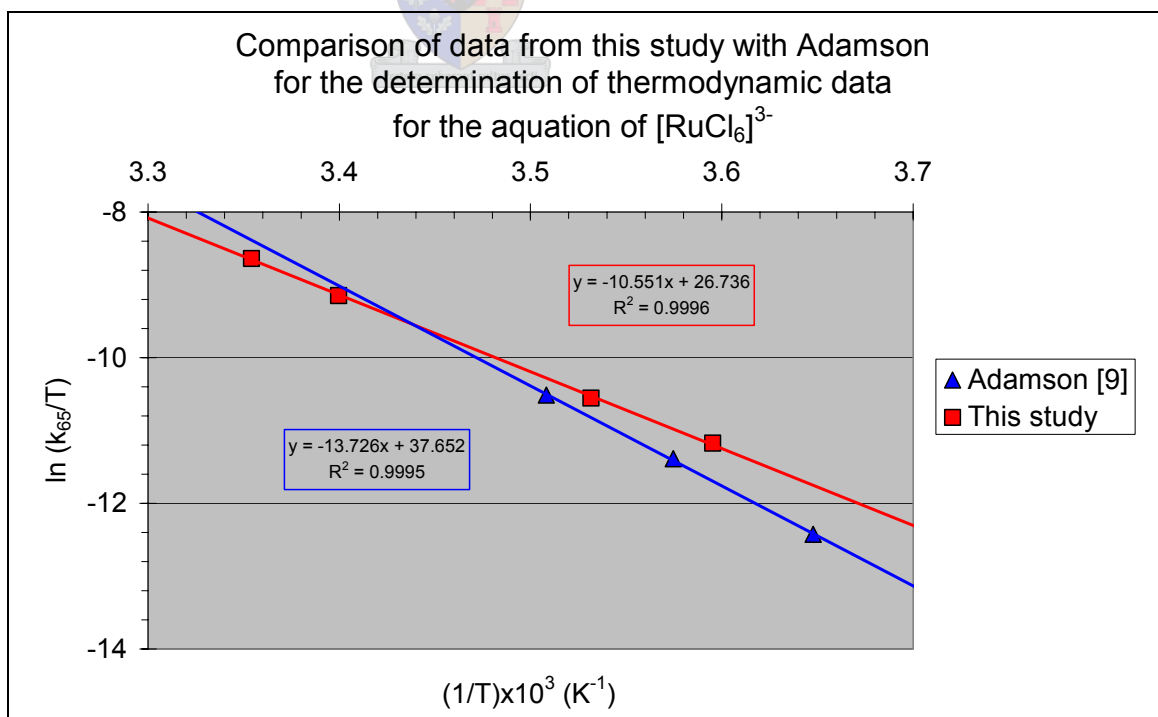**Figure 3-8:** Comparison of k_{65} versus 1/T for Adamson[9] and this study.

Figure 3-9: Comparison of k_{65}/T versus 1/T for Adamson[9] and this study.

The data in table 3-4 were calculated from figures 3-8 and 3-9 and compares data from this study with that of Adamson's unpublished data[9].

Table 3-4: A direct comparison of the data from Adamson[9] and this study.

	Adamson[9]	This study
k_{65} (s^{-1}) at 25°C	6.80 (±0.012) $\times 10^{-2}$	5.21 (±0.37) $\times 10^{-2}$
E_a $(kJ.mol^{-1})$	116.4 (±1.4)	90.1 (±1.2)
A (s^{-1})	1.71 (±0.6) $\times 10^{19}$	3.20 (±0.5) $\times 10^{14}$
$\Delta H^{\ddagger}$ $(kJ.mol^{-1})$	114.1 (±1.4)	87.7 (±1.2)
$\Delta S^{\ddagger}$ $(J.K^{-1}.mol^{-1})$	115.5 (±5.0)	24.7 (±4.3)
$\Delta G^{\ddagger}$ $(kJ.mol^{-1})$ at 25°C	79.7 (±1.5)	80.4 (±1.2)

The rate constant for the aquation of $[RuCl_6]^{3-}$ (k_{65}) determined in this study is smaller than the value determined by Adamson[9] at 25°C and they are not within experimental error. At 25°C the lines (figure 3-9) are close to their intercept (290.9K) and therefore the best comparison between the rate constants will be around the intercept. Adamson manually inserted reagents into the viewing cell of the spectrophotometer before mixing the reagents with air, in-situ, while in this study a stopped-flow kinetics accessory (SFA-20, figure 2-1) with a dead-time of less than 8ms were used. The use of this equipment will increase the reproducibility of the experimental results. The thermodynamic constants of the two studies do not compare well but the Gibbs free energies do compare well. The difference between the values determined in this study and that determined by Adamson could be due to the way the data was determined, manually versus automatic injection.

3.2.1.2 Comparison of the rate constants of ruthenium(III), rhodium(III) and iridium(III)

The rate of aquation of $[RuCl_6]^{3-}$ and the rate of anation of $[RuCl_5(H_2O)]^{2-}$ was compared to the analogous reactions of iridium(III) and rhodium(III) because of close proximity of these elements in the periodic table and other similarities that have been reported.   The data for the aquation of $[MCl_6]^{3-}$ data is compiled in table 3-5 and figures 3-10 and 3-11 and the chloride anation of $[MCl_5(H_2O)]^{2-}$ in table 3-6 and figures 3-12 and 3-13.

Table 3-5: Data for the aquation of $[MCl_6]^{3-}$.

Ru(III)	Temp (°C)	5.0	10.0	21.0	**25.0**
	$(1/T) \times 10^3$	3.60	3.53	3.40	**3.35**
	$k_{65} \times 10^{-3}$ (s^{-1})	3.82	7.6	31.8	**52.1**
Rh(III) [39]	Temp (°C)	-	15	20	**25**
	$(1/T) \times 10^3$	-	3.47	3.41	**3.35**
	$k_{65} \times 10^{-3}$ (s^{-1})	-	0.43	1.1	**1.8**
Ir(III) [14]	Temp (°C)	6	**25**	50.5	-
	$(1/T) \times 10^3$	3.58	**3.35**	3.09	-
	$k_{65} \times 10^{-3}$ (s^{-1})	0.00023	**0.0094**	0.4	-

The aquation rate constant, k_{65}, for Ru(III) is faster than the aquation rate constant of Rh(III), which in turn is faster than that of Ir(III).   A general statement for the aquation rate constants (k_{65}) of the hexachloro species for the metals would be: Ru(III) > Rh(III) > Ir(III).
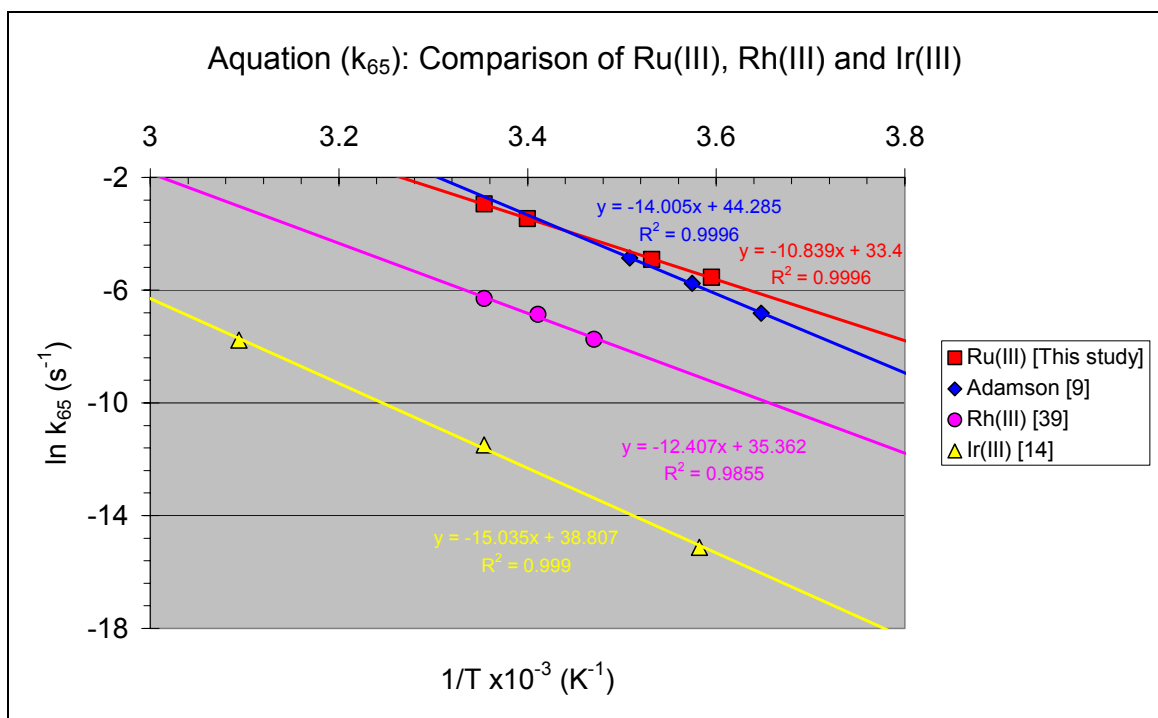
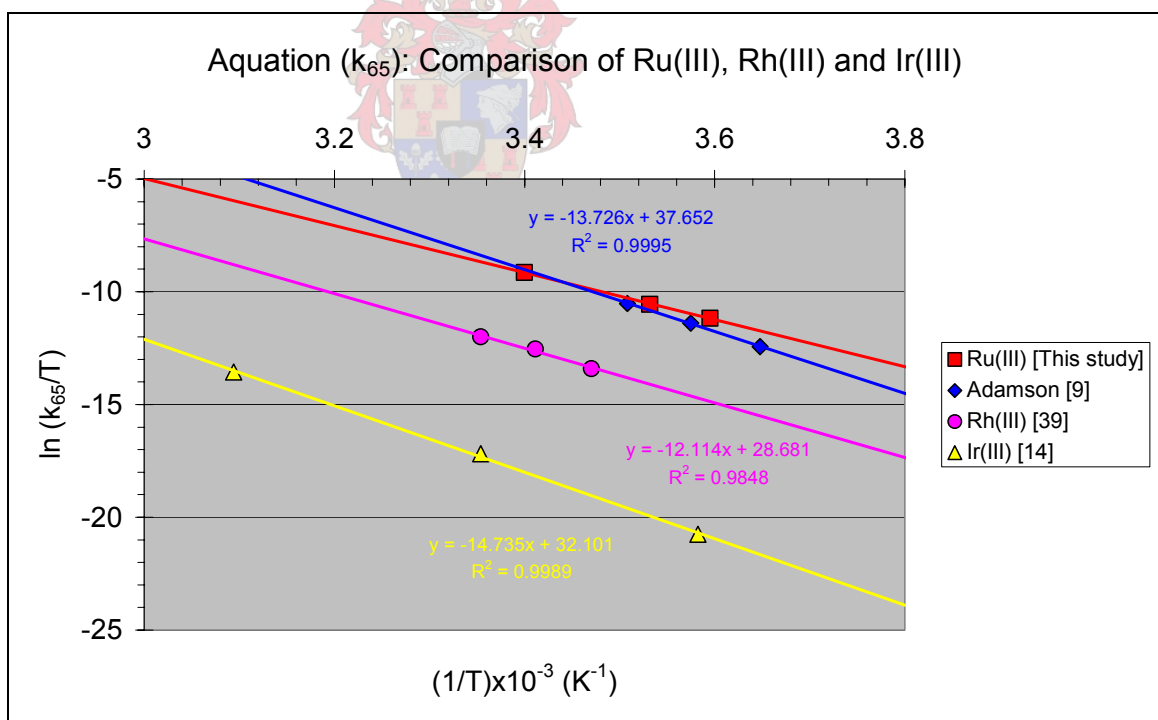**Figure 3-10:** Aquation data comparison for $[MCl_6]^{3-}$, where M = Ru(III), Rh(III) and Ir(III).

Figure 3-11: Aquation data comparison for $[MCl_6]^{3-}$, where M = Ru(III), Rh(III) and Ir(III).

Table 3-6: Data for the chloride anation of $[MCl_5(H_2O)]^{2-}$:

Ru(III)	Temp (°C)	5.0	10.0	21.0	**25.0**
	$(1/T)x10^3$	3.60	3.53	3.40	**3.35**
	$k_{56} \; x10^{-3} \; (s^{-1})$	0.126	0.246	1.00	**1.62**
Rh(III) [39]	Temp (°C)	-	15	20	**25**
	$(1/T)x10^3$	-	3.47	3.41	**3.35**
	$k_{56} \; x10^{-3} \; (s^{-1})$	-	0.083	0.147	**0.22**
Ir(III) [14]	Temp (°C)	-	**25**	50.5	-
	$(1/T)x10^3$	-	**3.35**	3.09	-
	$k_{56} \; x10^{-3} \; (s^{-1})$	-	**0.002**	0.05	-
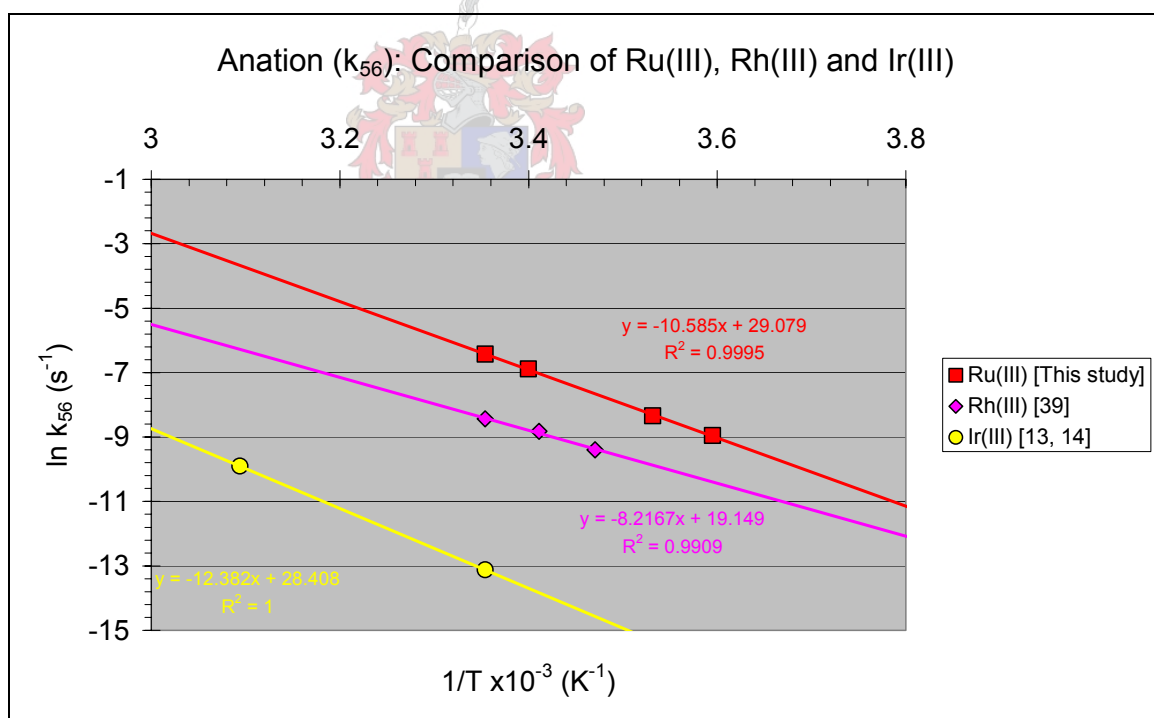
Figure 3-12: Anation data comparison for $[MCl_5(H_2O)]^{2-}$, where M = Ru(III), Rh(III) and Ir(III).
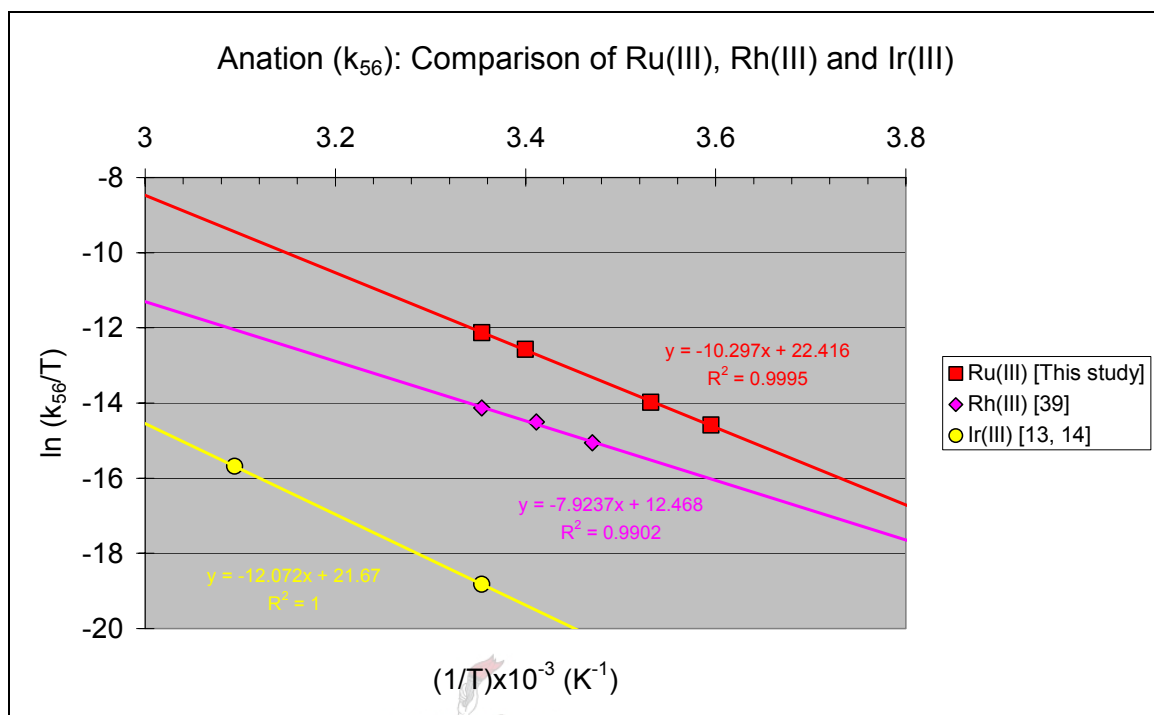
Figure 3-13: Anation data comparison for $[MCl_5(H_2O)]^{2-}$, where M = Ru(III), Rh(III) and Ir(III).

The trend for the aquation rate constants, k_{65}, of the hexachloro metal species is the same as that for the corresponding anation rate constants (k_{56}) of the aquapentachloro species, i.e. Ru(III) > Rh(III) > Ir(III).   The two values for Ir(III) were obtained from different sources[13, 15] and the resulting thermodynamic constants are expected to be an indication of the true values.

The thermodynamic data obtained from the graphs are summarised in table 3-7 below:

Table 3-7: Calculated thermodynamic data for the aquation and anation of Ru(III), Rh(III) and Ir(III).

|		E_a (kJ.mol^{-1})	A (s^{-1})	$\Delta H^{\ddagger}$ (kJ.mol^{-1})	$\Delta S^{\ddagger}$ (J.K^{-1}.mol^{-1})	$\Delta G^{\ddagger}$ (kJ.mol^{-1}) at 25°C
Aquation	Ru(III)	90.1 ±1.24	3.2 (±0.52) x10^{14}	87.7 ±1.23	24.7 ±4.3	80.4 ±1.23
	Rh(III)	103.1 ±7.3	2.2x10^{15}	100.6 ±7.3	40.7 ±0.025	88.5 ±7.3
	Ir(III)	126.9 ±2.5	1.38x10^{17}	124.4 ±2.5	74.8 ±0.0085	102.1 ±2.5
Anation	Ru(III)	88.0 ±1.36	4.26 (±0.57) x10^{12}	85.6 ±1.36	-11.2 ±4.7	87.01 ±1.36
	Rh(III)	68.4 ±3.8	2.11x10^8	65.9 ±3.8	-93.7 ±0.013	93.9 ±3.8
	Ir(III)	102.9 ±5.1	2.17x10^{12}	100.4 ±5.0	-17.4 ±0.89	105.6 ±5.3

The smaller the $\Delta G^{\ddagger}$ value, the smaller the activation barrier for the reaction and therefore less energy is required to form the activated complex and thus the complex. The Gibbs function of activation ($\Delta G^{\ddagger}$) is smaller in the aquation and anation reactions for Ru(III) than for Rh(III) and Ir(III). It therefore follows the trend for $\Delta G^{\ddagger}$ Ru(III) > Rh(III) > Ir(III).

The influence of the temperature on the equilibrium constants for Ru(III) and Rh(III)[39] can be seen in table 3-8 where the equilibrium values decrease with increasing temperature for both elements. The decrease in the equilibrium constants points to the formation of the pentachloro species ($[RuCl_5(H_2O)]^{2-}$) being favoured in the reaction at

equilibrium (equation 1-2)♠ at increased temperature. Although not linear, figure 3-14 graphically shows the definite decrease in the equilibrium constants for Ru(III) and Rh(III) with increasing temperature.

Table 3-8: The equilibrium constant (K_6) values for Ru(III) and Rh(III) at different temperatures.

		Ru(III)	Rh(III)[39]
Temp (°C)	T (K)	K_6 (M^{-1})	K_6 (M^{-1})
5	278.15	0.03312	-
10	283.15	0.03258	-
15	288.15	-	0.1923
20	293.15	-	0.1397
21	294.15	0.03183	-
25	298.15	0.03108	0.1182
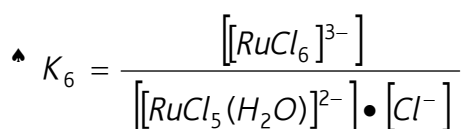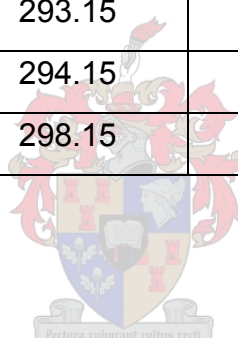
♠ $K_6 = \dfrac{\left[[RuCl_6]^{3-}\right]}{\left[[RuCl_5(H_2O)]^{2-}\right] \bullet \left[Cl^-\right]}$ **Equation 1-2**
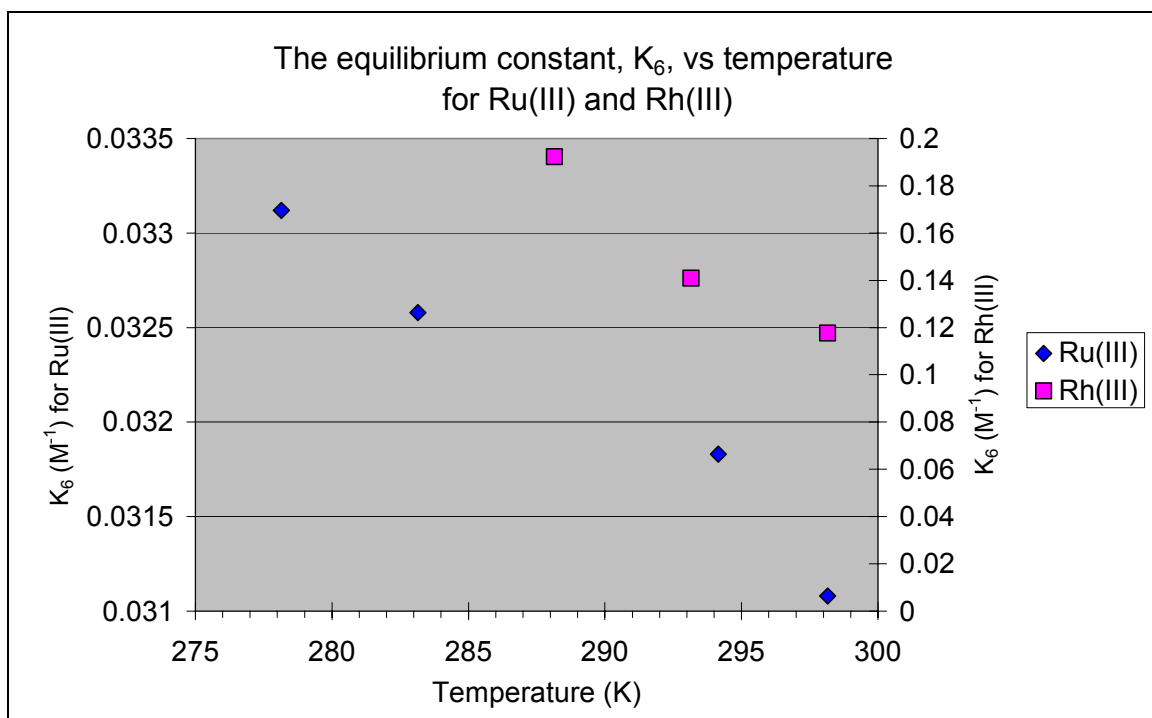
Figure 3-14: The equilibrium constants, K_6, for Ru(III) and Rh(III)[39] at different temperatures.

3.2.2 The effect of ionic strength on the aquation rate constant of $[RuCl_6]^{3-}$

The ionic strength of a solution can influence the rate of a reaction taking place in the solution[11], usually a higher ionic strength slows a reaction down. The non-reactive ions in solution around the reagent ions decrease the possibility of the reagents colliding and reacting with each other. This effect is seen in the Ir(III) kinetic studies[14] where the aquation rate constant (k_{65}) decreases with increasing ionic strength. The aquation rate constant for Rh(III) is dependant on the chloride ion concentration and possibly on the ionic strength[39]. Adamson[9] indicated, on the grounds of preliminary studies, that the rate constant for the aquation of $[RuCl_6]^{3-}$ could be dependent on the ionic strength, increasing with decreasing ionic strength.

To examine this possibility the ionic strength of the solution was adjusted using lithium chloride dissolved in water and added to the diluent solution in predetermined concentrations. The rate constants at various ionic strengths were then determined using the stopped-flow kinetic accessory, varying the ionic strength but keeping the temperature constant at $10°C$. The results are provided in Appendix C and the summarised results are in table 3-9.

The ionic strength and the chloride ion concentration (table 3-9) are very similar because the adjustment was done with the addition of LiCl. This causes doubt on whether the changes seen in the rate constants are due to ionic strength or chloride ion concentration as the chloride ion plays a major part in the reaction under investigation. The rate constant k_{65} is expected to decrease if the chloride ion concentration increase because the rate of the reverse reaction (anation, k_{56}) will increase, according to the reaction: $[RuCl_6]^{3-}$ + H_2O $\rightleftarrows$ $[RuCl_5(H_2O)]^{2-}$ + Cl^-, to maintain the equilibrium. Therefore, it can be said that the rate constant for the aquation of $[RuCl_6]^{3-}$ is dependent on

the hydrochloric acid concentration of the solution, decreasing with increasing hydrochloric acid concentration (figure 3-15); a similar trend is expected for an increase in ionic strength.   This corresponds to what Adamson reported from initial experiments and thus Ru(III) is similar to Ir(III) in that for both elements in oxidation state +3 the ionic strength of the solution influences the aquation rate of the hexachloro species.

Table 3-9: The influence of ionic strength on the aquation rate constant, k_{65}, of $[RuCl_6]^{3-}$ at a constant temperature of 10°C.

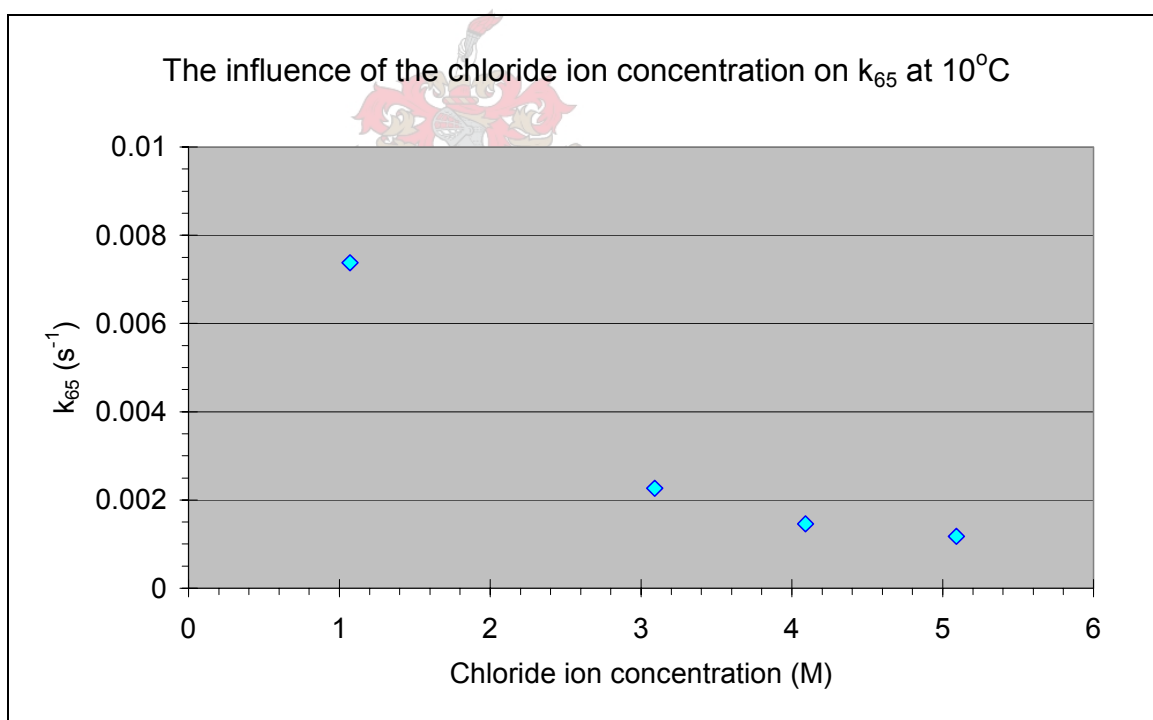| Ionic strength, μ (M)	1.07	3.10	4.10	5.10
Chloride ion concentration (M)	1.07	3.09	4.09	5.09
k_{65} x10^{-3} (s^{-1})	7.37 (±0.51)	2.26 (±0.070)	1.46 (±0.055)	1.17 (±0.060)

Figure 3-15: The influence of the chloride ion concentration on the aquation rate constant, k_{65}, of $[RuCl_6]^{3-}$ at 10°C.

3.2.2.1 The influence of chloride ion concentration on the spectrum of Ru(III)

Experiments were performed to determine the influence of the chloride ion concentration on the spectrum of Ru(III). The chloride concentration of a sample of $[RuCl_6]^{3-}$ was adjusted using lithium chloride. Diluent solutions were made up of 6M HCl with the appropriate amount of 12M LiCl added to the solution to adjust the total chloride concentration from 7M to 12M (6 solutions in total). This adjusted solution was used to dilute an aliquot of $[RuCl_6]^{3-}$ in 12M HCl. The spectrum of each solution was taken after the baseline of each was measured (figure 3-16). From the collected spectra, the increase in the absorbance as the chloride concentration increases can be seen at wavelengths 310nm and 347nm. The minimum at 329nm is lower in 12M HCl and 12M LiCl than at any other concentration.
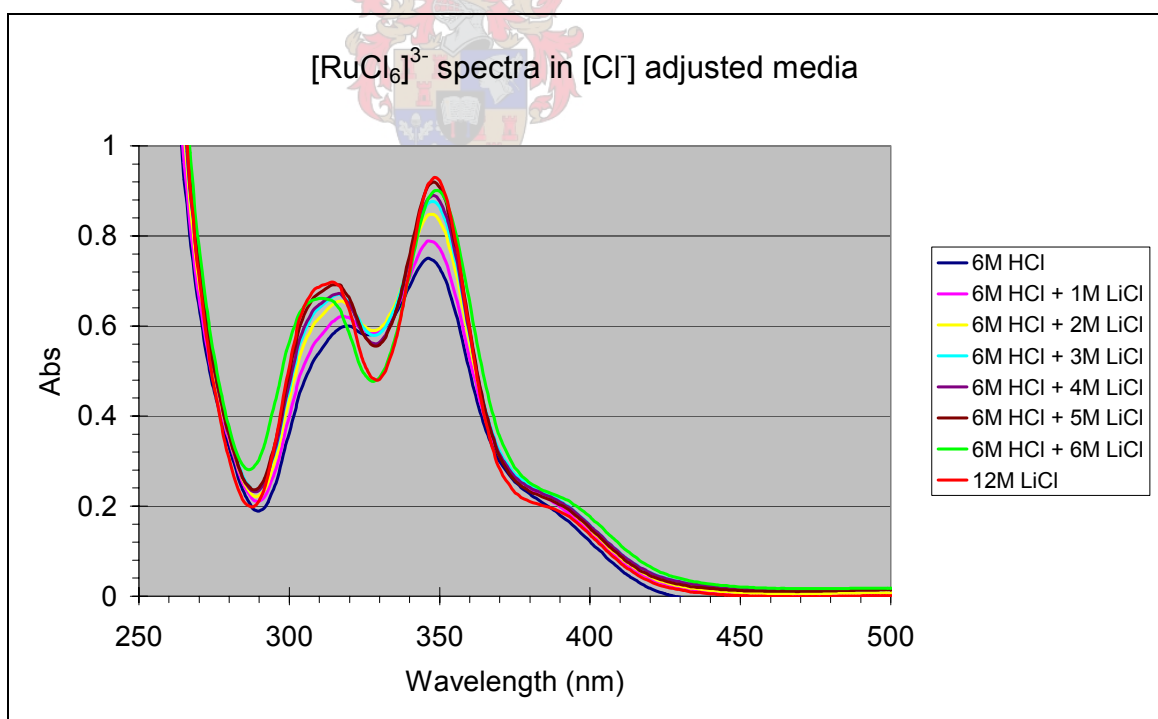

Figure 3-16: Spectrum of $[RuCl_6]^{3-}$ in chloride adjusted media.

The chloride ion concentration of a solution containing Ru(III) was increased above 12M to ascertain whether the spectrum of $[RuCl_6]^{3-}$ in

12M is the actual spectrum of the species and not a mixture of $[RuCl_6]^{3-}$ and $[RuCl_5(H_2O)]^{2-}$. Dissolving an amount of LiCl in 12M HCl enabled a chloride concentration of higher than 12M to be achieved. The spectra of three solutions at chloride concentrations of 12M, 13M and 14M look very similar (figure 3-17). This could mean that the spectrum of Ru(III) in 12M HCl is that of $[RuCl_6]^{3-}$ exclusively. Alternatively, the same amount of $[RuCl_5(H_2O)]^{2-}$ is present at 12M, 13M and 14M chloride concentration; that is, the equilibrium is unchanged.
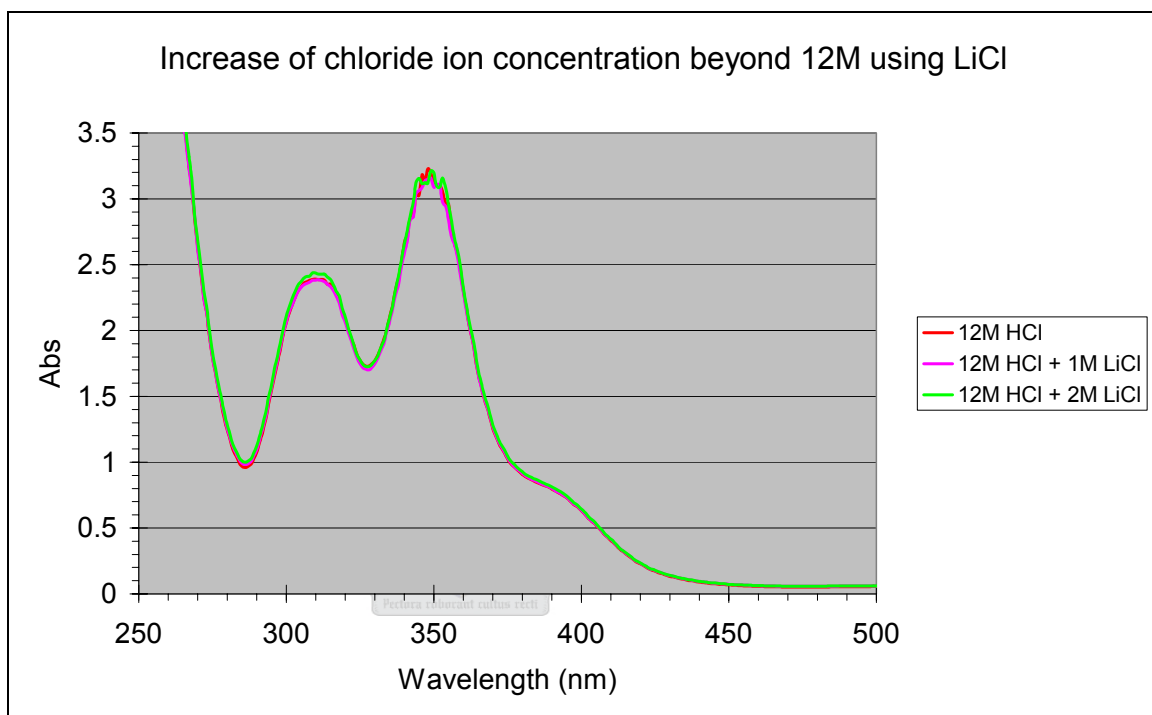

Figure 3-17: Spectrum of $[RuCl_6]^{3-}$ in chloride media above 12M.

3.2.3 Distribution diagram for the ruthenium(III) species in aqueous hydrochloric acid medium

The equilibrium constant for a reaction can also be influenced by chloride ion concentration, as in the case of K_6 for the aqua-chloro species of Ir(III)[40]. The equilibrium constants (K_6 and K_5) for Ir(III) at different hydrochloric acid concentrations was determined by Drake[40] and is shown in figure 3-18*. The equilibrium constants, previously assumed constant throughout the range of chloride ion concentrations[14, 15, 16], increase as the chloride ion concentration increase.
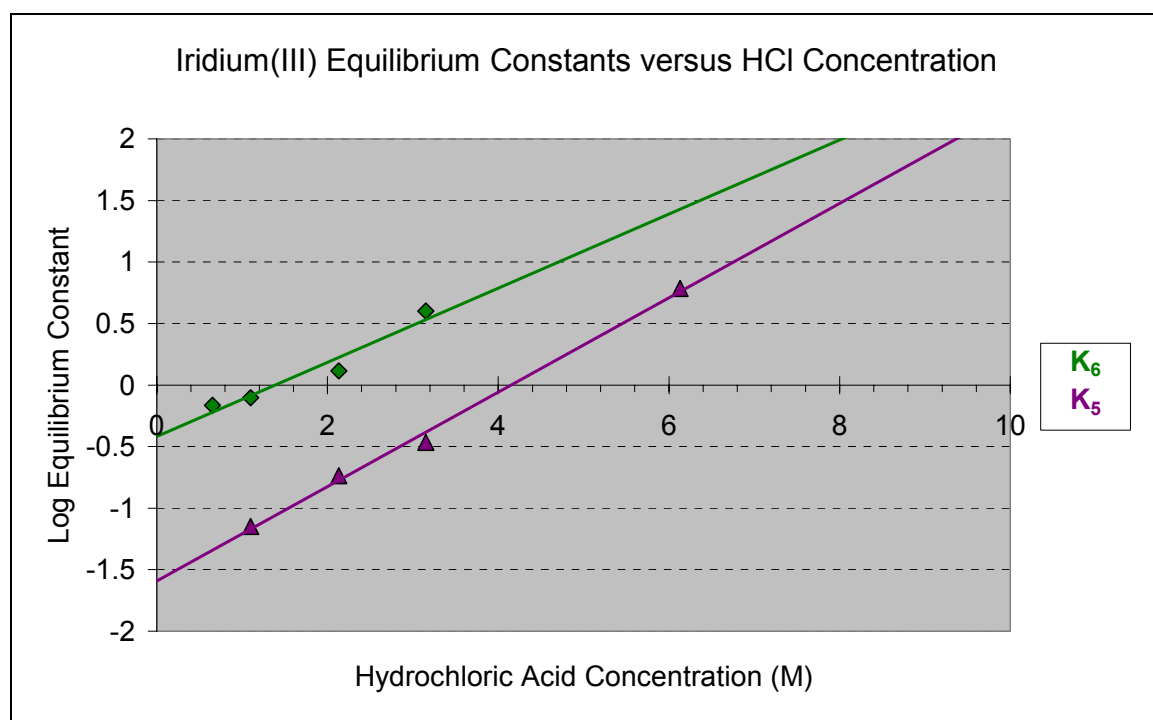

Figure 3-18: The influence of HCl concentration on the equilibrium constants of Ir(III), adapted and redrawn from Drake.[40]

---

* Note that the units of the equilibrium constant was changed for the purposes of comparison to this study because Drake uses the following equation for calculating

the equilibrium constant: $K_6 = \dfrac{\left[[IrCl_5(H_2O)]^{2-}\right] \cdot \left[Cl^-\right]}{\left[[IrCl_6]^{3-}\right]}$ (compare to equation1-2)

To determine whether the equilibrium constant, K_6, for the aqua-chloro Ru(III) system also change with the chloride ion concentration, the value determined in this study was compiled with values available in literature. It has been noted previously that Fine's data[24] for K_6 increases quite considerably at concentrations of 7M HCl and higher. In addition, it has to be noted, that Connick[21] only gave an estimate of the K_6 value at 5M ionic strength. As the change in K_6 at different HCl concentration would influence the distribution diagram, the values of K_6 at each HCl concentration need to be determined. Rejecting the values for K_6 above 7M HCl of Fine and Connick's estimate value, the values for K_6 in table 3-10 were used to construct a regression line for the determination of K_6 at different HCl concentrations. From figure 3-19, the estimated values for K_6 at different HCl concentrations can be calculated and used in determining the distribution diagrams and as can be seen, K_6 increase at increased HCl concentration. This should be taken into consideration when the equilibrium diagram for Ru(III) is constructed.

Table 3-10: Equilibrium constants K_6 values at different HCl concentrations.

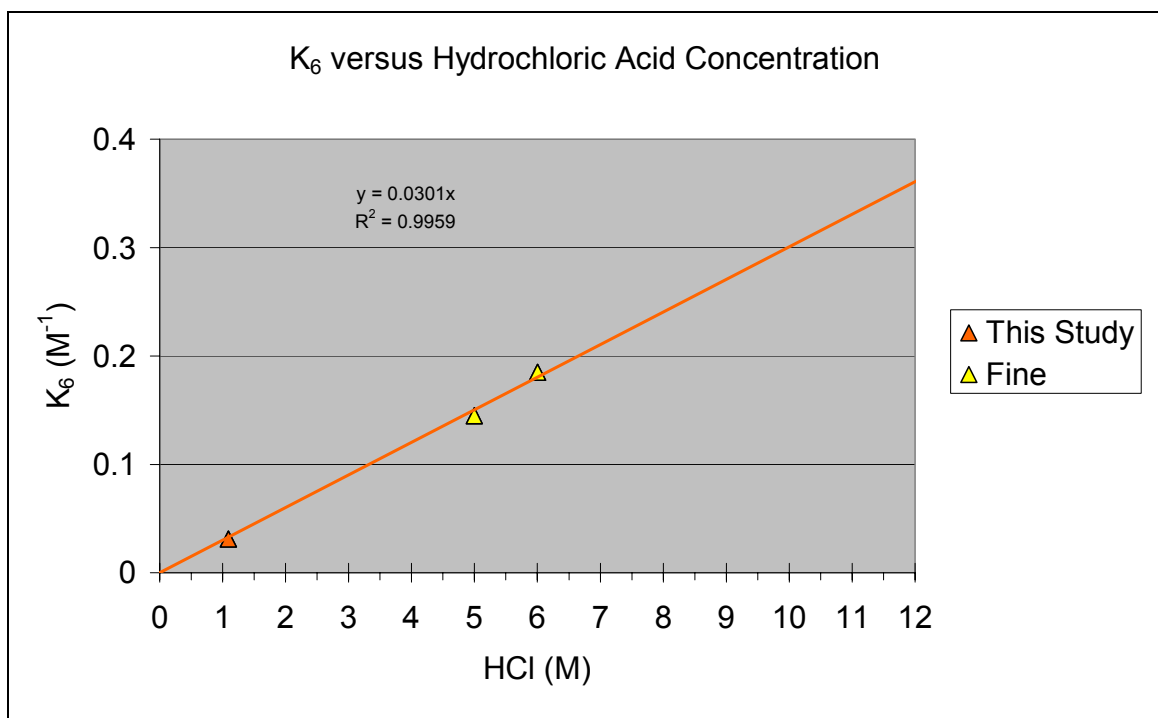| HCl concentration (M)	K_6 (M^{-1})	Reference
1.09	0.0311	This study
5	0.145	24
6	0.185	24

Figure 3-19: Equilibrium constant K_6 versus HCl concentration for the estimation of K_6 at various HCl concentrations.

From the equilibrium constant data determined in this study and by Connick[21] and Fine[24], distribution diagrams can be constructed. There is however no value for K_1 in the literature and this has to be accommodated in the calculations of the amount of species present at different chloride concentrations.

Using the equations that were used to describe the determination of the equilibrium constants, the total ruthenium concentration in solution can be related to the amount of $[RuCl_5(H_2O)]^{2-}$. This is then used to construct a distribution diagram for the series $[RuCl_{6-n}(H_2O)_n]^{n-3}$. The equations used to calculate the data and the data for the distribution diagrams are available in Appendix D.

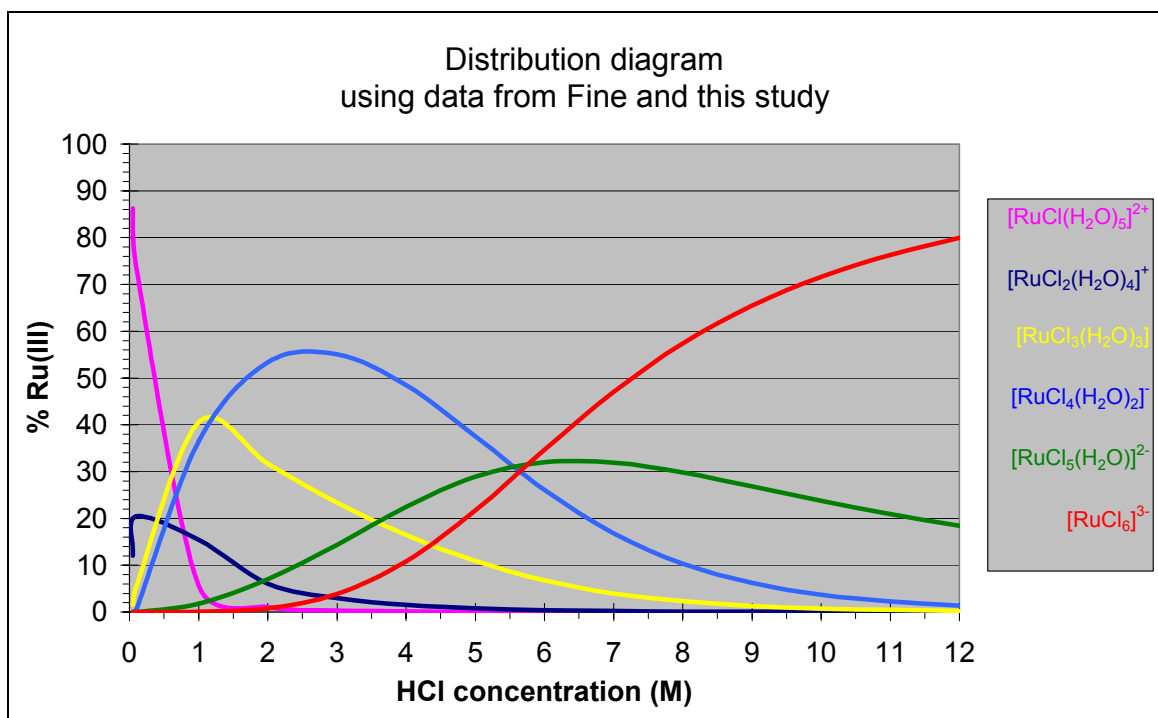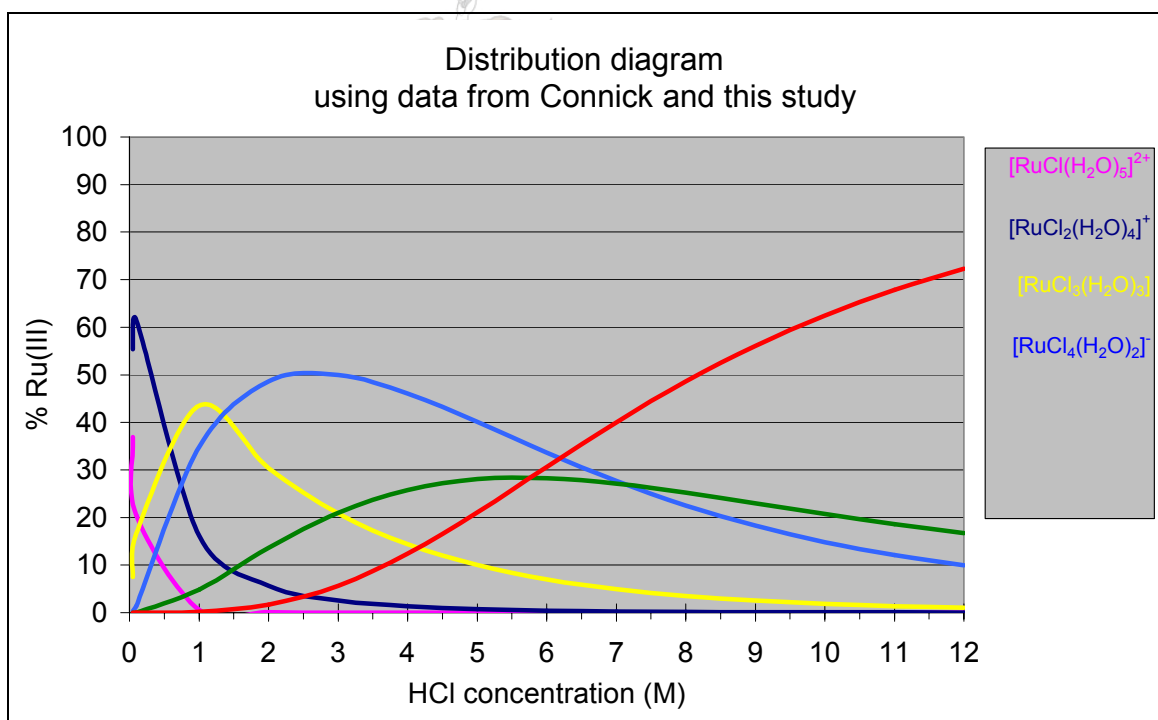**Figure 3-20:** Distribution diagram from Fine[24] and this study.

**Figure 3-21:** Distribution diagram from Connick[21] and this study.

A distribution diagram (figure 1-21) constructed from Connick's[21] equilibrium constant values shows 41.97% $[RuCl_6]^{3-}$ in 12M HCl while Fine[24] assumed 100% $[RuCl_6]^{3-}$ in 12M HCl (figure 1-20). The

distribution diagram constructed using the calculated K_6 values from this study and combining it with Fine's (figure 3-20) and Connick's (figure 3-21) equilibrium constants gives an amount of 79.9% and 72.3% $[RuCl_6]^{3-}$ in 12M HCl, respectively.   It is clear that Fine's assumption is inaccurate as the rate of aquation is extremely fast and it would be expected that at least some of the aquation product is present at 12M HCl, Fine cautions about this assumption in his thesis[24].   The rest of the species' distribution looks very similar to the original distribution diagram constructed with Connick's equilibrium constant data, except at around 12M HCl.   The distribution of the species using Fine's data is much smoother as the large increases reported by Fine were smoothed out.   Connick's equilibrium values do not change with HCl concentration and it was shown that the HCl concentration does influence the equilibrium constant.   The distribution diagrams are an indication only of the amount of species present at various HCl concentrations at equilibrium.   The equilibrium data from Fine, used in the calculation of the distribution diagram, was extrapolated over a wide range (0.05M to 12M HCl) and this would introduce errors in the values of the equilibrium constants.   The two different distribution diagrams do agree well when the differences in the equilibrium constants used are taken into consideration, suggesting that the true distribution diagram will not be radically different, depending on the correctness of the reported equilibrium constants from Fine and Connick.

4   CONCLUSIONS

Crystals of diethylenetriamine hexachlororuthenate(III) was prepared and identified by CHN analysis and x-ray crystallography.   Poor crystal structure resulted in a high final R index and high standard deviations on reported bond lengths.   The hexachlororuthenate(III) anion is in pseudo octahedral geometry and two crystallographic independent molecules were identified.   The good yield (99.59%) for the compound makes this a convenient method to separate the hexachlororuthenate(III) anion in solution with other Ru(III) species.

The rate constants for the reaction

$$[RuCl_6]^{3-} + H_2O \underset{k_{56}}{\overset{k_{65}}{\rightleftarrows}} [RuCl_5(H_2O)]^{2-} + Cl^- \qquad \textbf{Equation 1-4-1}$$
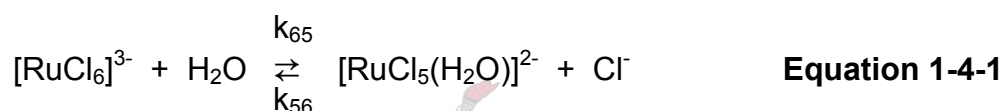
were not available in literature but information on the aquation rate constant was found in unpublished papers by Adamson[9].   The aquation (k_{65}) and anation (k_{56}) rate constants as well as the equilibrium constant, K_6 for the reaction, were determined in this study (figure 4-1).   Influences of temperature and chloride ion concentration on the aquation rate constant of $[RuCl_6]^{3-}$ were successfully determined.   The aquation rate constant showed an increase as the temperature increases; constructing a straight line through the points makes it possible to predict the rate constant at any temperature.   An increase in the chloride ion concentration causes a decrease in the rate constant and an analogous effect is expected for the ionic strength of the solution.   The influence of temperature on the chloride anation rate constant of $[RuCl_5(H_2O)]^{2-}$ was determined; the rate constant showing an increase as the temperature increase.   The influence of the chloride ion strength on the anation rate constant was not determined.

The data obtained in this study was compared to corresponding data for Ir(III) and Rh(III) and several trends were observed and confirmed.

It is well known that the elements of a group are chemically related but there are also similarities between elements in adjacent groups in the transition elements of the periodic table. An example of this is that higher oxidation states are more stable moving down in a group, for instance Rh(IV) is not very stable but Ir(IV) is and Ru(VIII) is not as stable as Os(VIII). The trends between elements in groups can be seen in the parameters for ruthenium, rhodium and iridium, for example it has been noted that in all the cases the rate of aquation decrease in the series going from $[MCl_6]^{3-}$ to $[MCl(H_2O)_5]^{2-}$. A property that changes in the Ru(III)-Rh(III)-Ir(III) series is the decreasing rate of ligand substitution (Ru(III) > Rh(III) > Ir(III)). The influences of temperature and chloride ion strength on the equilibrium constants, K_6 for each of these elements were summarised in table 4-1. Assumptions were made on the influence of the ionic strength on the aquation rate constant, k_{65}, from the results obtained from the chloride ion strength experiments.

The calculated distribution diagrams made use of data determined in this study combined with the data published by Connick[21] and Fine[24]. The equilibrium constants published by Connick were given at only one ionic strength and it appears that this was based on the assumption that the equilibrium constant does not vary with ionic strength. It is clear from this study that the equilibrium constant, K_6, does vary with chloride ion concentration and thus quite possibly ionic strength as well. Thus the distribution diagram using Fine's data is felt to be more reliable although some of Fine's equilibrium constant data had to be discarded because it showed large increases, as the chloride concentration increases, that are uncharacteristic of equilibrium constants. The actual distribution diagram for the aqua-chloro ruthenate(III) series is thought to be somewhere between these two distribution diagrams. All the gaps in the rate constant data (figure 4-1) will have to be filled in order for the true distribution diagram to be calculated. With the true distribution diagram in hand, the behaviour of the aqua-chloro Ru(III) species in solutions of varying chloride ion

strength can be predicted.   This will be of great use for refining purposes.

Table 4-1: Summary of the influences of temperature and ionic strength on the equilibrium constants of Ru(III), Rh(III) and Ir(III).

Ru(III) – K_6	Rh(III) – K_6
varies with chloride ion strength (and ionic strength) [This study, 21, 24] varies with T [This study]	does not vary with ionic strength [38] varies with T [38]
	Ir(III) – K_6 varies with ionic strength [14] variation with T unknown
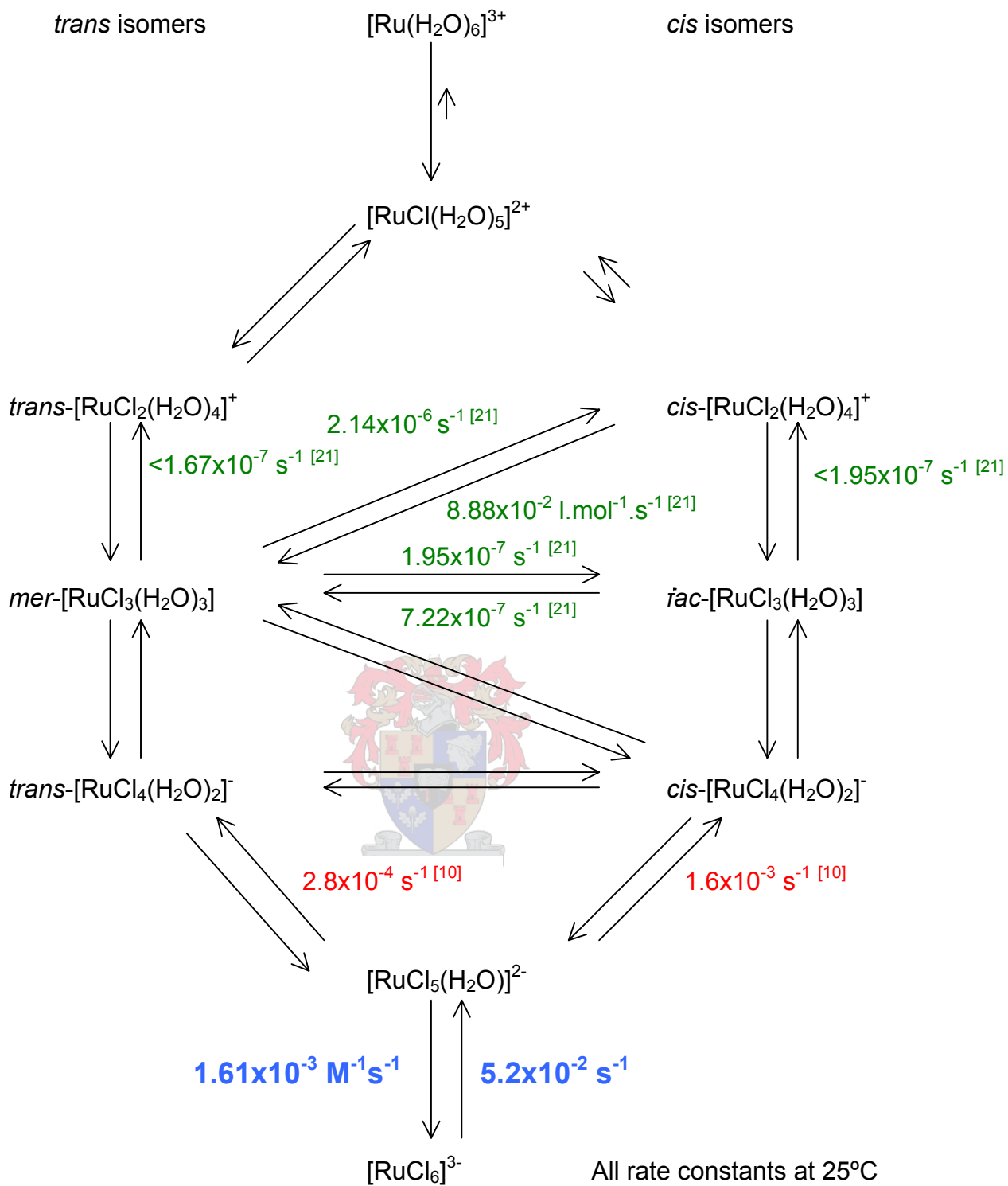
Figure 4-1: Scheme of Ru(III) with all rate constants available in literature and the new rate constants determined in this study.

5   REFERENCES

1.   R.A. Grant, 3 December 1998, personal communication.

2.   N.N. Greenwood and A. Earnshaw, *Chemistry of the Elements*, Butterworth Heineman, Oxford, 1995.

3.   S.E. Livingstone, Pergamon Texts in Inorganic Chemistry Volume 25, *The Chemistry of Ruthenium, Rhodium, Palladium, Osmium, Iridium and Platinum*, Pergamon Press, 1980.

4.   Platinum Today, www.platinum.matthey.com, 13 March 2002.

5.   R.A. Grant in *Precious Metals Recovery and Refining,* ed. L. Manzick , International Precious Metals Institute, Allentown, Pa, 1990.

6.   P. Charlesworth, *Platinum Metals Review*, 1981, **25**.

7.   J.L. Woodhead and J.M. Fletcher, *Report AERE R-4123*, UK Atomic Energy Research Group, 1962.

8.   R.A. Grant, 7 November 2000, personal communication.

9.   M.G. Adamson and R.E. Connick, unpublished work.

10.   M.G. Adamson, R.E. Connick and R. Hasty, unpublished work.

11.   J.H. Espenson, *Chemical Kinetics and Reaction Mechanisms*, McGraw-Hill International Editions, 2nd Ed, 1995.

12.   D.A. Skoog, D.M. West and F.J. Holler, *Fundamentals of Analytical Chemistry*, Saunders College Publishing, 6th Ed, 1992.

13.   R.A. Grant, *Amplats and Johnson Matthey Refining Conference 2000*.

14.   I.A. Poulsen and C.S. Garner, *J.A.C.S.*, 1962, **84**, 2032-2037.

15.   J.C. Chang and C.S. Garner, *Inorg Chem*, 1965, **4**, 209-215.

16.   A.A. El-Awady, E.J. Bounsall, *et al*, *Inorg Chem*, 1967, **6**, 79-86.

17.   D.A. Palmer and G.M. Harris, *Inorg Chem*, 1974, **14**, 1316-1321.

18.   W. Robb and M.M. De V. Steyn, *Inorg Chem*, 1967, **6**, 616-619.

19.   R.A. Grant and C.S. Smith (Johnson Matthey/Matthey Rustenburg Refiners) GB Patent 2293372, 1998.

20.   W. Frank and G.J. Reiss, *Z Anorg Allg Chem*, 1996, **622**, 729-733.

21. R.E. Connick in *Advances in the Chemistry of the Coordination Compounds*, Ed. S. Kirschner, MacMillan, 1961.

22. H.H. Cady and R.E. Connick, *J.A.C.S.*, 1959, **80**, 2646-2652.

23. R.E. Connick and D.A. Fine *J.A.C.S.*, 1960, **82** (August), 4187-4191.

24. D.A. Fine, Thesis, University of California at Berkeley, 1958.

25. E.E. Mercer and W.A. McAllister, *Inorg. Chem.*, 1965, **4**(10), 1414-1416.

26. M.G. Adamson, R.E. Connick and D.A. Fine, Unpublished.

27. T.E. Hopkins, A. Zalkin, *et al.*, *Inorg. Chem.*, 1966, **5**(8), 1427-1431.

28. E. Ohyoshi, A. Ohyoshi, *et al.*, *Radiochimica Acta*, 1969, **13**(1), 10-18.

29. M.M. Taqui Khan, G. Ramachandraiah, *et al.*, *Inorg. Chem.*, 1988, **27**, 3274-3278.

30. T.E. Hopkins, A. Zalkin, *et al.*, *Inorg. Chem.*, 1966, **5**(8), 1431-1433.

31. T.E. Hopkins, A. Zalkin, *et al.*, *Inorg. Chem.*, 1969, **8**(11), 2421-2425.

32. B.R. James and R.S. McMillan, *Inorg Nucl Chem Lett*, 1975, **11**, 837.

33. M.G. Adamson, *J Chem Soc*, 1968, **A**, 1370.

34. H.H. Cady and R.E. Connick, *J.A.C.S.*, 1957, **79**, 4242-4243.

35. R.E. Connick and D.A. Fine, 1961, *J.A.C.S.*, 1957, **83**, 3414-3416.

36. E.E. Mercer and R.R. Buckley, *Inorg Chem*, 1965, **4**: 1692.

37. Hi-Tech Scientific, http://www.hi-techsci.co.uk, 8 August 2002.

38. H. Su, Report of the data collection, reduction and refinement for diethylenetriamine hexachlororuthenate(III), 1 November 2002.

39. W. Robb and G.M. Harris, *J.A.C.S.*, 1965, **87**, 4472.

40. V.A. Drake and R.A. Grant, *Amplats and Johnson Matthey Refining Conference 1994.*

41. J.N. Miller, *Analyst*, 1991, **116**: 3.

42. Rules for error propagation, http://chem.unk.edu/chem475/propagation_rules.html, 18 February 2003.
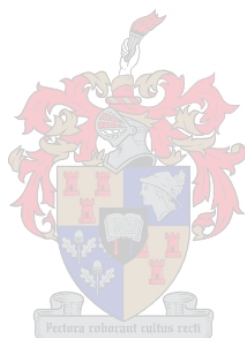
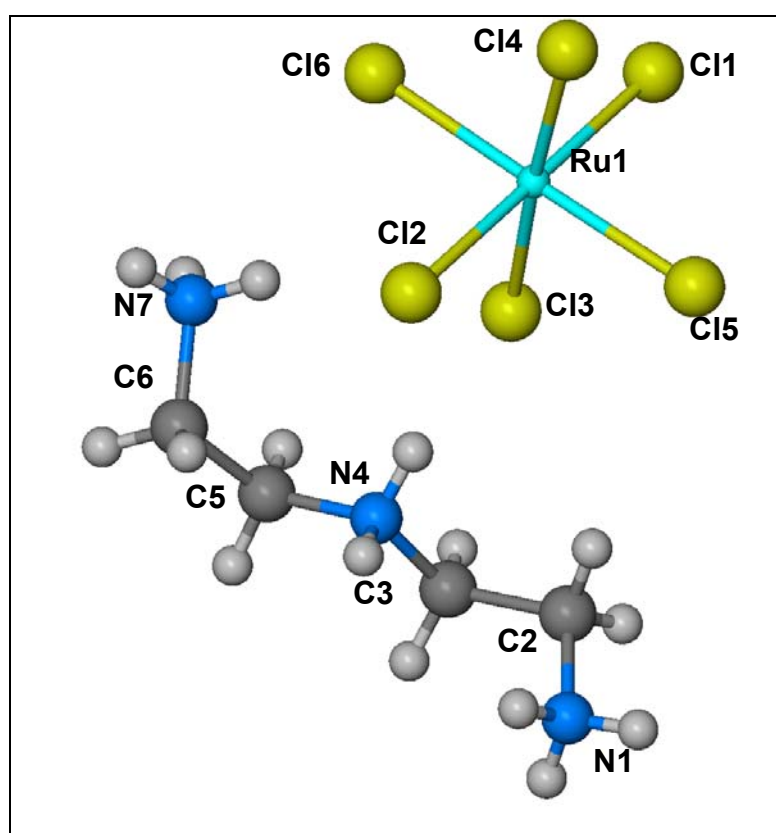# APPENDIX A: CRYSTALLOGRAPHIC DATA FOR DIETHYLENETRIAMINE HEXACHLORORUTHENATE(III) CRYSTALS

Figure A-1: The atomic labeling scheme for diethylenetriamine hexachlororuthenate(III).

Table A-1: Atomic coordinates (x10^4) and equivalent isotropic displacement parameters (Å^2 x10^3) for diethylenetriamine hexachlororuthenate(III).

	x	y	z	U(eq)
Ru(1A)	4659(1)	2149(2)	2955(2)	26(1)
Ru(1B)	7150(1)	17674(2)	5415(2)	19(1)
Cl(3B)	7476(2)	17955(7)	7445(4)	18(1)
Cl(1A)	4331(2)	2021(7)	4297(4)	17(1)
Cl(3A)	5213(2)	-176(7)	3884(5)	27(1)
Cl(6B)	6591(2)	20050(8)	5258(5)	26(1)
Cl(6A)	5196(2)	4410(8)	4091(5)	34(2)
Cl(1B)	6610(2)	15486(8)	5511(5)	29(1)
Cl(5B)	7701(2)	15414(9)	5606(6)	38(2)
Cl(4A)	4104(2)	4469(9)	1969(5)	37(2)
Cl(5A)	4117(2)	-101(12)	1869(6)	50(2)
Cl(2B)	7694(2)	19966(10)	5408(6)	46(2)
Cl(4B)	6831(3)	17488(12)	3454(6)	51(2)
Cl(2A)	4981(3)	2470(10)	1601(6)	44(2)
N(1A)	5002(6)	-2950(20)	1902(15)	17(3)
C(2A)	5509(7)	-3120(30)	2069(17)	20(4)
N(4A)	5899(6)	30(20)	2513(13)	16(3)
C(3A)	5704(8)	-1440(30)	1657(18)	26(4)
N(4B)	8386(9)	15490(30)	8350(20)	47(6)
N(1B)	7508(9)	12620(30)	7180(20)	36(6)
C(5A)	6105(6)	1480(20)	2038(15)	15(3)
C(6A)	6297(8)	3120(30)	2862(19)	27(4)
C(3B)	8164(13)	13990(50)	8720(30)	66(9)
C(2B)	8029(11)	12490(40)	8070(30)	52(8)
N(7A)	6801(7)	2850(30)	3692(17)	26(4)
C(5B)	8598(11)	16920(40)	9230(20)	46(7)
N(7B)	9293(10)	17720(40)	9010(20)	53(7)
C(6B)	8791(15)	18320(60)	8900(40)	72(10)

Table A-2: Bond lengths (Å) and angles (°) for diethylenetriamine hexachlororuthenate(III).

Ru(1A)-Cl(5A)	2.360(8)
Ru(1A)-Cl(3A)	2.365(5)
Ru(1A)-Cl(1A)	2.367(6)
Ru(1A)-Cl(2A)	2.379(8)
Ru(1A)-Cl(4A)	2.380(6)
Ru(1A)-Cl(6A)	2.380(7)
Ru(1B)-Cl(5B)	2.319(7)
Ru(1B)-Cl(4B)	2.329(8)
Ru(1B)-Cl(1B)	2.364(6)
Ru(1B)-Cl(2B)	2.387(8)
Ru(1B)-Cl(6B)	2.408(6)
Ru(1B)-Cl(3B)	2.417(6)
N(1A)-C(2A)	1.50(3)
C(2A)-C(3A)	1.57(3)
N(4A)-C(3A)	1.49(3)
N(4A)-C(5A)	1.50(2)
N(4B)-C(3B)	1.48(4)
N(4B)-C(5B)	1.48(4)
N(1B)-C(2B)	1.55(4)
C(5A)-C(6A)	1.56(3)
C(6A)-N(7A)	1.49(3)
C(3B)-C(2B)	1.34(4)
C(5B)-C(6B)	1.35(5)
N(7B)-C(6B)	1.56(5)
Cl(5A)-Ru(1A)-Cl(3A)	89.01(19)
Cl(5A)-Ru(1A)-Cl(1A)	89.9(2)
Cl(3A)-Ru(1A)-Cl(1A)	92.1(2)
Cl(5A)-Ru(1A)-Cl(2A)	92.2(3)
Cl(3A)-Ru(1A)-Cl(2A)	90.6(2)
Cl(1A)-Ru(1A)-Cl(2A)	176.6(2)
Cl(5A)-Ru(1A)-Cl(4A)	90.4(3)
Cl(3A)-Ru(1A)-Cl(4A)	178.2(3)
Cl(1A)-Ru(1A)-Cl(4A)	89.5(2)

Cl(2A)-Ru(1A)-Cl(4A)	87.7(2)
Cl(5A)-Ru(1A)-Cl(6A)	178.3(3)
Cl(3A)-Ru(1A)-Cl(6A)	91.0(2)
Cl(1A)-Ru(1A)-Cl(6A)	88.4(2)
Cl(2A)-Ru(1A)-Cl(6A)	89.5(3)
Cl(4A)-Ru(1A)-Cl(6A)	89.70(19)
Cl(5B)-Ru(1B)-Cl(4B)	91.8(3)
Cl(5B)-Ru(1B)-Cl(1B)	90.7(2)
Cl(4B)-Ru(1B)-Cl(1B)	91.9(3)
Cl(5B)-Ru(1B)-Cl(2B)	91.0(3)
Cl(4B)-Ru(1B)-Cl(2B)	90.7(3)
Cl(1B)-Ru(1B)-Cl(2B)	176.8(3)
Cl(5B)-Ru(1B)-Cl(6B)	178.7(3)
Cl(4B)-Ru(1B)-Cl(6B)	89.4(3)
Cl(1B)-Ru(1B)-Cl(6B)	89.8(2)
Cl(2B)-Ru(1B)-Cl(6B)	88.4(2)
Cl(5B)-Ru(1B)-Cl(3B)	89.6(2)
Cl(4B)-Ru(1B)-Cl(3B)	178.4(3)
Cl(1B)-Ru(1B)-Cl(3B)	88.8(2)
Cl(2B)-Ru(1B)-Cl(3B)	88.5(3)
Cl(6B)-Ru(1B)-Cl(3B)	89.2(2)
N(1A)-C(2A)-C(3A)	114.6(17)
C(3A)-N(4A)-C(5A)	108.3(14)
N(4A)-C(3A)-C(2A)	114.1(17)
C(3B)-N(4B)-C(5B)	113(2)
N(4A)-C(5A)-C(6A)	111.8(16)
N(7A)-C(6A)-C(5A)	112.1(18)
C(2B)-C(3B)-N(4B)	118(3)
C(3B)-C(2B)-N(1B)	112(3)
C(6B)-C(5B)-N(4B)	114(3)
C(5B)-C(6B)-N(7B)	108(3)

Table A-3: Hydrogen coordinates (x10^4) and isotropic displacement parameters (Å^2 x10^3) for diethylenetriamine hexachlororuthenate(III).

	x	y	z	U(eq)
H(1A1)	4974	-2009	2308	26
H(1A2)	4912	-3984	2131	26
H(1A3)	4815	-2768	1166	26
H(2A1)	5538	-4207	1666	24
H(2A2)	5708	-3312	2874	24
H(4A1)	6129	-432	3160	19
H(4A2)	5665	503	2677	19
H(3A1)	5954	-1857	1438	31
H(3A2)	5446	-937	982	31
H(4B1)	8163	16008	7719	57
H(4B2)	8617	15020	8172	57
H(1B2)	7315	12076	7441	54
H(1B1)	7481	12063	6537	54
H(1B3)	7425	13798	7029	54
H(5A2)	5860	1904	1318	18
H(5A1)	6365	957	1892	18
H(6A1)	6275	4229	2424	33
H(6A2)	6098	3293	3271	33
H(3B1)	8388	13616	9474	79
H(3B2)	7884	14485	8785	79
H(2B2)	8062	11431	8553	62
H(2B1)	8238	12315	7689	62
H(7A1)	6821	1849	4106	39
H(7A3)	6899	3826	4149	39
H(7A2)	6986	2714	3320	39
H(5B1)	8351	17394	9436	55
H(5B2)	8844	16363	9900	55
H(7B1)	9465	17302	9716	80
H(7B2)	9443	18682	8880	80
H(7B3)	9262	16837	8510	80
H(6B1)	8819	19386	9368	86
H(6B2)	8589	18637	8109	86

Table A-4: Torsion angles (°) for diethylenetriamine hexachlororuthenate(III).

C(5A)-N(4A)-C(3A)-C(2A)	175.8(16)
N(1A)-C(2A)-C(3A)-N(4A)	87(2)
C(3A)-N(4A)-C(5A)-C(6A)	177.2(16)
N(4A)-C(5A)-C(6A)-N(7A)	88(2)
C(5B)-N(4B)-C(3B)-C(2B)	-170(3)
N(4B)-C(3B)-C(2B)-N(1B)	-91(4)
C(3B)-N(4B)-C(5B)-C(6B)	-178(3)
N(4B)-C(5B)-C(6B)-N(7B)	-80(4)
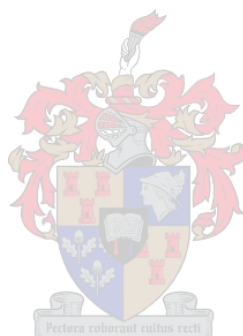
APPENDIX B – RATE CONSTANT TEMPERATURE DATA

The percentage of the ruthenium(III) species under investigation in solution versus time was plotted for each experiment. The half-life time ($t_{1/2}$) was determined by calculating the time at which 50% of the ruthenium(III) species was present. The value for $t_{1/2}$ was then used in equation 1-12 to determine the rate constant for the reaction.

B.1   AQUATION OF $[RuCl_6]^{3-}$

B.1.1 The aquation of $[RuCl_6]^{3-}$ at 25°C

Table B-5: Data for the aquation of $[RuCl_6]^{3-}$ at 25°C.

Run no.	Ru(III) Concentration (M)	HCl Concentration (M)	Ionic strength (M)	k_{65} (min^{-1})	k_{65} (s^{-1})
A	2.862×10^{-3}	1.09	1.12	3.142	0.05236
B	2.862×10^{-3}	1.09	1.12	3.180	0.05300
D	2.862×10^{-3}	1.09	1.12	3.197	0.05328
Average				3.173	0.05288
Std dev				0.02816	0.000473
% RSD				0.89%	0.89%
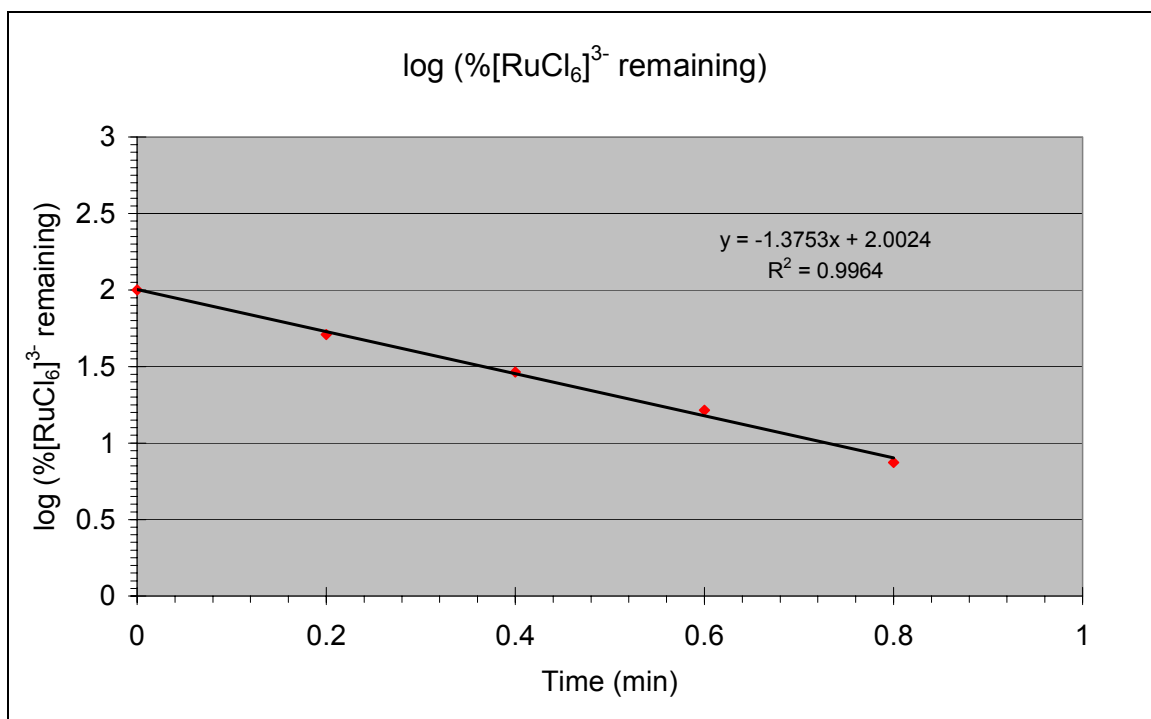
Figure B-2: Run A: Aquation of $[RuCl_6]^{3-}$ at $25°C$.
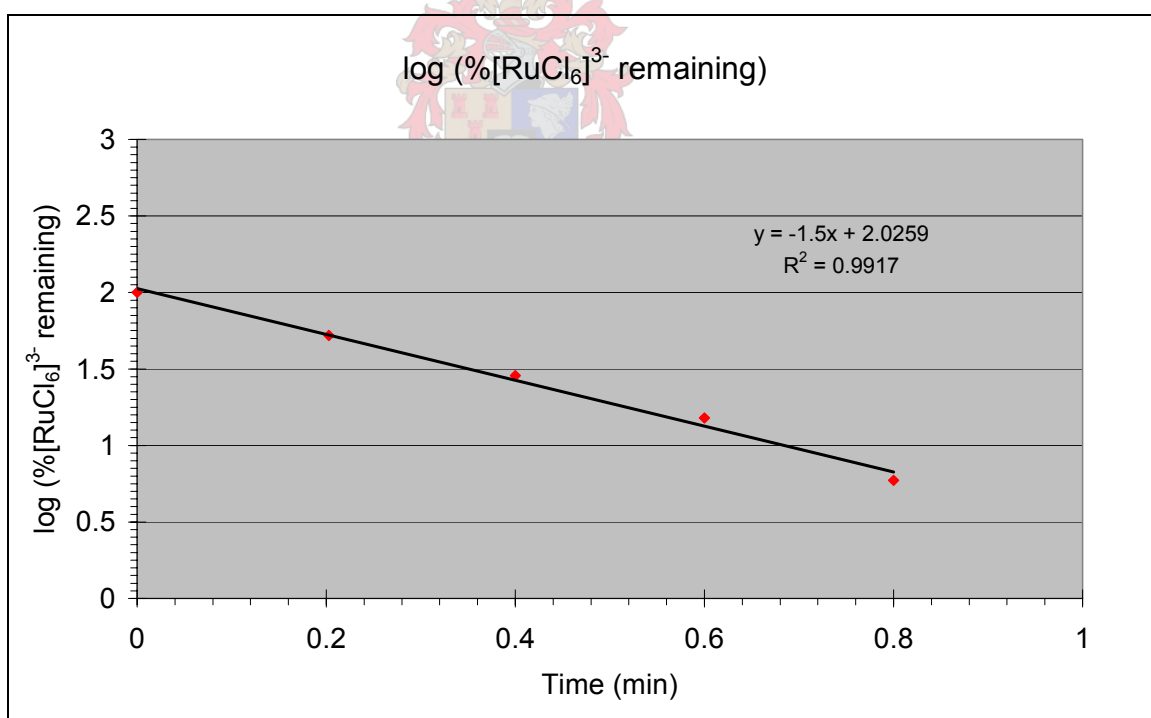
Figure B-3: Run B: Aquation of $[RuCl_6]^{3-}$ at $25°C$.
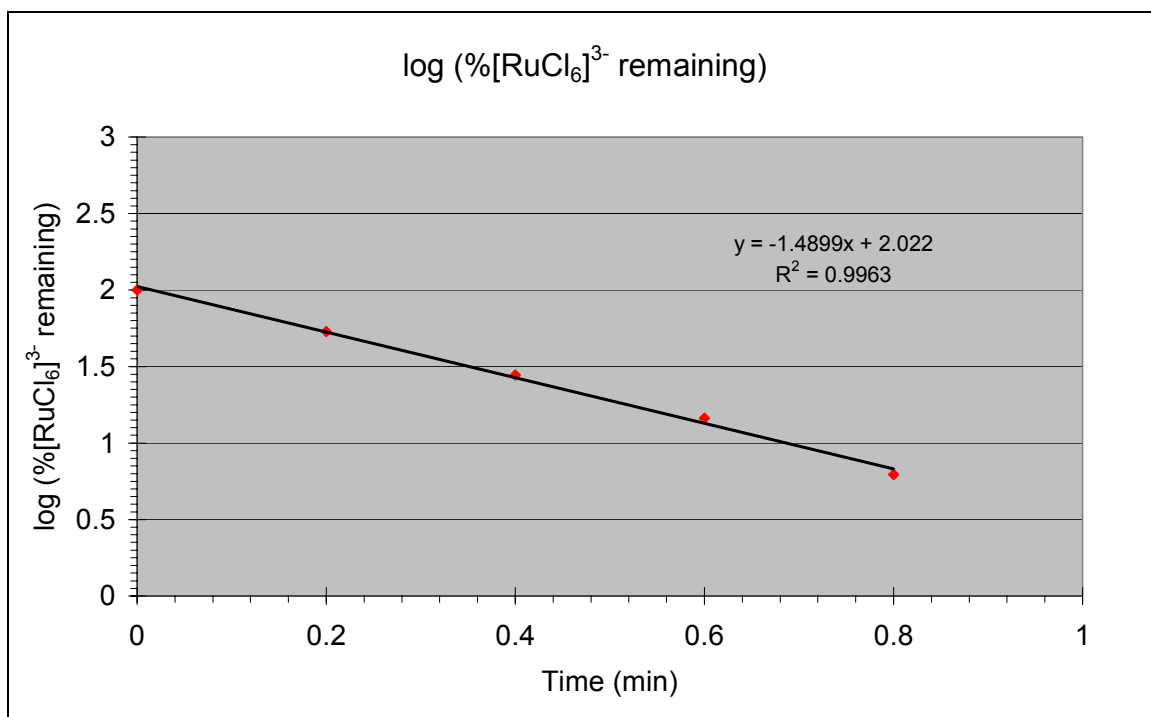
Figure B-4: Run D: Aquation of $[RuCl_6]^{3-}$ at $25^\circ C$.
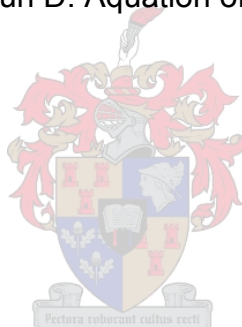
B.1.2. The aquation of $[RuCl_6]^{3-}$ at 21°C

Table B-6: Data for the aquation of $[RuCl_6]^{3-}$ at 21°C.

Run no.	Ru(III) Concentration (M)	HCl Concentration (M)	Ionic strength (M)	k_{65} (min^{-1})	k_{65} (s^{-1})
Test	5.675x10^{-4}	1.09	1.10	1.623	0.02705
A	2.862x10^{-3}	1.09	1.12	2.143	0.03572
B	2.862x10^{-3}	1.09	1.12	2.222	0.03704
C	2.862x10^{-3}	1.09	1.12	1.628	0.02713
D	2.862x10^{-3}	1.09	1.12	1.800	0.03001
Average				1.883	0.03139
Std dev				0.2837	0.004732
% RSD				15.1%	15.1%
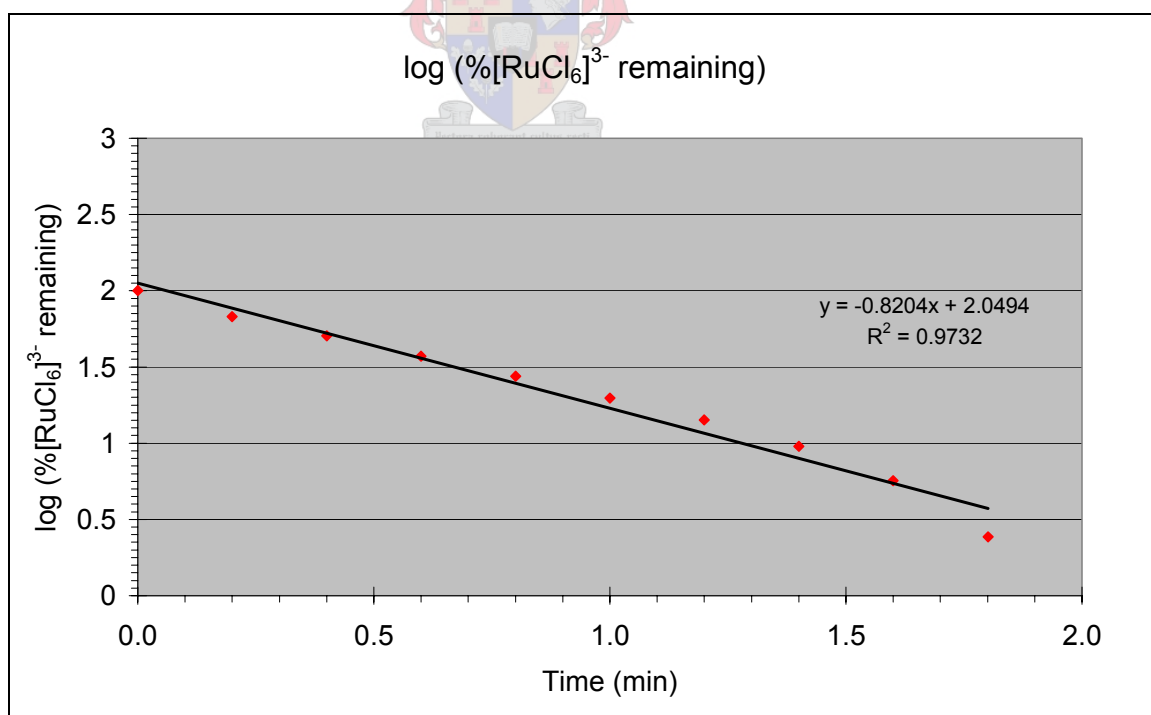
Figure B-5: Run test: Aquation of $[RuCl_6]^{3-}$ at 21°C.
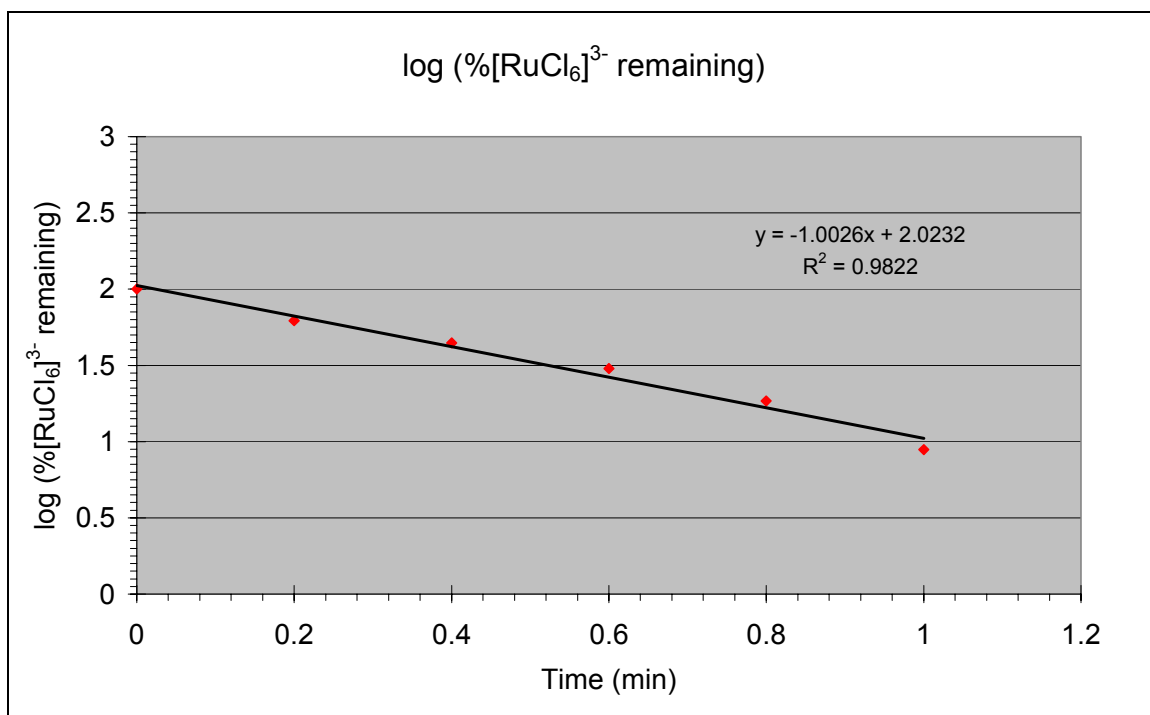
Figure B-6: Run A: Aquation of $[RuCl_6]^{3-}$ at 21°C.
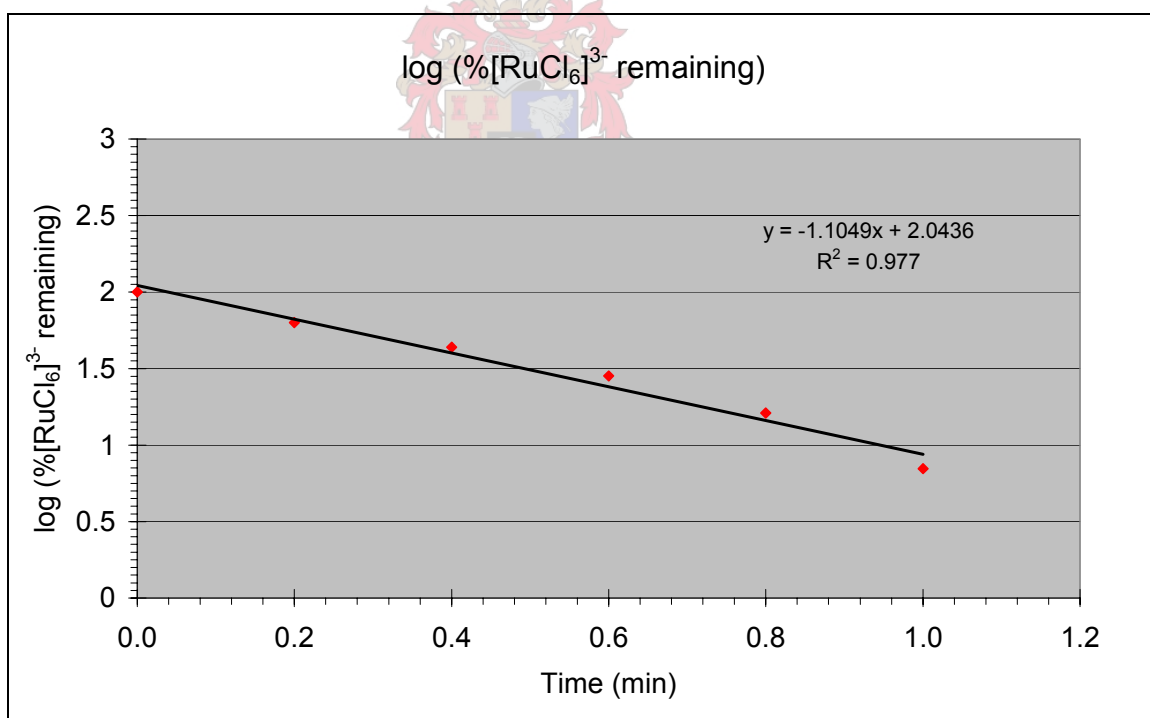
Figure B-7: Run B: Aquation of $[RuCl_6]^{3-}$ at 21°C.
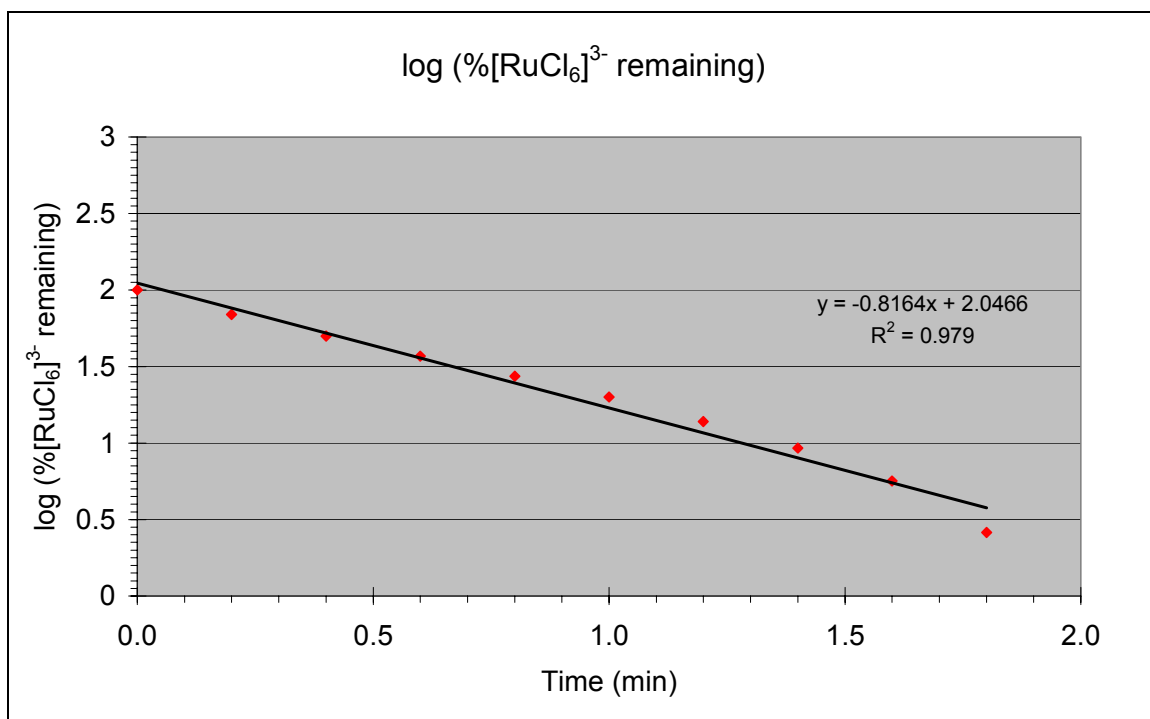
Figure B-8: Run C: Aquation of $[RuCl_6]^{3-}$ at 21°C.
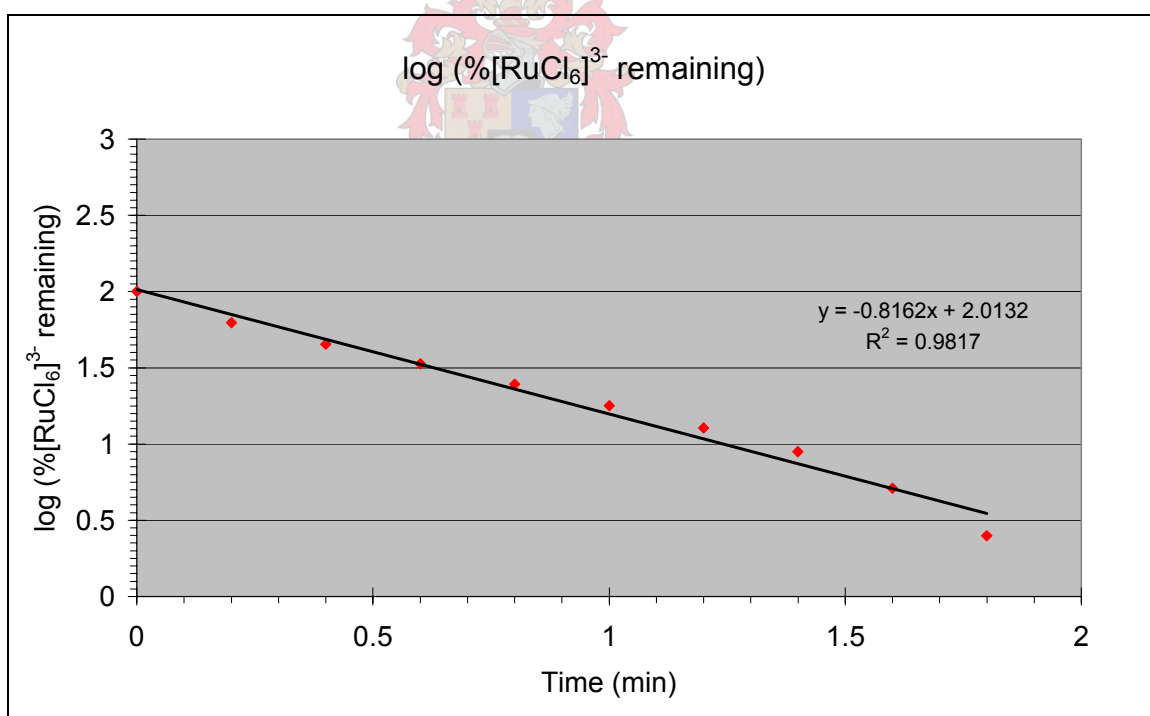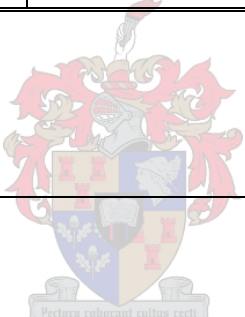
Figure B-9: Run D: Aquation of $[RuCl_6]^{3-}$ at 21°C.

B.1.3 The aquation of $[RuCl_6]^{3-}$ at 10°C

Table B-7: Data for the aquation of $[RuCl_6]^{3-}$ at 10°C.

Run no.	Ru(III) Concentration (M)	HCl Concentration (M)	Ionic strength (M)	k_{65} (min^{-1})	k_{65} x10^{-3}(s^{-1})
A	2.862x10^{-3}	1.07	1.10	0.4373	7.288
B	2.862x10^{-3}	1.07	1.10	0.4708	7.847
C	2.862x10^{-3}	1.07	1.10	0.4620	7.701
D	2.862x10^{-3}	1.07	1.10	0.4708	7.847
E	2.862x10^{-3}	1.07	1.10	0.4117	6.862
F	2.862x10^{-3}	1.07	1.10	0.4014	6.691
Average				0.4423	7.373
Std dev				0.0305	0.5080
% RSD				6.89%	6.89%
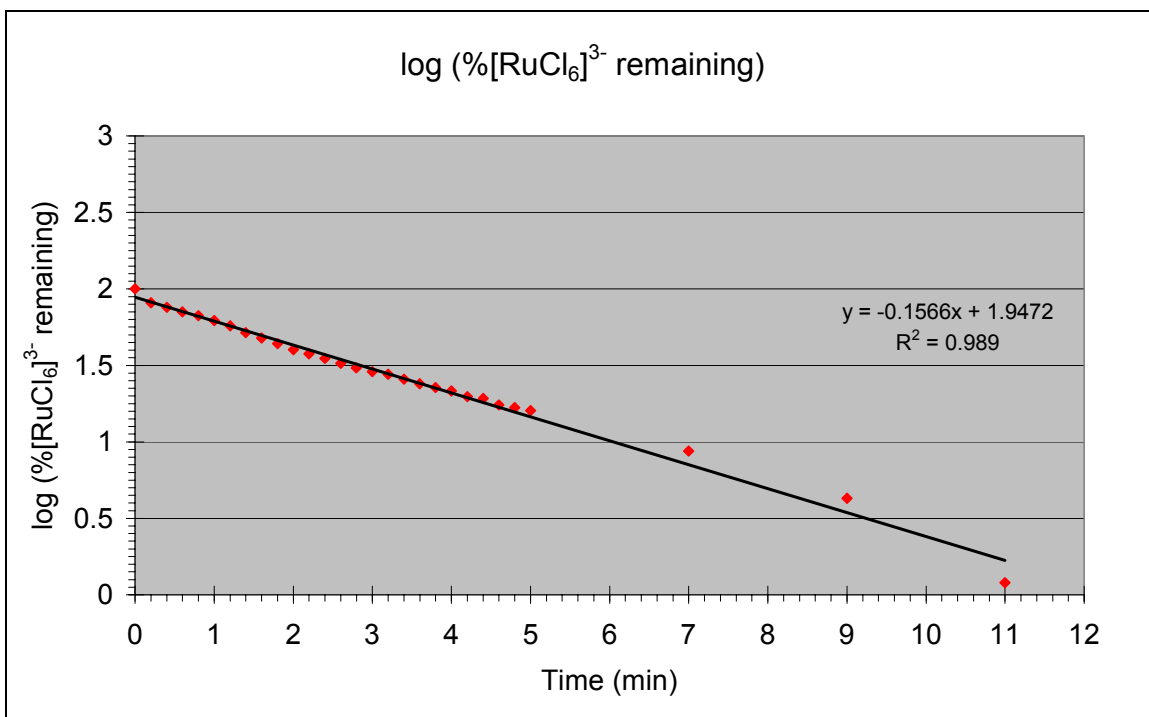
Figure B-10: Run A: Aquation of $[RuCl_6]^{3-}$ at 10°C.
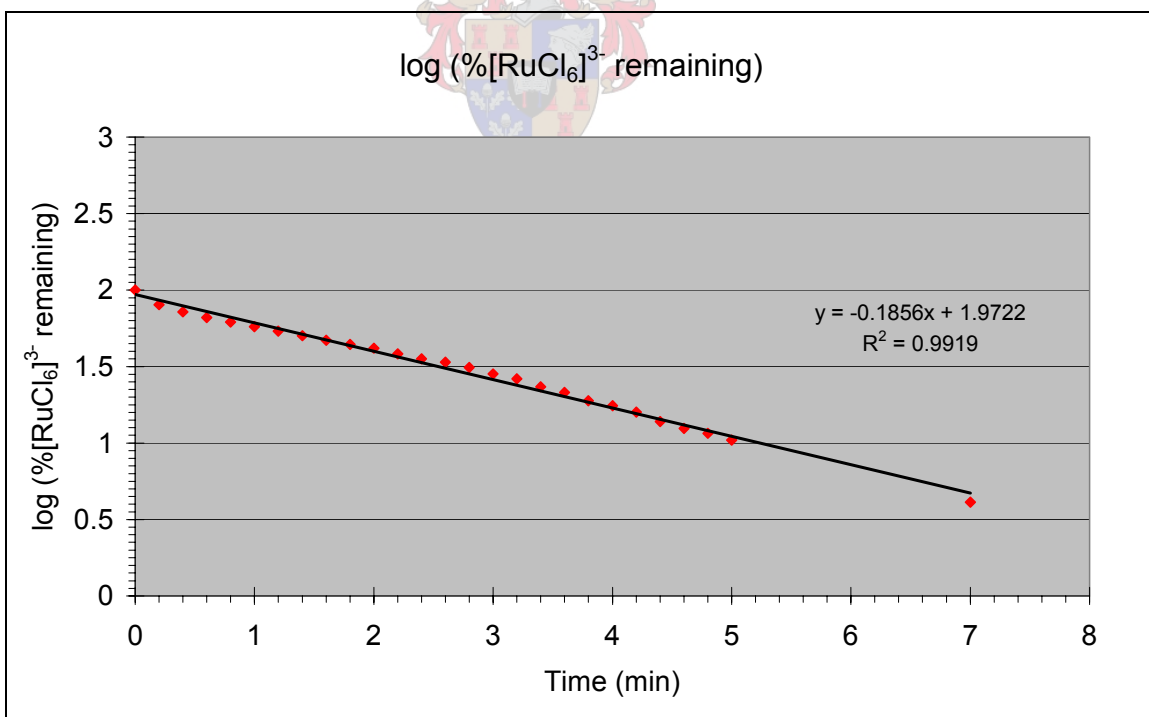
Figure B-11: Run B: Aquation of $[RuCl_6]^{3-}$ at 10°C.
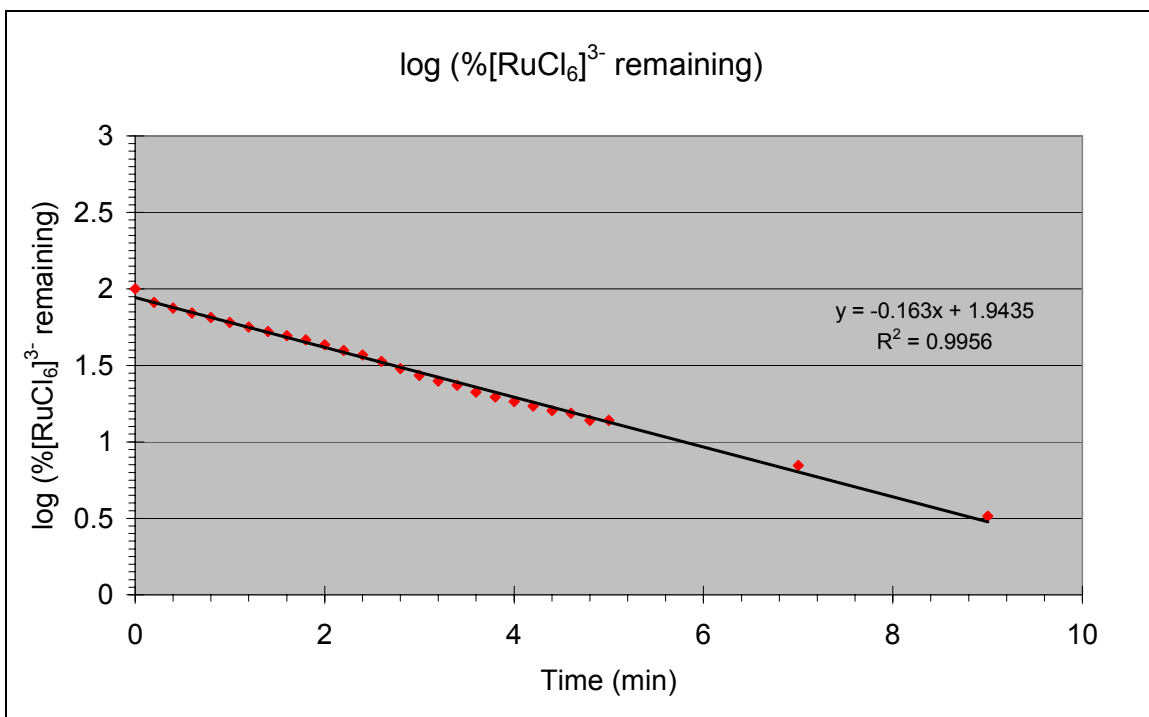
Figure B-12: Run C: Aquation of $[RuCl_6]^{3-}$ at $10^\circ C$.
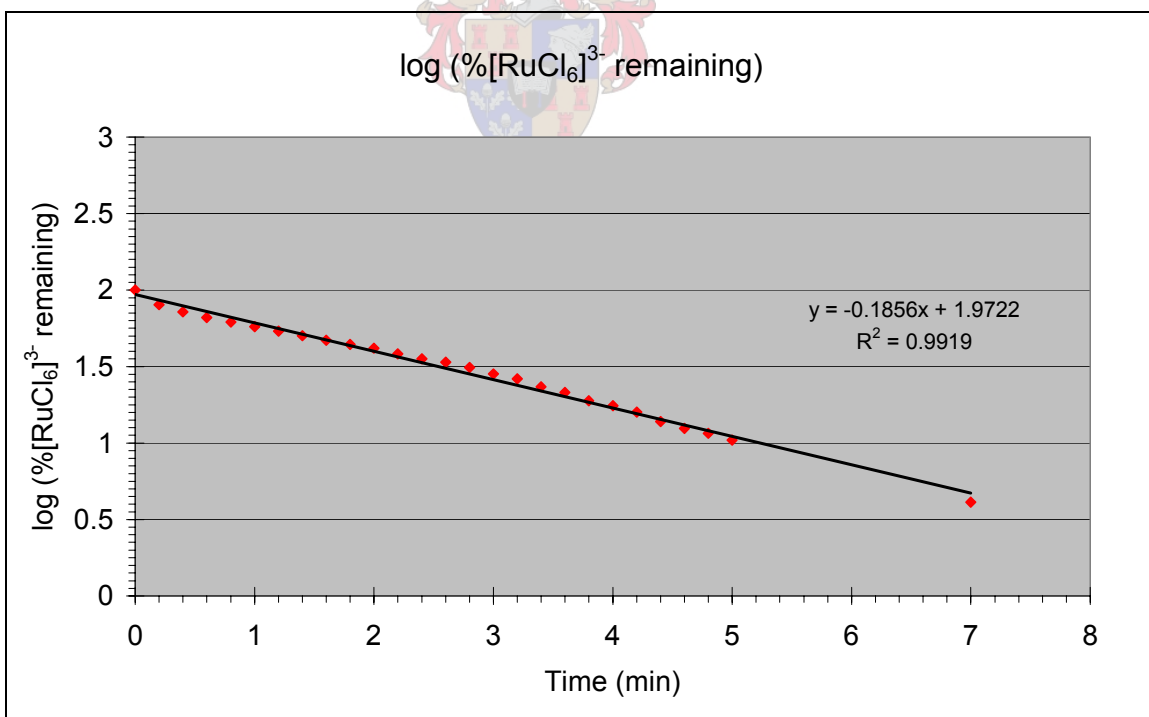
Figure B-13: Run D: Aquation of $[RuCl_6]^{3-}$ at $10^\circ C$.
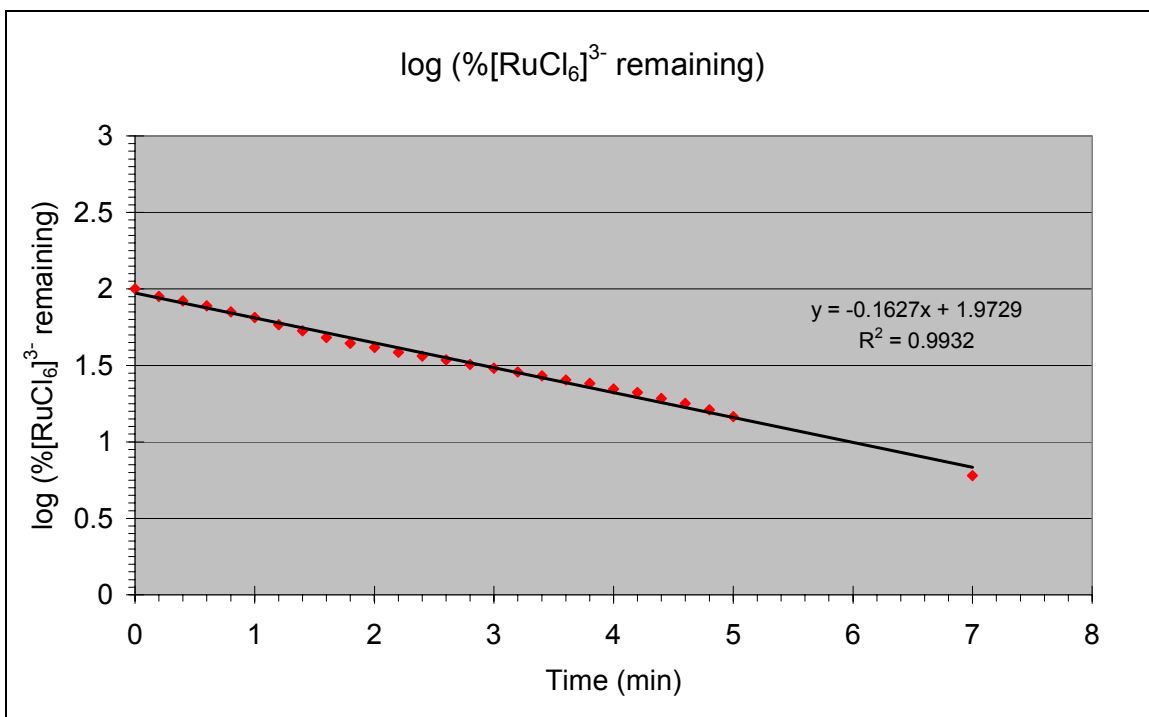
Figure B-14: Run E: Aquation of $[RuCl_6]^{3-}$ at 10°C.
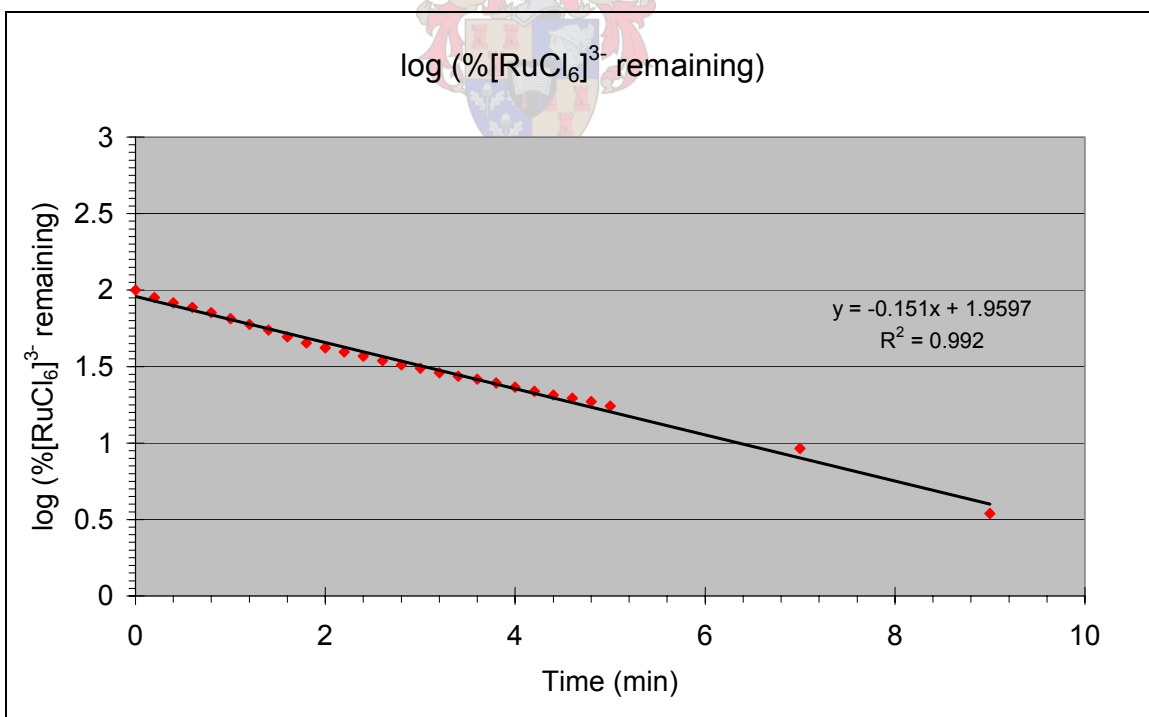
Figure B-15: Run F: Aquation of $[RuCl_6]^{3-}$ at 10°C.

B.1.4 The aquation of $[RuCl_6]^{3-}$ at 5°C

Table B-8: Data for the aquation of $[RuCl_6]^{3-}$ at 5°C.

Run no.	Ru(III) Concentration (M)	HCl Concentration (M)	Ionic strength (M)	k_{65} (min^{-1})	k_{65} x10^{-3} (s^{-1})
A	2.862x10^{-3}	1.07	1.10	0.2653	4.422
B	2.862x10^{-3}	1.07	1.10	0.2178	3.629
C	2.862x10^{-3}	1.07	1.10	0.2151	3.585
D	2.862x10^{-3}	1.07	1.10	0.2373	3.955
Average				0.2339	3.898
Std dev				0.02317	0.3865
% RSD				9.91%	9.92%
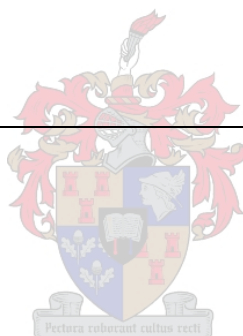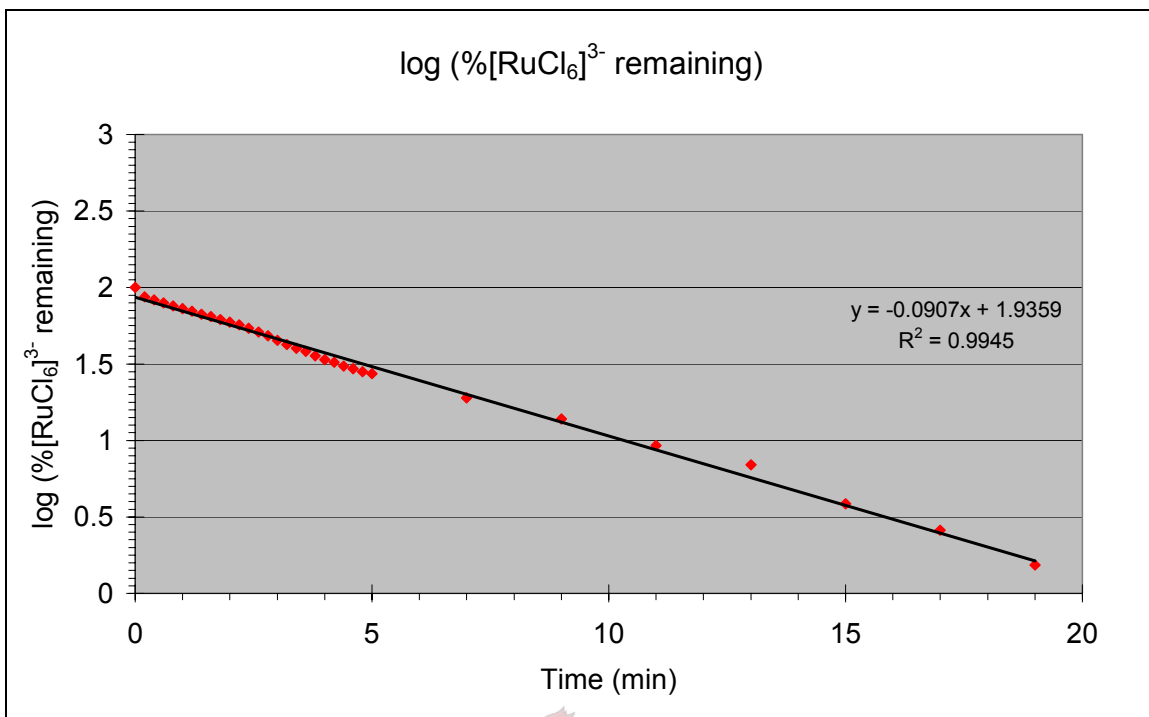
Figure B-16: Run A: Aquation of $[RuCl_6]^{3-}$ at $5°C$.
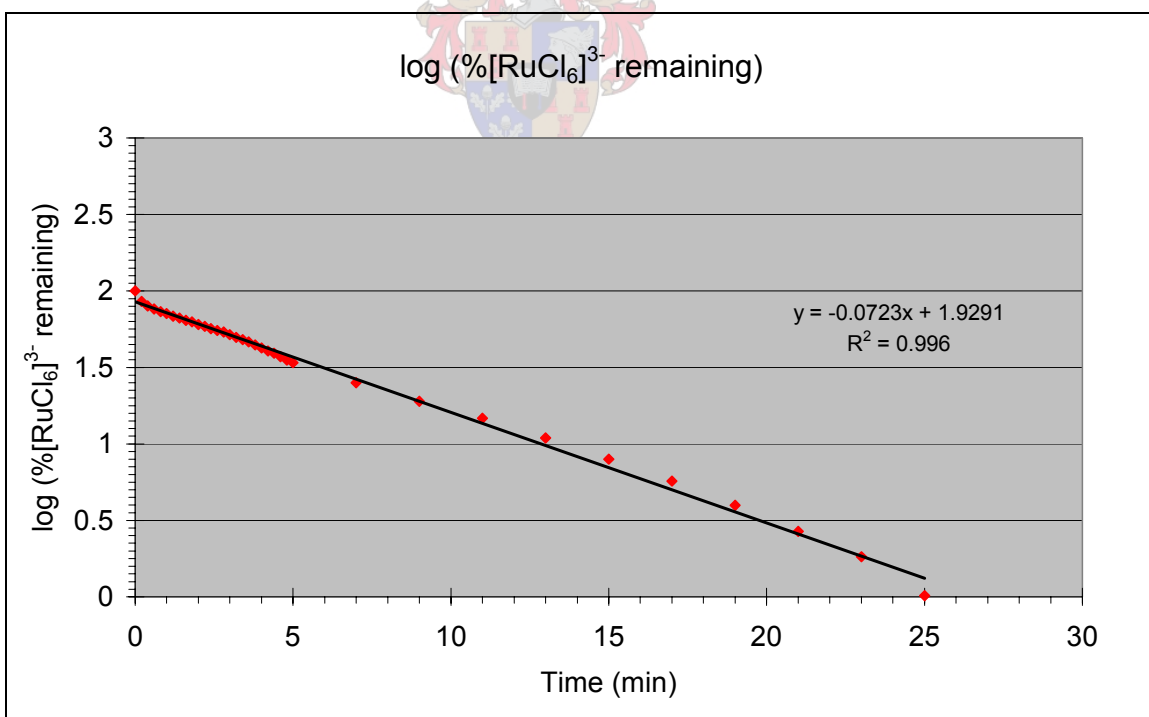
Figure B-17: Run B: Aquation of $[RuCl_6]^{3-}$ at $5°C$.
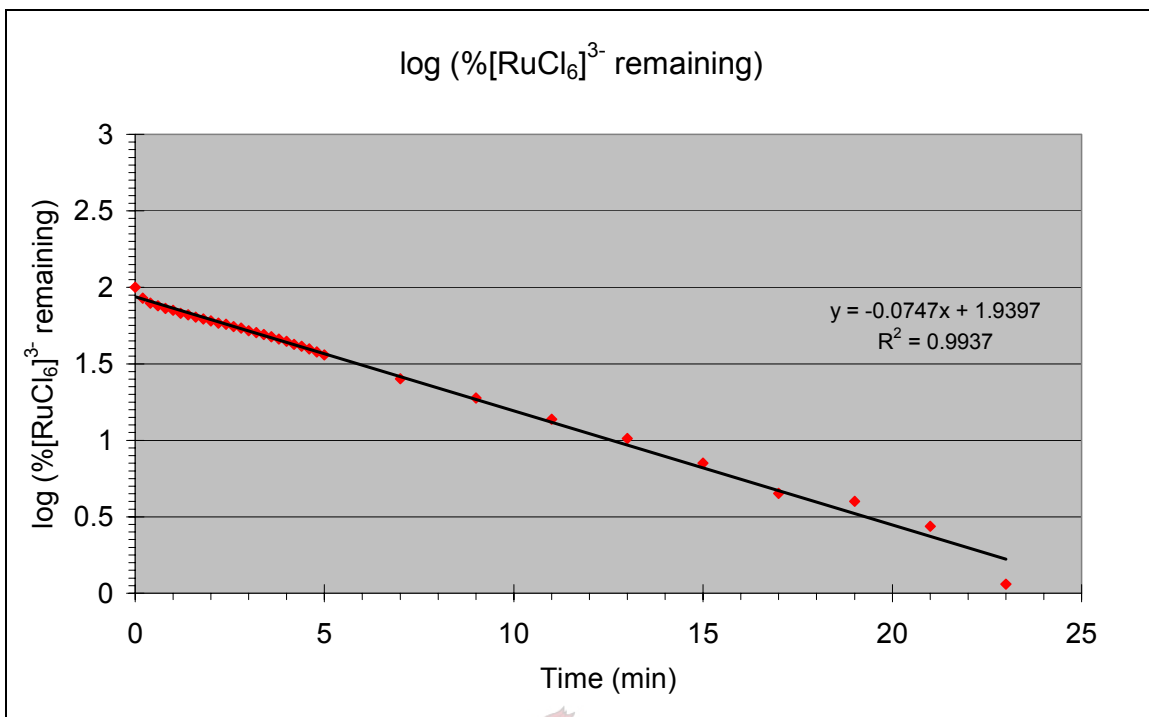
Figure B-18: Run C: Aquation of $[RuCl_6]^{3-}$ at 5°C.
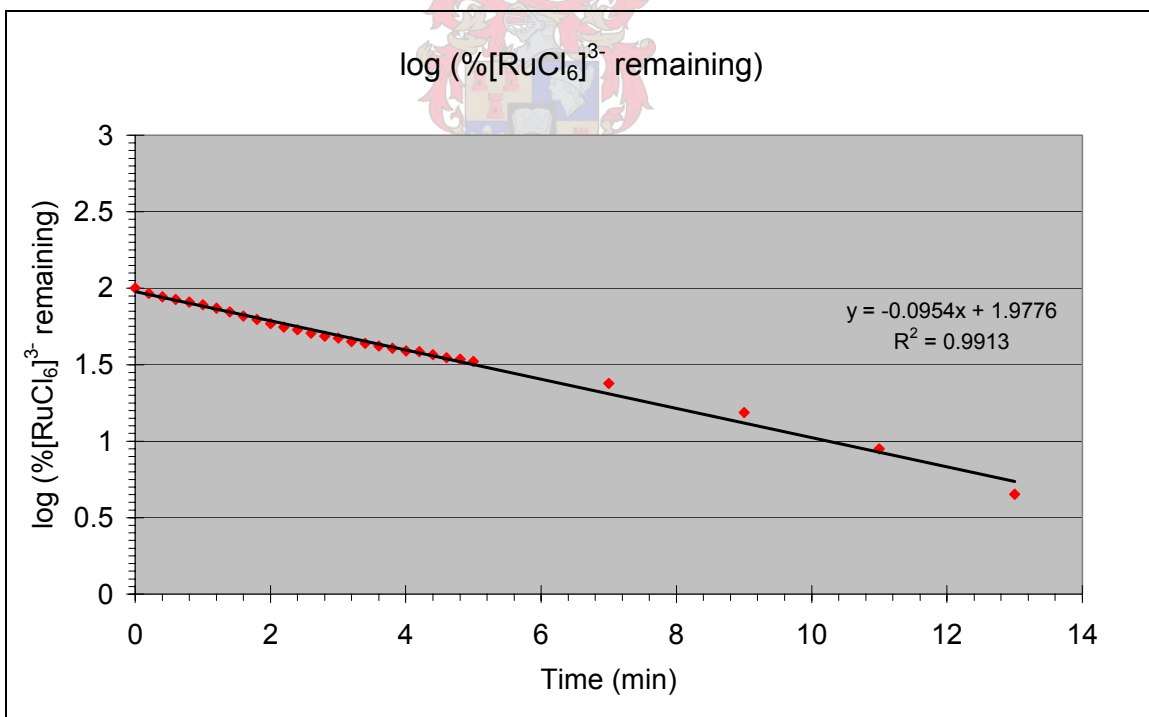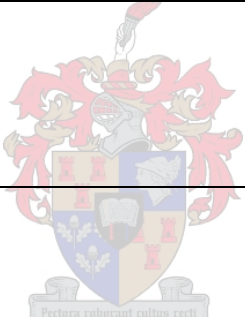
Figure B-19: Run D: Aquation of $[RuCl_6]^{3-}$ at 5°C.

B.2 CHLORIDE ANATION OF [RuCl$_5$(H$_2$O)]$^{2-}$

B.2.1 The anation of [RuCl$_5$(H$_2$O)]$^{2-}$ at 25°C

Table B-9: Data for the anation of [RuCl$_5$(H$_2$O)]$^{2-}$ at 25°C.

Run no.	Ru(III) Concentration (M)	HCl Concentration (M)	Ionic strength (M)	k_{56} (M^{-1}.min^{-1})	k_{56} x10^{-3} (M^{-1}s^{-1})
C	3.045x10^{-3}	11.18	11.21	0.06056	1.009
D	3.045x10^{-3}	11.18	11.21	0.06467	1.078
E	3.045x10^{-3}	11.18	11.21	0.05887	0.9812
F	3.045x10^{-3}	11.18	11.21	0.06189	1.031
Average				0.06150	1.025
Std dev				0.00245	0.04090
% RSD				4.0%	4.0%

Figure B-20: Run K: Anation of $[RuCl_5(H_2O)]^{2-}$ at 25°C.
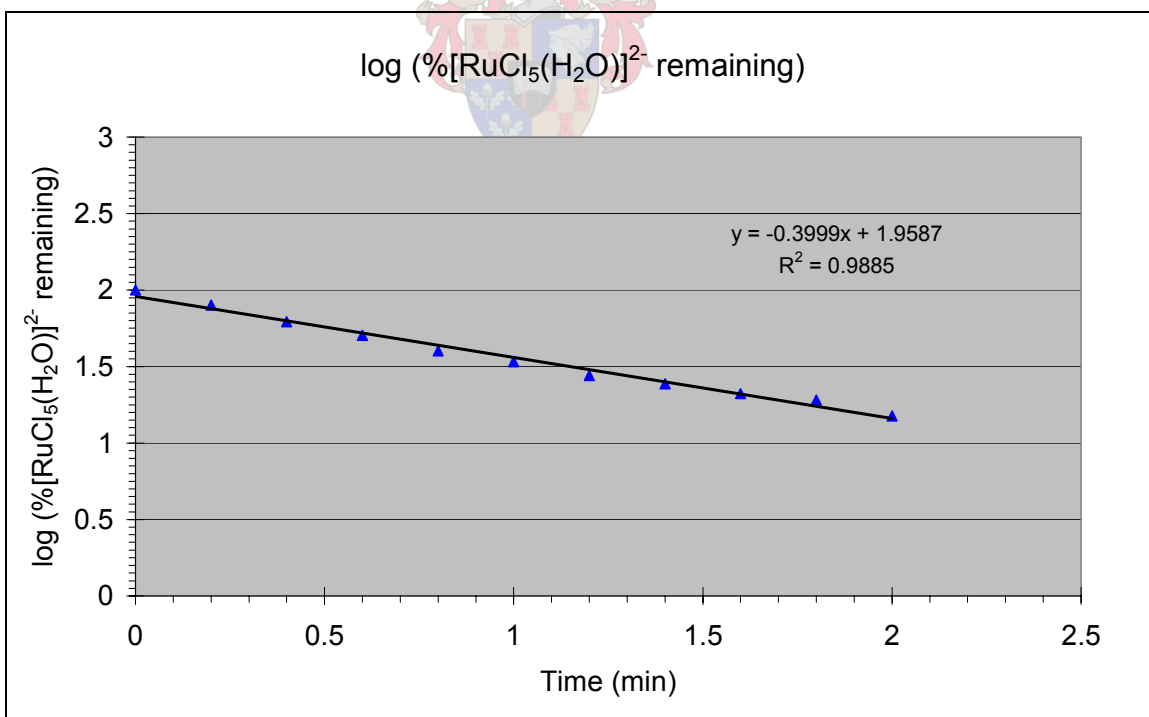
Figure B-21: Run M: Anation of $[RuCl_5(H_2O)]^{2-}$ at 25°C.
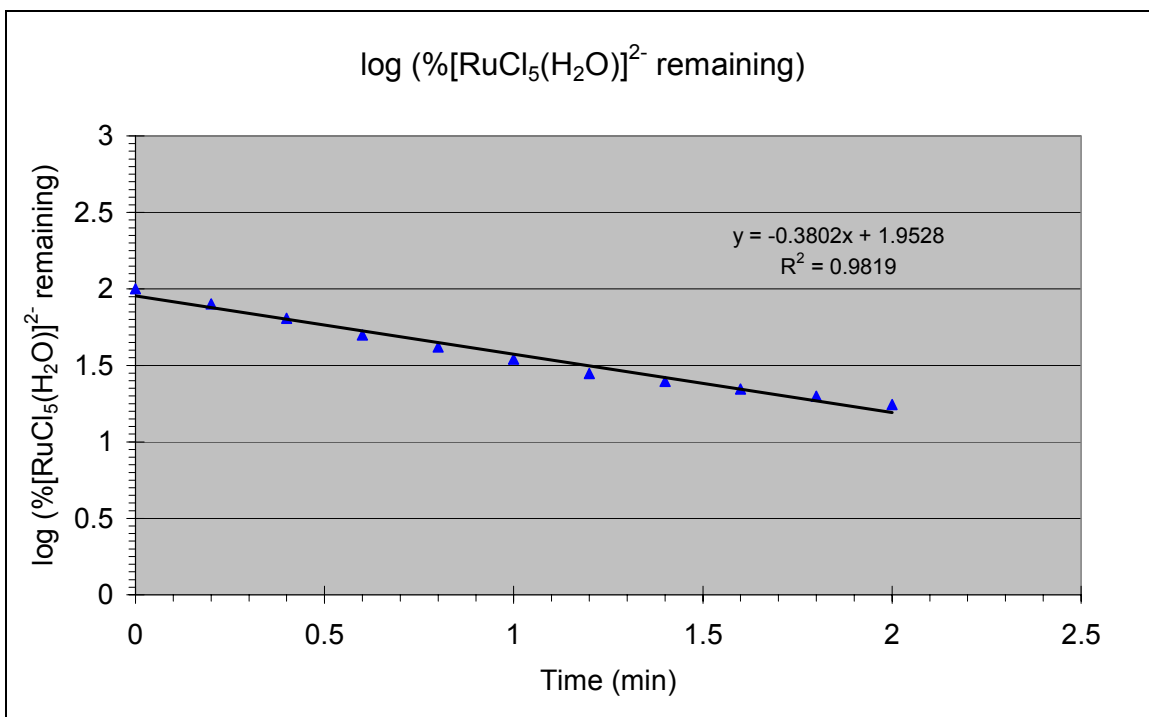
Figure B-22: Run N: Anation of $[RuCl_5(H_2O)]^{2-}$ at 25°C.

B.2.2 The anation of $[RuCl_5(H_2O)]^{2-}$ at 21°C

Table B-10: Data for the anation of $[RuCl_5(H_2O)]^{2-}$ at 21°C.

Run no.	Ru(III) Concentration (M)	HCl Concentration (M)	Ionic strength (M)	k_{56} $(M^{-1}.min^{-1})$	k_{56} $\times 10^{-3}$ $(M^{-1}s^{-1})$
C	3.007×10^{-3}	11.18	11.21	0.06056	1.009
D	3.007×10^{-3}	11.18	11.21	0.06467	1.078
E	3.007×10^{-3}	11.18	11.21	0.05887	0.9812
F	3.007×10^{-3}	11.18	11.21	0.06189	1.031
Average				0.06150	1.025
Std dev				0.00245	0.04090
% RSD				4.0%	4.0%

Figure B-23: Run C: Anation of $[RuCl_5(H_2O)]^{2-}$ at 21°C.
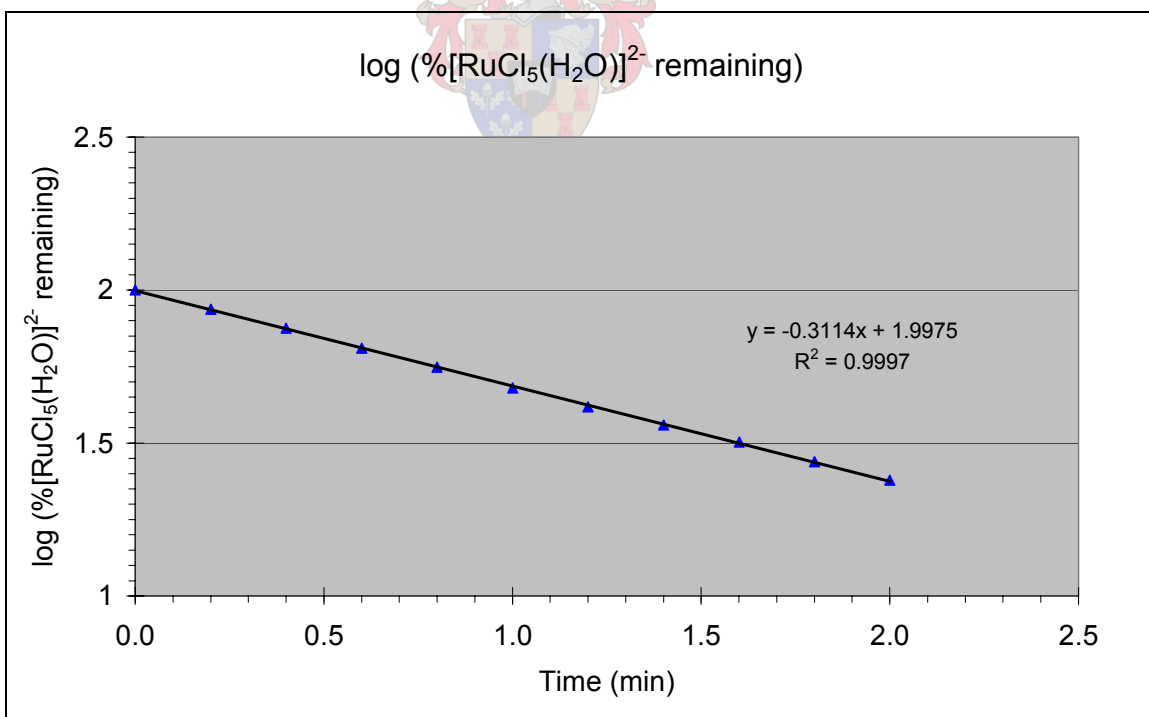
Figure B-24: Run D: Anation of $[RuCl_5(H_2O)]^{2-}$ at 21°C.
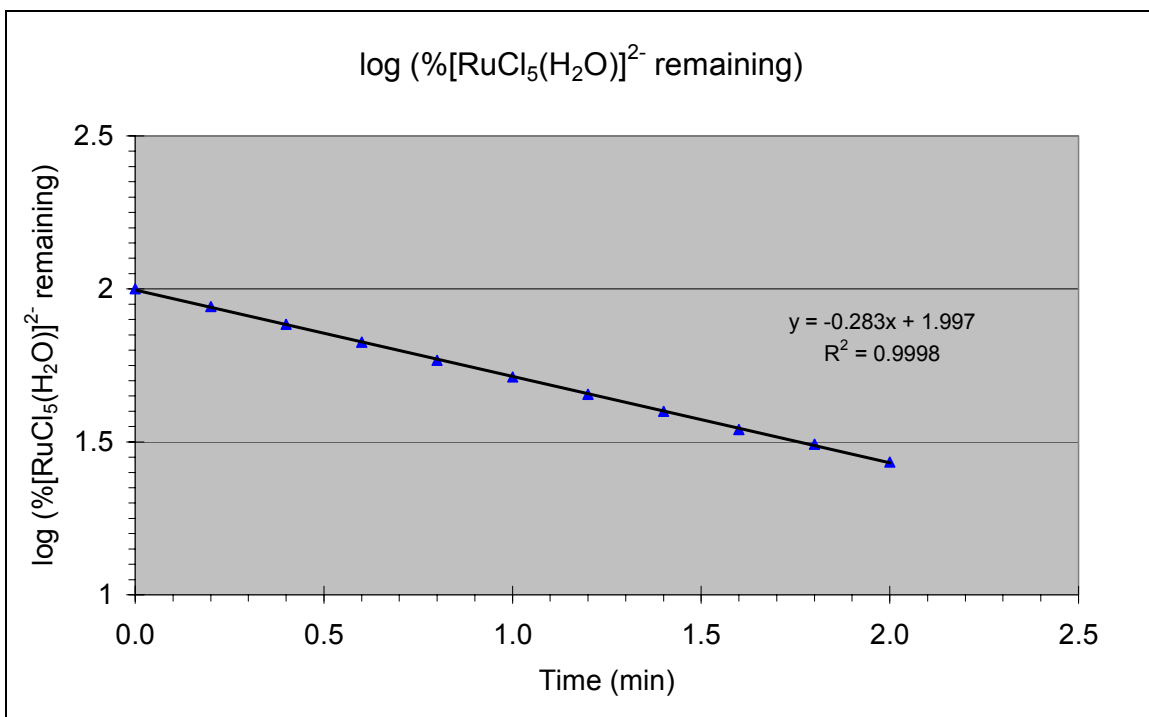
Figure B-25: Run E: Anation of $[RuCl_5(H_2O)]^{2-}$ at 21°C.
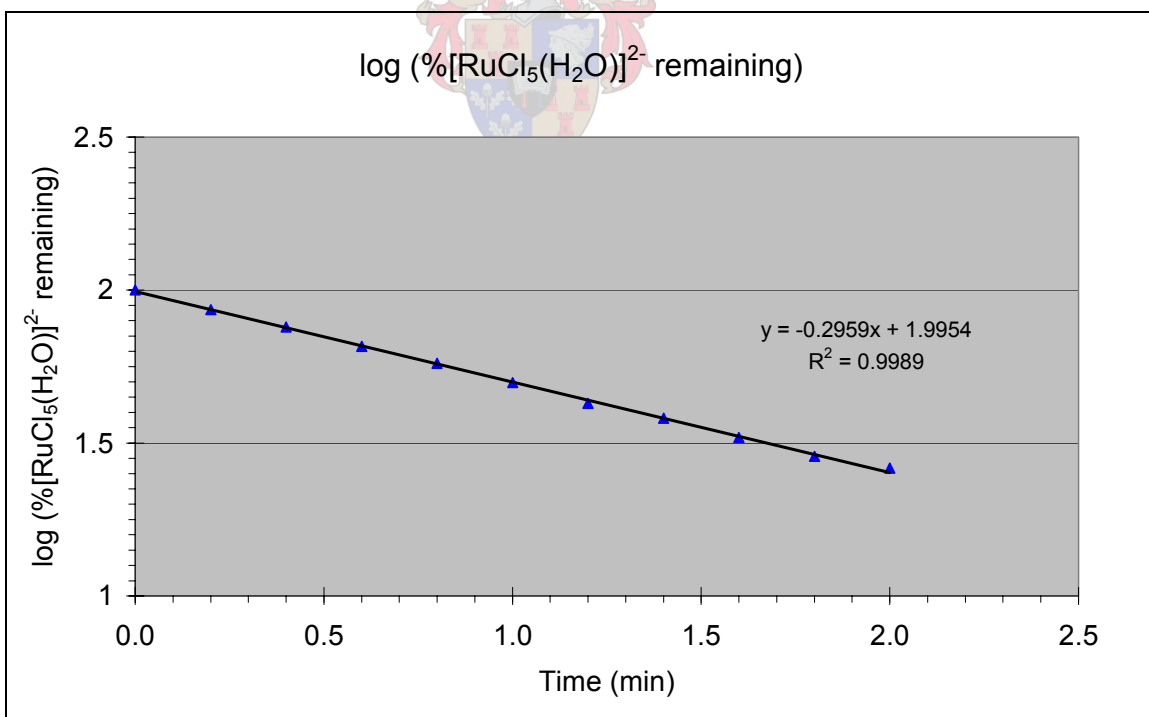
Figure B-26: Run F: Anation of $[RuCl_5(H_2O)]^{2-}$ at 21°C.

B.2.3 The anation of $[RuCl_5(H_2O)]^{2-}$ at 10°C

Table B-11: Data for the anation of $[RuCl_5(H_2O)]^{2-}$ at 10°C.

Run no.	Ru(III) Concentration (M)	HCl Concentration (M)	Ionic strength (M)	k_{56} $(M^{-1}.min^{-1})$	k_{56} x10^{-3} $(M^{-1}s^{-1})$
A	3.007×10^{-3}	11.18	11.21	0.01435	0.2392
B	3.007×10^{-3}	11.18	11.21	0.01495	0.2492
C	3.007×10^{-3}	11.18	11.21	0.01397	0.2328
D	3.007×10^{-3}	11.18	11.21	0.01428	0.2380
Average				0.01439	0.2398
Std dev				0.000411	0.00685
% RSD				2.86%	2.86%
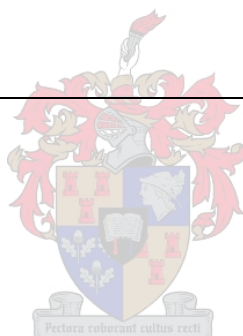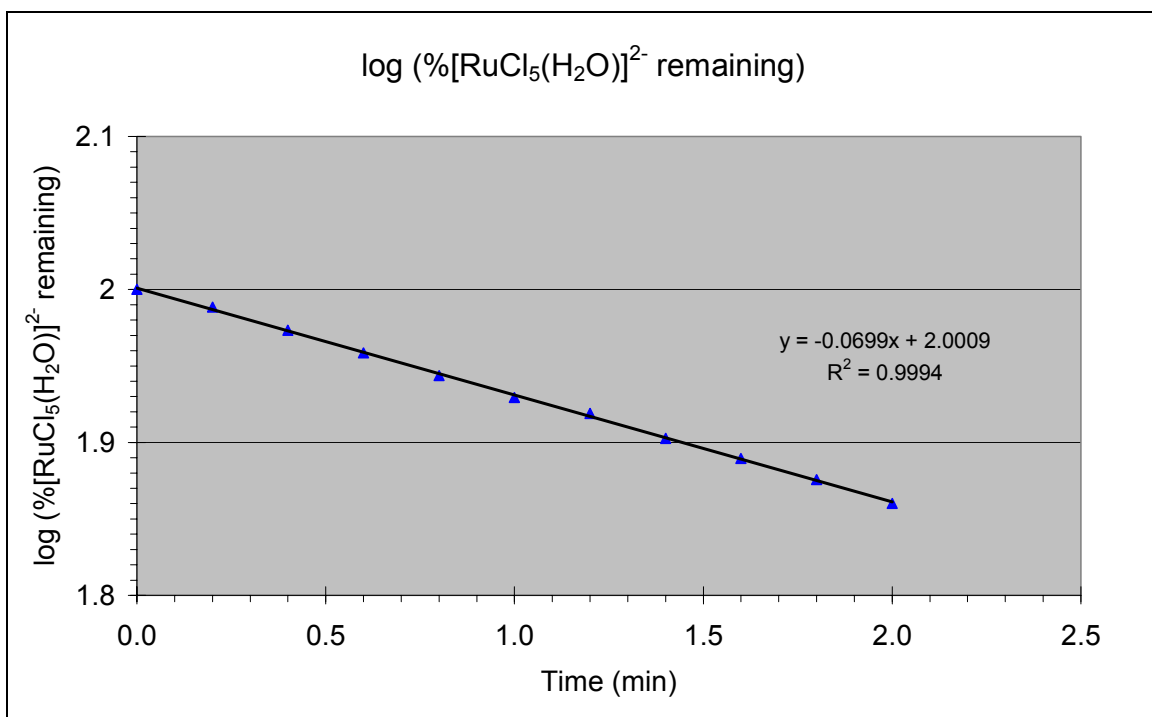
Figure B-27: Run A: Anation of $[RuCl_5(H_2O)]^{2-}$ at $10°C$.
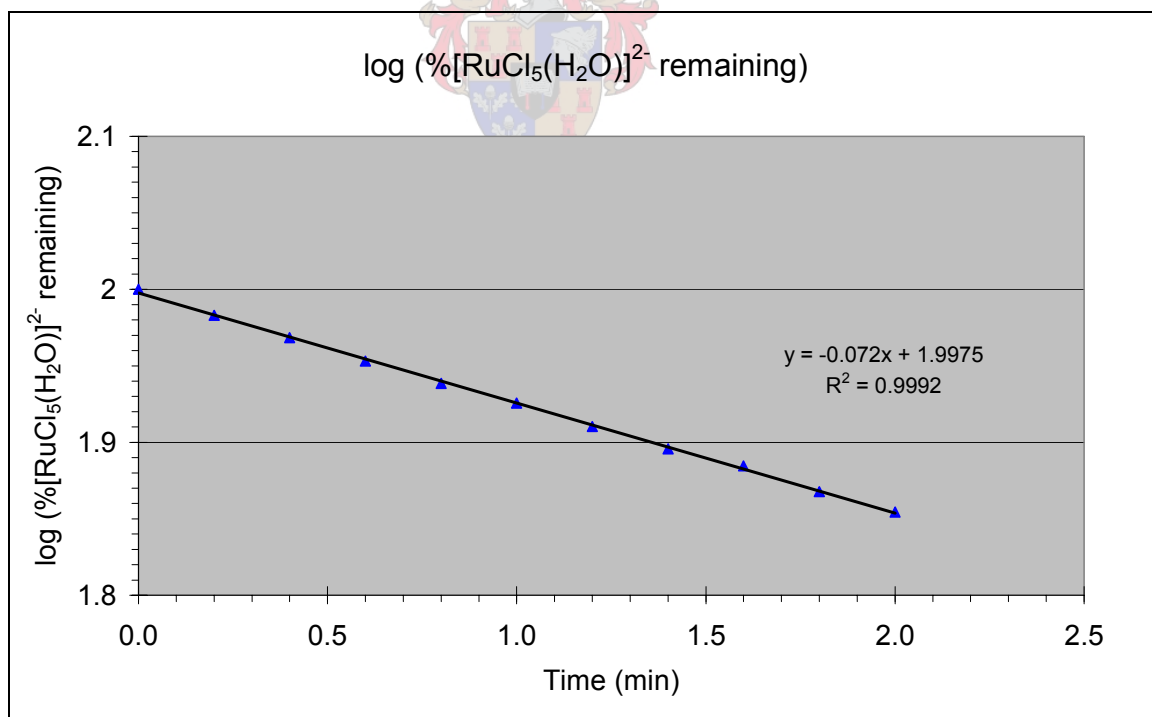
Figure B-28: Run B: Anation of $[RuCl_5(H_2O)]^{2-}$ at $10°C$.
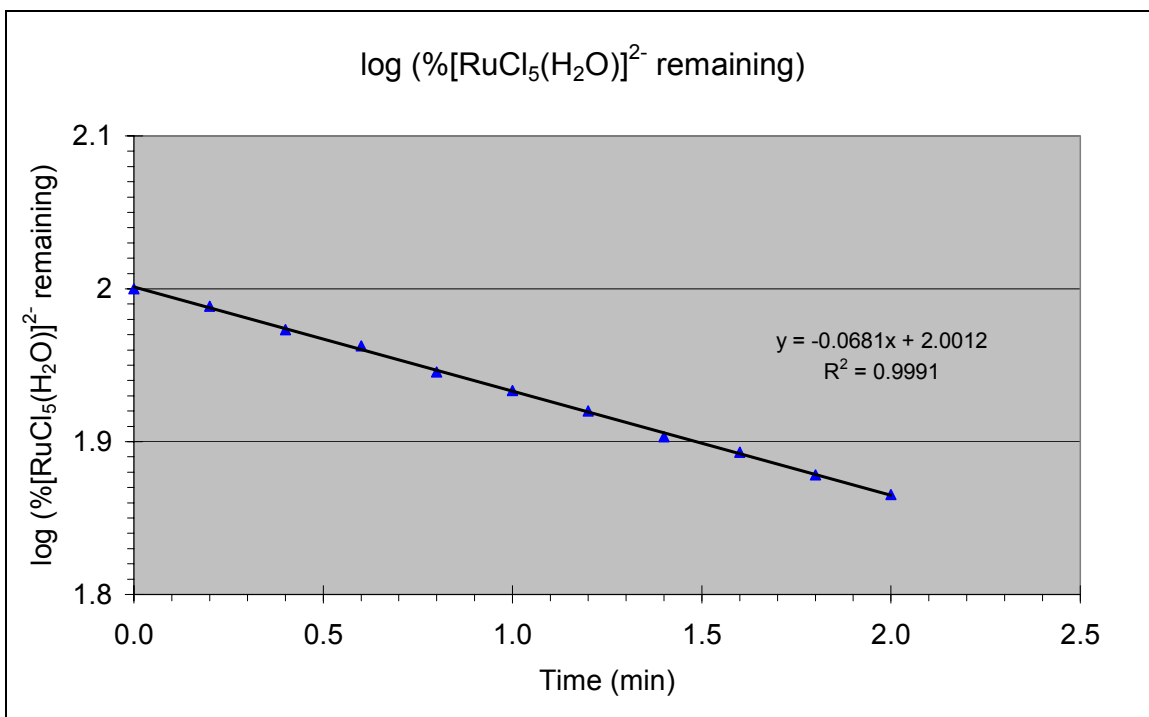
Figure B-29: Run C: Anation of $[RuCl_5(H_2O)]^{2-}$ at 10°C.
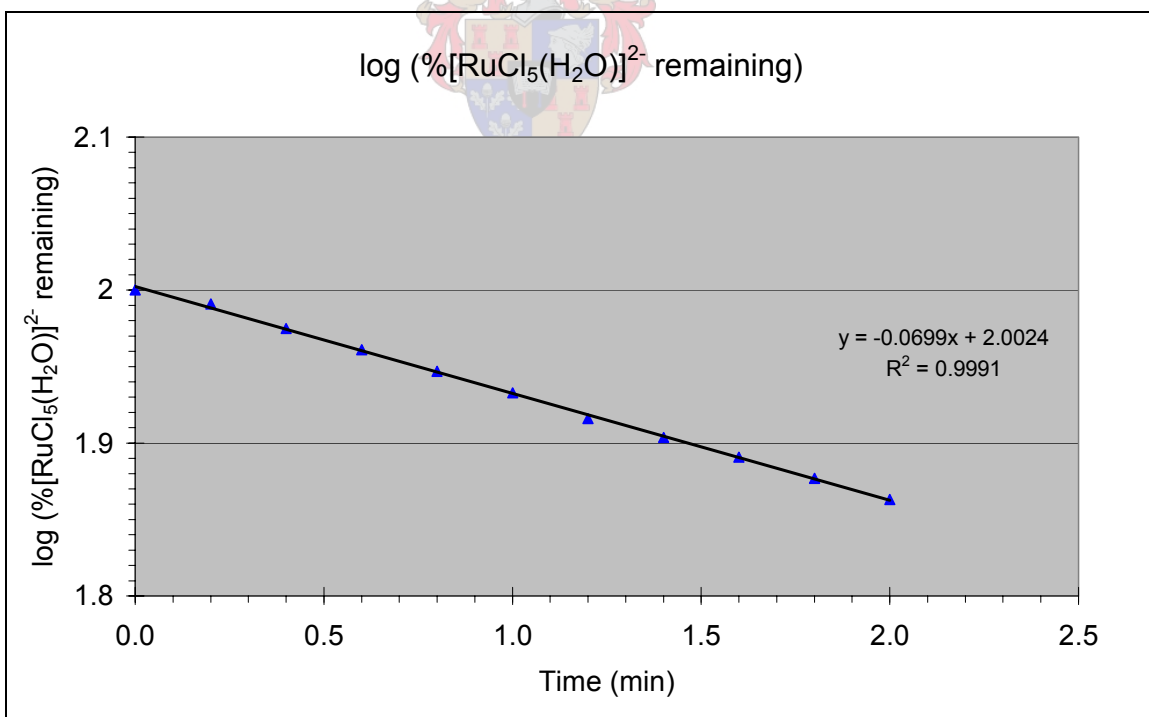
Figure B-30: Run D: Anation of $[RuCl_5(H_2O)]^{2-}$ at 10°C.

B.2.4 The anation of $[RuCl_5(H_2O)]^{2-}$ at 5°C

Table B-12: Data for the anation of $[RuCl_5(H_2O)]^{2-}$ at 5°C.

Run no.	Ru(III) Concentration (M)	HCl Concentration (M)	Ionic strength (M)	k_{56} $(M^{-1}.min^{-1})$	k_{56} x10^{-3} $(M^{-1}s^{-1})$
A	$3.007x10^{-3}$	11.18	11.21	0.008202	0.1367
B	$3.007x10^{-3}$	11.18	11.21	0.007397	0.1233
C	$3.007x10^{-3}$	11.18	11.21	0.007987	0.1331
D	$3.007x10^{-3}$	11.18	11.21	0.007386	0.1231
Average				0.007743	0.1291
Std dev				0.000415	0.00692
% RSD				5.36%	5.36%
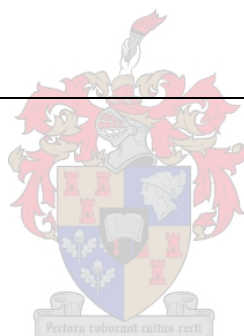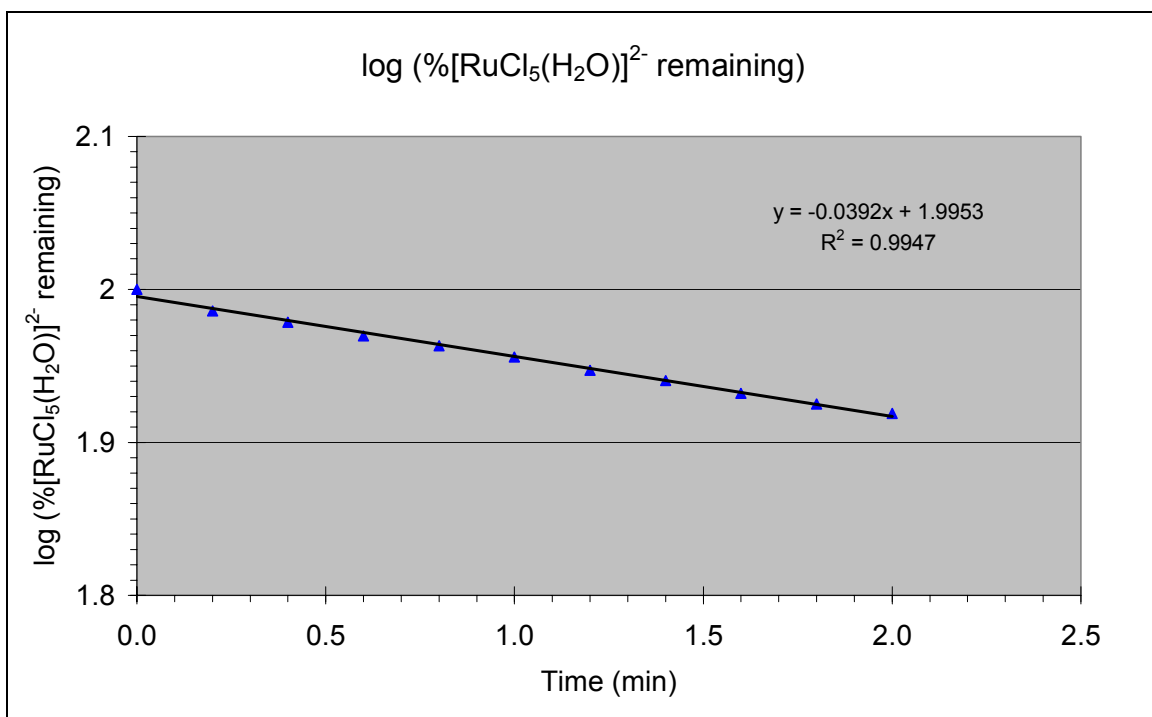
Figure B-31: Run A: Anation of $[RuCl_5(H_2O)]^{2-}$ at 5°C.
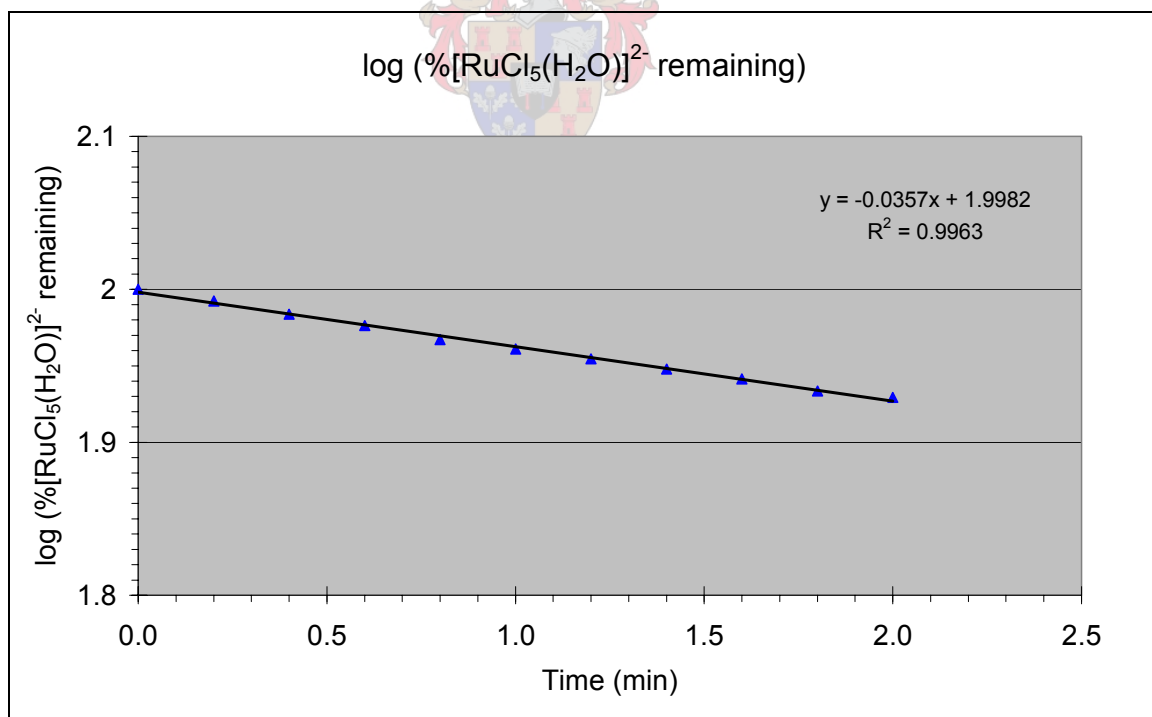
Figure B-32: Run B: Anation of $[RuCl_5(H_2O)]^{2-}$ at 5°C.
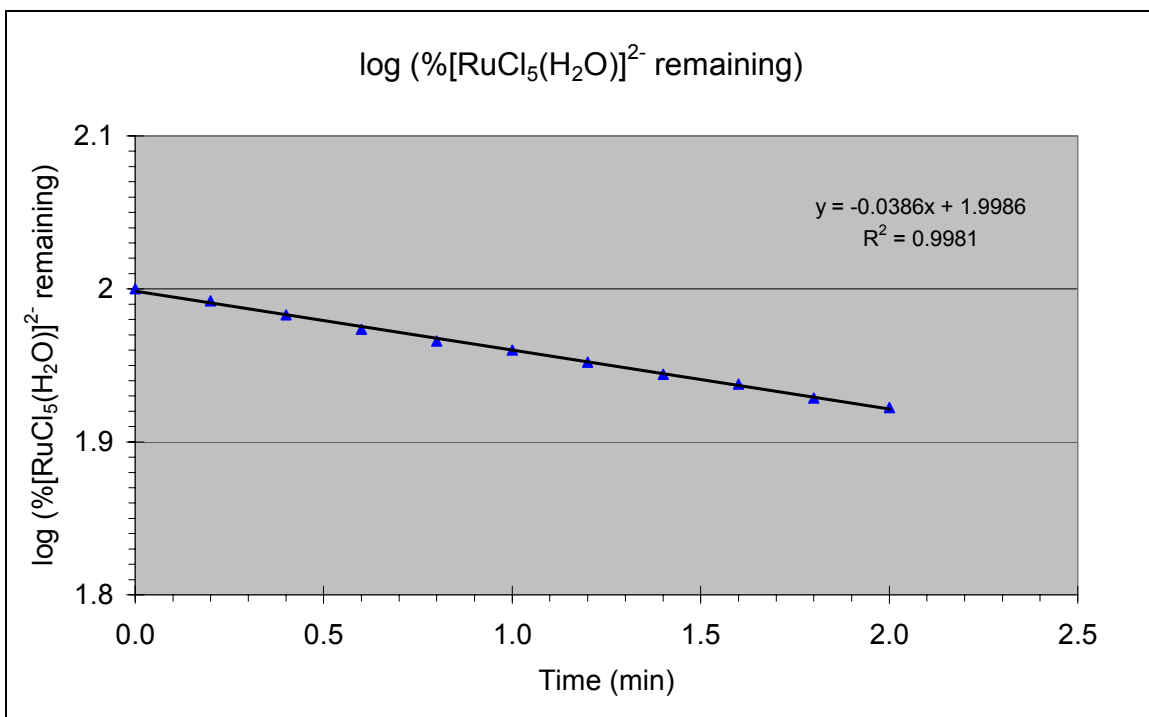
Figure B-33: Run C: Anation of $[RuCl_5(H_2O)]^{2-}$ at $5°C$.
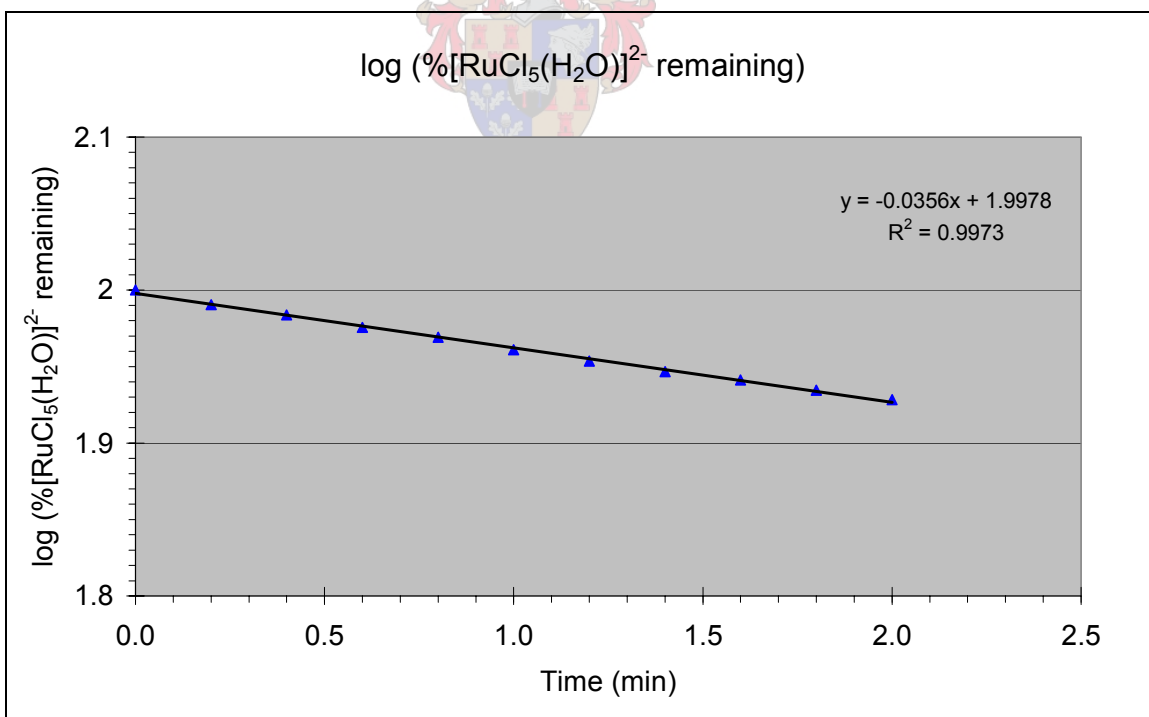

Figure B-34: Run D: Anation of $[RuCl_5(H_2O)]^{2-}$ at $5°C$.

B.3   STATISTICAL MANIPULATION OF RATE CONSTANT DATA

B.3.1 Weighted regression

The standard deviation for rate constants is expected to increase as the temperature at which the constants were determined, increase.   For this reason weighted regression[41] was attempted because all the points on the regression line would not have an equal weighting.

Table B-13: Weights calculated for the aquation rate constant data.

1/T*10^3 (K^{-1})	5°C		10°C		21°C	
	3.595		3.532		3.340	
	k_{65} (s^{-1})	ln k_{65} (s^{-1})	k_{65} (s^{-1})	ln k_{65} (s^{-1})	k_{65} (s^{-1})	ln k_{65} (s^{-1})
	0.00442	-5.42	0.00729	-4.92	0.0271	-3.61
	0.00363	-5.62	0.00785	-4.85	0.0357	-3.33
	0.00359	-5.63	0.0077	-4.87	0.0370	-3.30
	0.00396	-5.53	0.00785	-4.85	0.0271	-3.61
			0.00686	-4.98	0.03	-3.51
			0.00669	-5.01		
Average	0.00390	-5.55	0.00737	-4.91	0.0314	-3.47
Std dev	0.000386	0.0968	0.000508	0.0698	0.00473	0.149
w_i	-	0.897	-	1.73	-	0.378

The calculated weights for the rate constant at 10°C is higher than that at 21°C.   The calculated weights do not reflect the premise that the rate constants at higher temperatures should have a higher standard deviation. The weighted regression line (y=-10.625x + 32.626) did not differ significantly from the normal regression line (y=-10.713x + 32.949).   This is to be expected because the function of a weighted regression calculation is to provide proper estimates of standard deviations and confidence limits.   The calculation of the confidence interval of an estimated value from the weighted regression line could not be determined as the negative of a square root value

was obtained in the calculation. It was concluded that the weighting scheme for heteroscedastic data is not valid for the sets of data in this study.

B.3.2 Extrapolated vs experimental values

The aquation and anation rate constants (k_{65} and k_{56}) were determined at 5°C, 10°C and 21°C. The values for the rate constants at 25°C were obtained by extrapolation; k_{65} = 0.0507 ($\pm$0.0040) s^{-1} and k_{56} = 0.00164 ($\pm$0.00017) M^{-1}s^{-1}. Extrapolation is not a desirable way to obtain results and it was thus decided to experimentally obtain the rate constant determinations at 25°C. The aquation rate constant, k_{65}, was determined as 0.0521 ($\pm$0.0033) s^{-1} and the anation rate constant, k_{56}, as 0.00162 ($\pm$0.00011) M^{-1}s^{-1}. The extrapolated results compares well with the experimental results.

B.3.3 95% Confidence interval

The 95% confidence interval for the regression line was calculated using the t-test (t $_{0.025,\ 2}$= 4.303) and the formula:
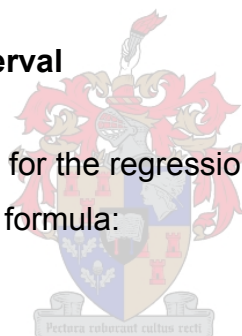
$$y\left(\pm\, t_{0.025,(n-2)} \times s\right)$$ **Equation B-1**

The calculated values are shown in table B-10 and the relative standard deviation values show a small increase as the temperature increase. This confirms the expectation that the standard deviation would increase as the temperature, at which the rate constant is determined, increase. The overall standard deviation is a product of individual standard deviations from factors influencing the rate, regression calculations, etc. The very small increase points to factors other than rate factors, such as the regression analysis, dominating the standard deviation of the rate constants determined.

Table B-14: The values for the 95% confidence interval for the aquation rate constant.

Temp (°C)	ln y	Error (s_a)	y (k_{65})	95% confidence interval	% RSD
25	-2.9542	0.014607	0.05212	0.062856	2.128%
21	-3.4485	0.014613	0.03179	0.062878	1.823%
10	-4.8801	0.014613	0.007597	0.06288	1.289%
5	-5.5682	0.014606	0.003817	0.06285	1.129%

The error of taking the antilog of the y value (ln k_{65}) was also taken into consideration using[42]:

$$\frac{s_y}{y} = s_a \qquad \text{for the calculation } e^y$$

where s_y is the error in the calculated value (y) (to be calculated) and s_a is the error in the value (ln y).
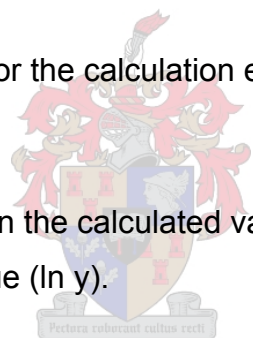
The values are shown in table B-11.

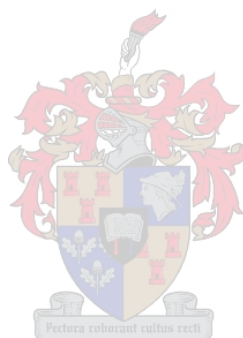**Table B-15:** The values of the standard deviations for the aquation rate constant calculated using error propagation.

Temp (°C)	ln y	Error (s_a)	y (k_{65})	s_y	% RSD
25	-2.9542	0.014607	0.05212	0.003276	6.286%
21	-3.4485	0.014613	0.03179	0.001999	6.288%
10	-4.8801	0.014613	0.007597	0.000478	6.288%
5	-5.5682	0.014606	0.003817	0.00024	6.285%

All the statistical manipulations were also applied to the anation rate constants.
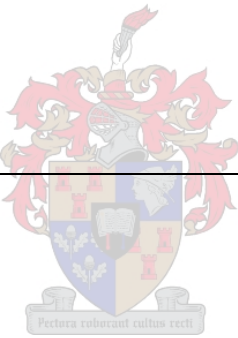
APPENDIX C – RATE CONSTANT IONIC STRENGTH DATA

C.1 THE INFLUENCE OF THE IONIC STRENGTH ON THE AQUATION RATE CONSTANT AT 10°C

C.1.1 The aquation of $[RuCl_6]^{3-}$ at 3M ionic strength

Table C-16: Data for the aquation of $[RuCl_6]^{3-}$ at 3M ionic strength.

Run no.	Ru(III) Concentration (M)	HCl Concentration (M)	Ionic strength (M)	k_{65} (min^{-1})	k_{65} x10^{-3}(s^{-1})
A	2.882×10^{-3}	1.091	3.104	0.1386	2.310
B	2.882×10^{-3}	1.091	3.104	0.1341	2.235
C	2.882×10^{-3}	1.091	3.104	0.1395	2.325
D	2.882×10^{-3}	1.091	3.104	0.1305	2.175
Average				0.1357	2.261
Std dev				0.004181	0.06969
% RSD				3.08%	3.08%
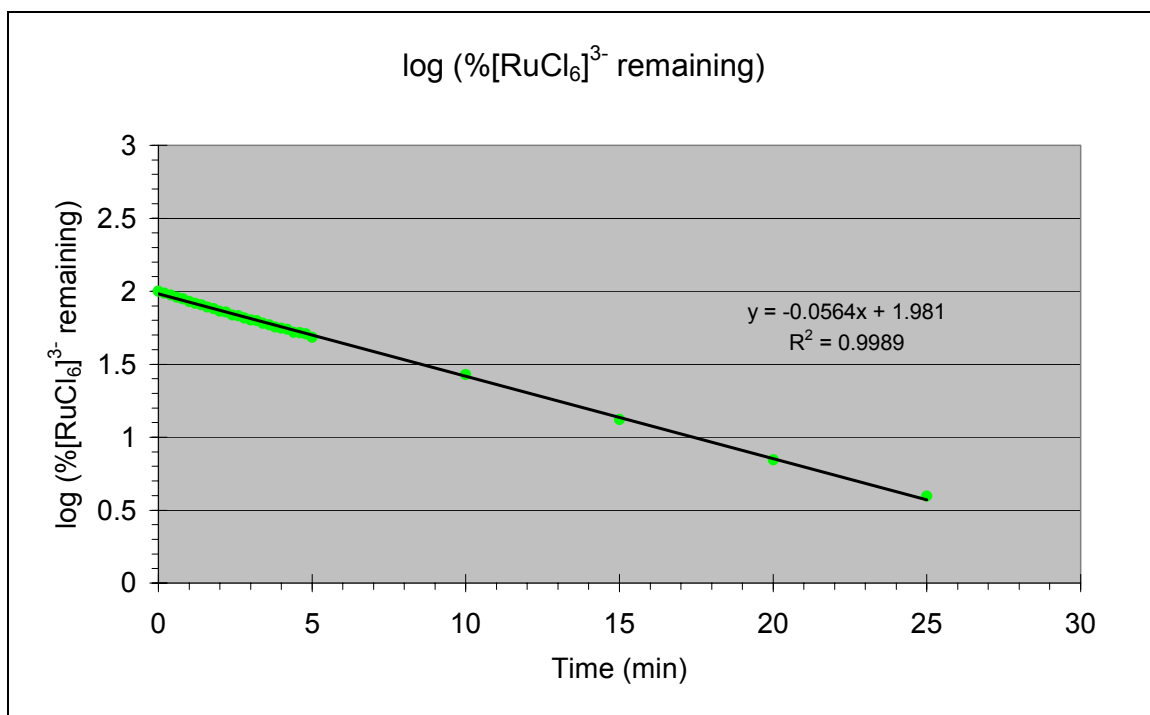
Figure C-35: Run A: Aquation of $[RuCl_6]^{3-}$ at $10°C$, 3M ionic strength.
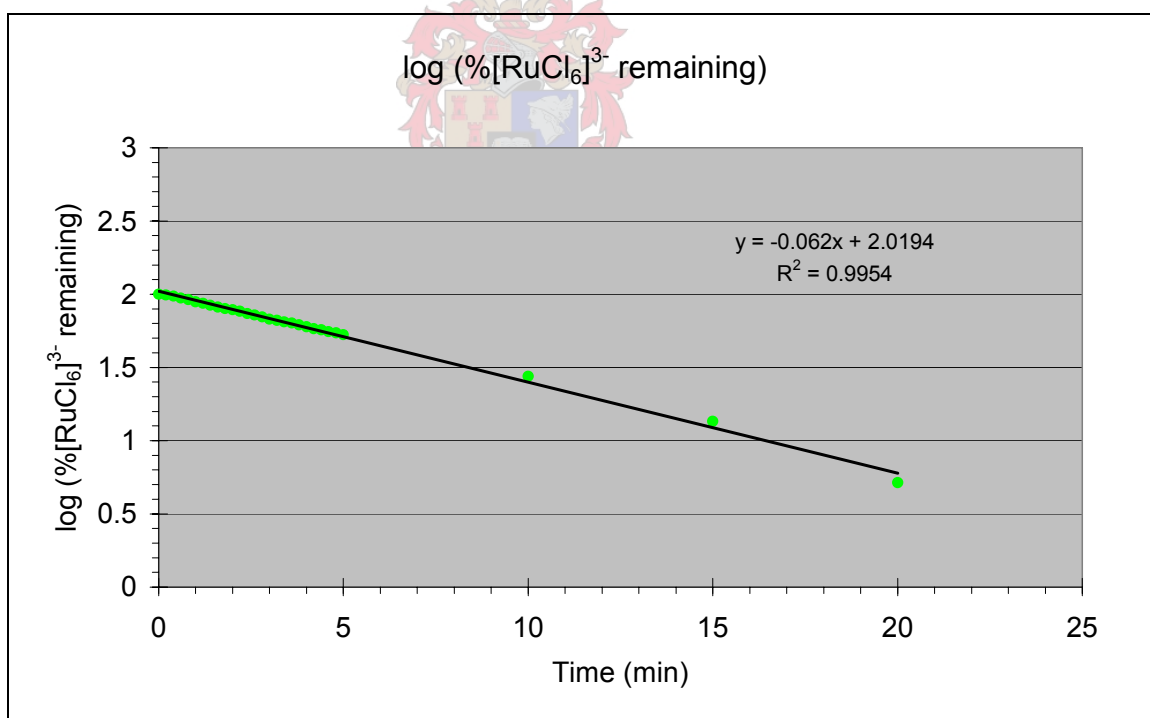
Figure C-36: Run B: Aquation of $[RuCl_6]^{3-}$ at $10°C$, 3M ionic strength.
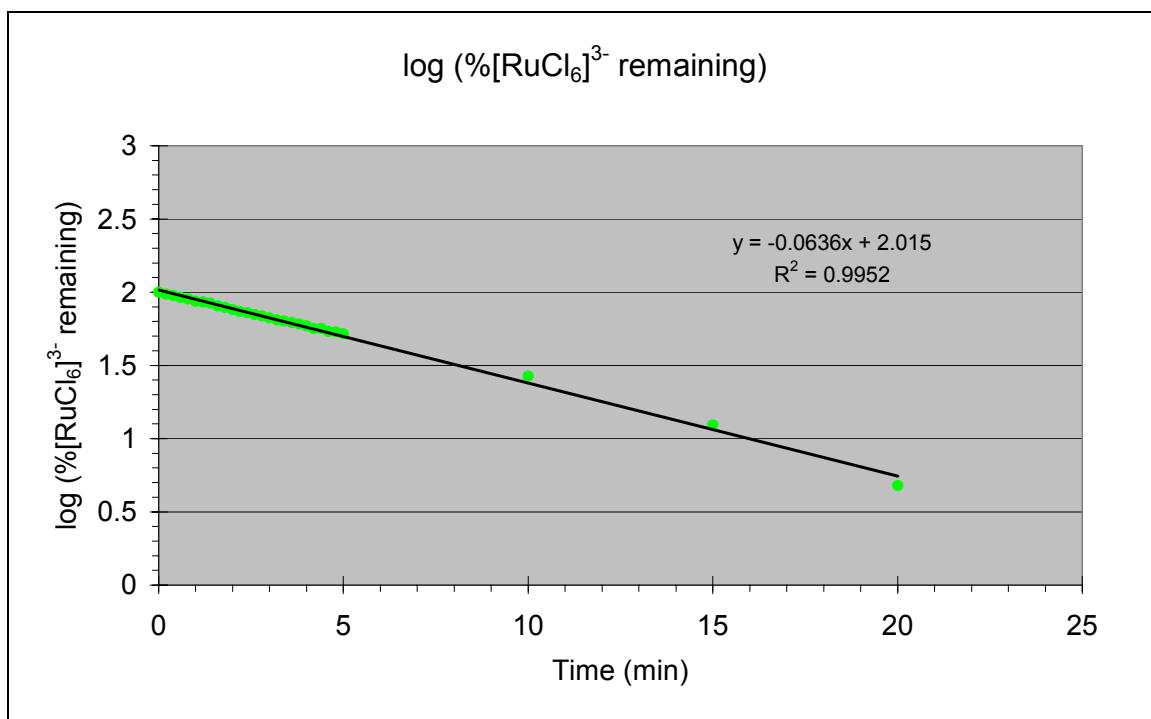
Figure C-37: Run C: Aquation of $[RuCl_6]^{3-}$ at 10°C, 3M ionic strength.
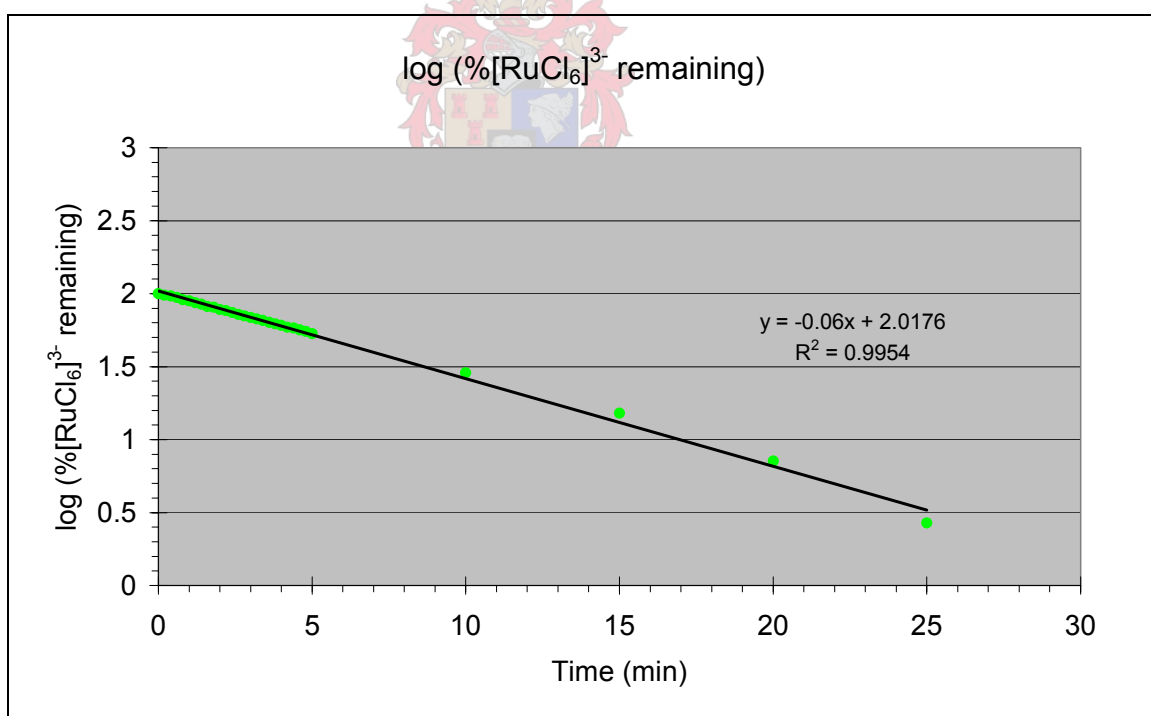

Figure C-38: Run D: Aquation of $[RuCl_6]^{3-}$ at 10°C, 3M ionic strength.

C.1.2 The influence of the ionic strength (4M) on the aquation rate constant at 10°C

Table C-17: Data for the aquation of $[RuCl_6]^{3-}$ at 4M ionic strength.

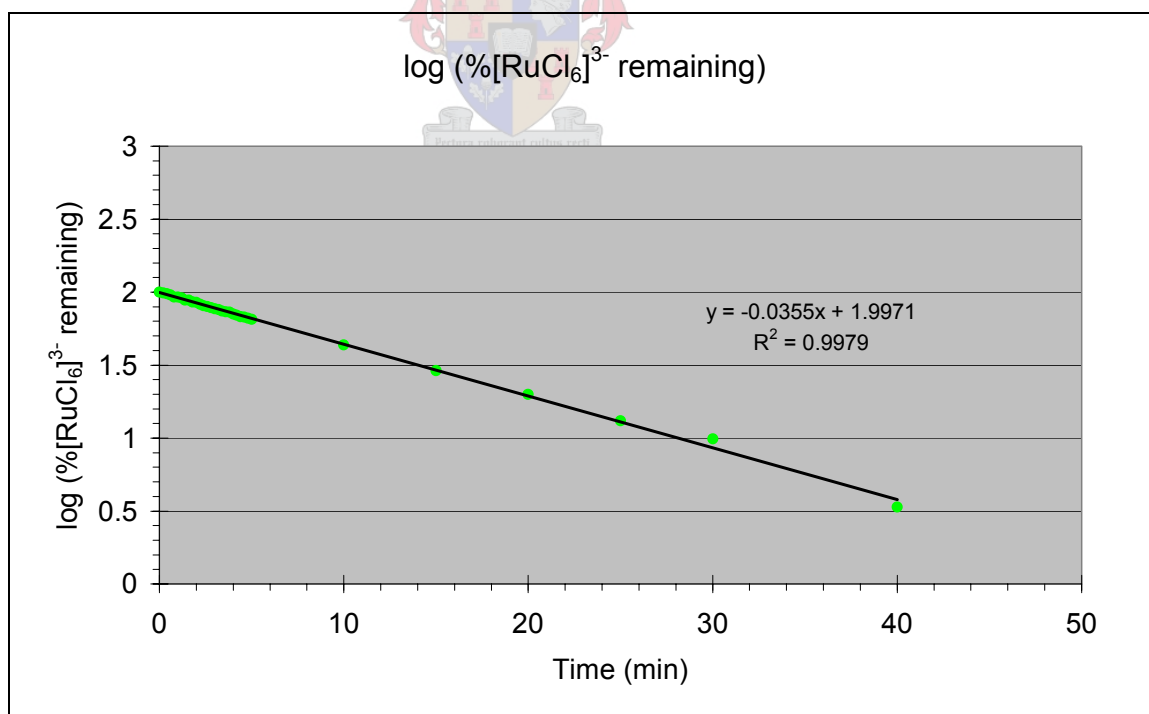| Run no.	Ru(III) Concentration (M)	HCl Concentration (M)	Ionic strength (M)	k_{65} (min^{-1})	k_{65} x10^{-3}(s^{-1})
B	2.882×10^{-3}	1.091	4.104	0.08254	1.376
C	2.882×10^{-3}	1.091	4.104	0.08874	1.479
E	2.882×10^{-3}	1.091	4.104	0.08832	1.472
F	2.882×10^{-3}	1.091	4.104	0.09007	1.501
Average				0.08742	1.457
Std dev				0.003336	0.05540
% RSD				3.82%	3.82%

Figure C-39: Run B: Aquation of $[RuCl_6]^{3-}$ at 10°C, 4M ionic strength.
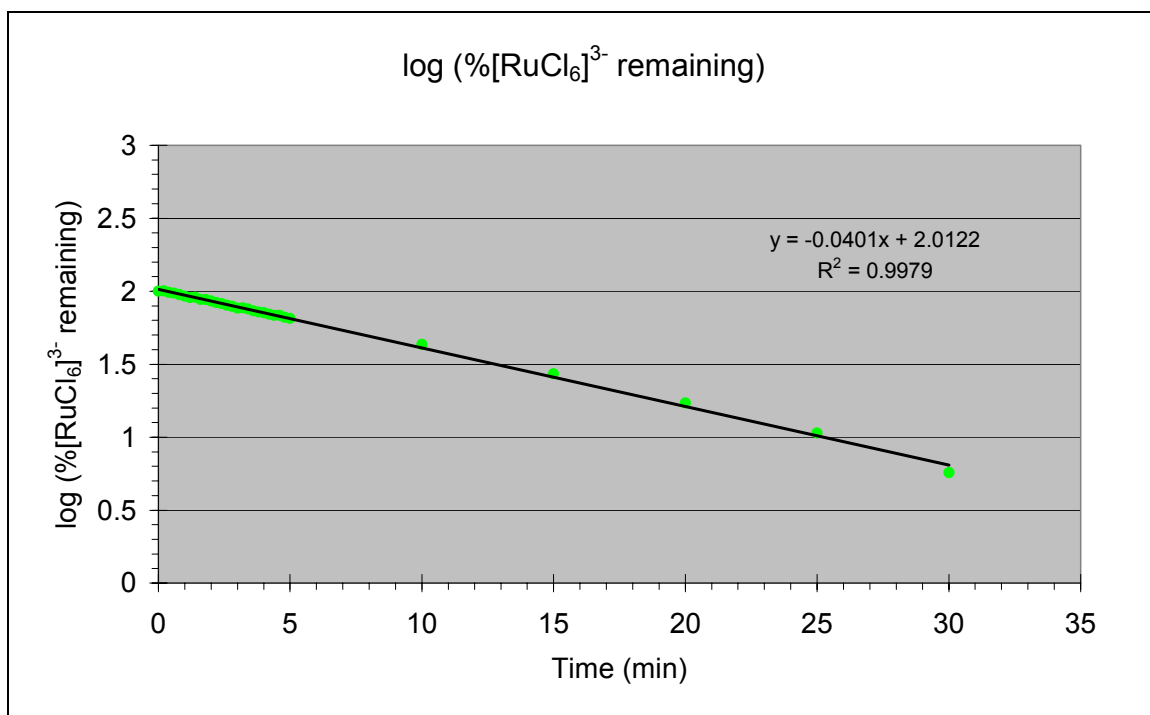
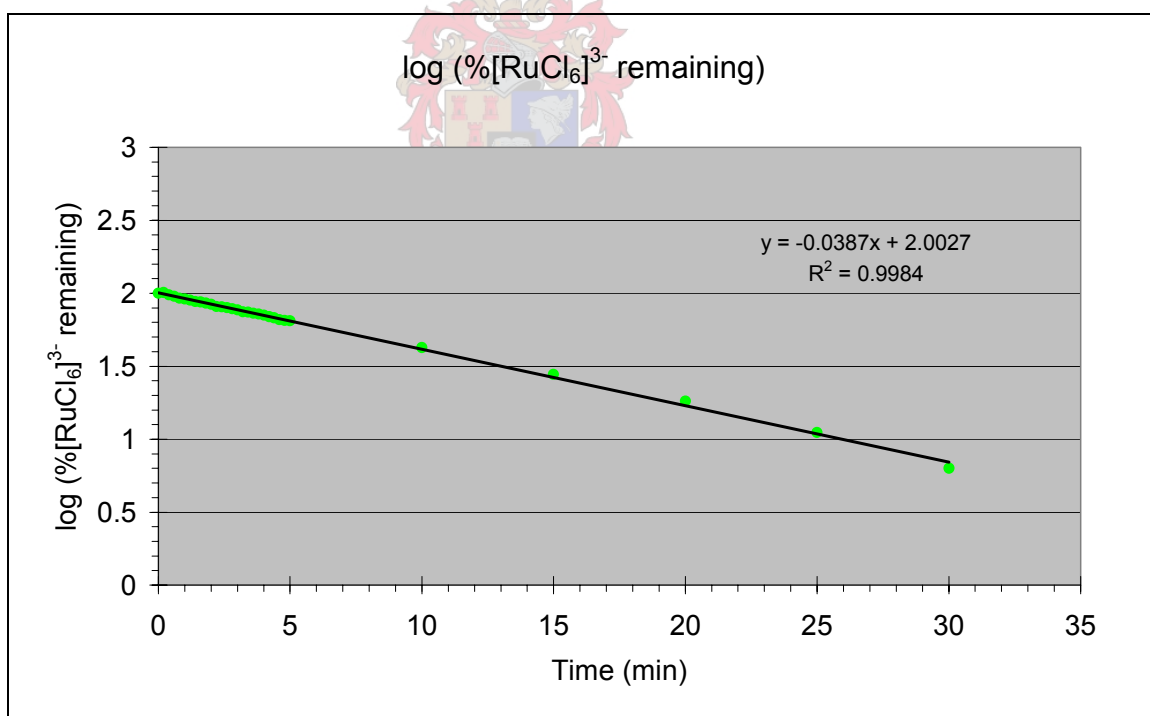**Figure C-40:** Run C: Aquation of $[RuCl_6]^{3-}$ at $10°C$, 4M ionic strength.

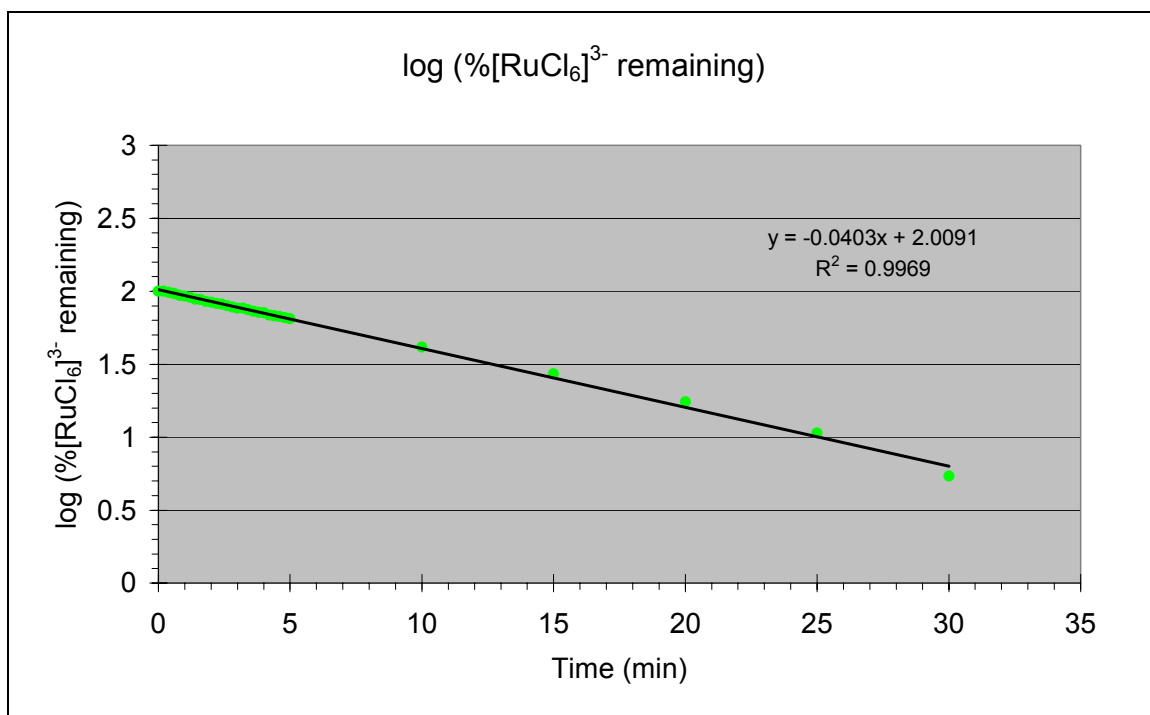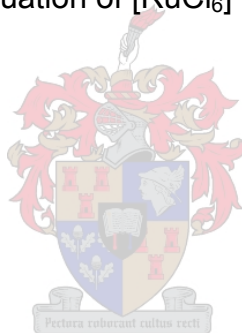**Figure C-41:** Run E: Aquation of $[RuCl_6]^{3-}$ at $10°C$, 4M ionic strength.

Figure C-42: Run F: Aquation of $[RuCl_6]^{3-}$ at $10°C$, 4M ionic strength.

C.1.3 The influence of the ionic strength (5M) on the aquation rate constant at 10°C

Table C-18: Data for the aquation of $[RuCl_6]^{3-}$ at 5M ionic strength.

Run no.	Ru(III) Concentration (M)	HCl Concentration (M)	Ionic strength (M)	k_{65} (min^{-1})	k_{65} x10^{-3}(s^{-1})
D	2.882×10^{-3}	1.091	5.104	0.06828	1.138
E	2.882×10^{-3}	1.091	5.104	0.06853	1.142
F	2.882×10^{-3}	1.091	5.104	0.07586	1.264
G	2.882×10^{-3}	1.091	5.104	0.06910	1.152
Average				0.07044	1.174
Std dev				0.003628	0.06029
% RSD				5.15%	5.15%
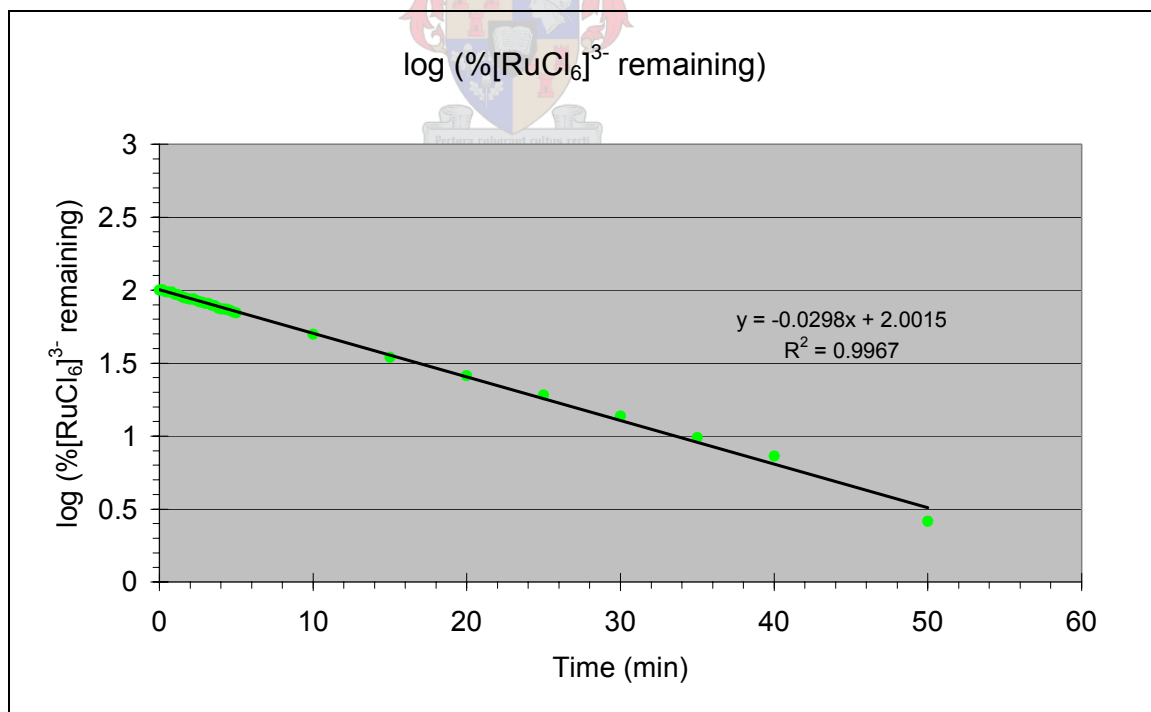
Figure C-43: Run D: Aquation of $[RuCl_6]^{3-}$ at 10°C, 5M ionic strength.
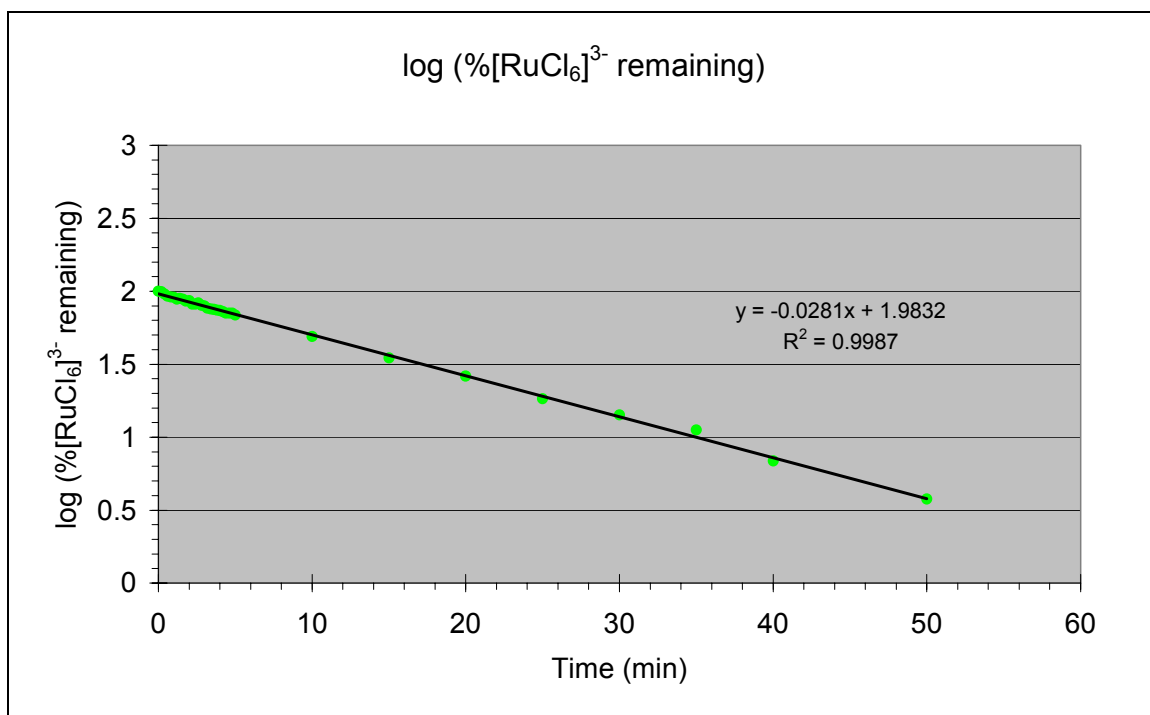
Figure C-44: Run E: Aquation of $[RuCl_6]^{3-}$ at $10°C$, 5M ionic strength.

Figure C-45: Run F: Aquation of $[RuCl_6]^{3-}$ at $10°C$, 5M ionic strength.

Figure C-46: Run G: Aquation of $[RuCl_6]^{3-}$ at $10°C$, 5M ionic strength.
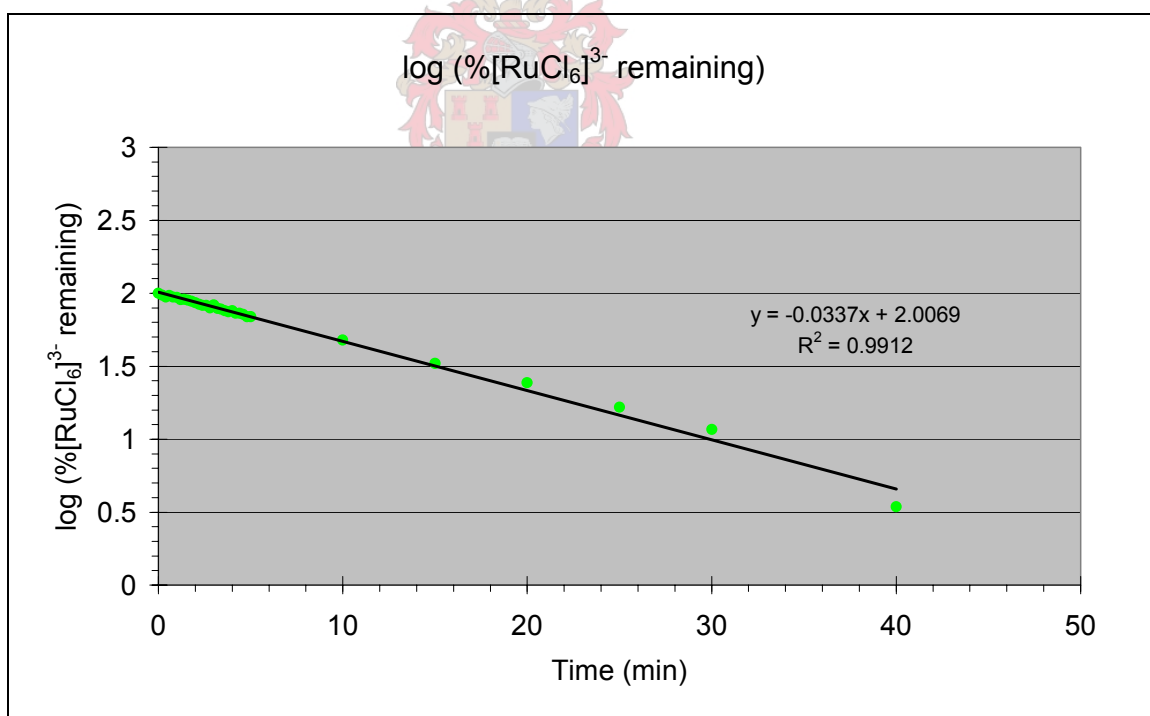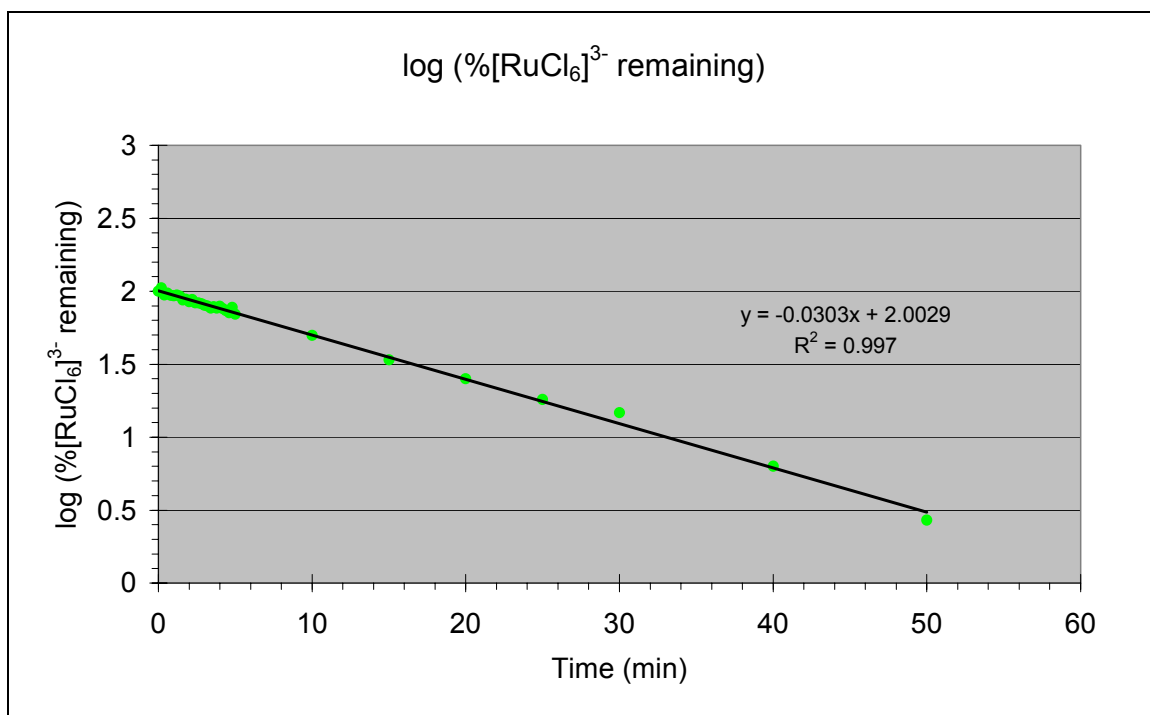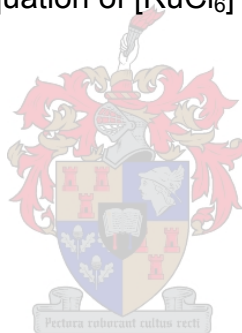
APPENDIX D – DISTRIBUTION DIAGRAM DATA

For the reaction

$$[RuCl_2(H_2O)_4]^+ + H_2O \rightleftharpoons [RuCl(H_2O)_5]^{2+} + Cl^-$$
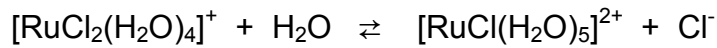
the equilibrium constant is defined as follows

$$K_2 = \frac{\left[[RuCl_2(H_2O)_4]^+\right]}{\left[[RuCl(H_2O)_5]^{2+}\right] \cdot \left[Cl^-\right]}$$
Equation D-2

The total ruthenium concentration ($[Ru]_t$) for this reaction is the sum of all the ruthenium species present

$$[Ru]_t = [[RuCl_2(H_2O)_4]^+] + [[RuCl(H_2O)_5]^{2+}]$$
Equation D-3

It follows from substitution from the equilibrium constant equation (equation D-1) and total ruthenium concentration (equation D-2):

$$[Ru]_t = K_2 [[RuCl(H_2O)_5]^{2+}][Cl^-] + [[RuCl(H_2O)_5]^{2+}]$$

Rearrangement of this gives:

$$[Ru]_t = [[RuCl(H_2O)_5]^{2+}] (K_2[Cl^-] + 1)$$

$$[[RuCl(H_2O)_5]^{2+}] = \frac{[Ru]_t}{(K_2[Cl^-] + 1)}$$
Equation D-4

Similarly, for the reaction of the neutral species, $[RuCl_3(H_2O)_3]$, can be used to calculate the amount of $[RuCl(H_2O)_5]^{2+}$

$$[RuCl_3(H_2O)_3] + H_2O \rightleftarrows [RuCl_2(H_2O)_4]^+ + Cl^-$$

$$K_3 = \frac{[[RuCl_3(H_2O)_3]]}{[[RuCl_2(H_2O)_4]^+] \cdot [Cl^-]}$$ **Equation D-5**

The total ruthenium concentration ($[Ru]_t$) for this reaction is the sum of all the ruthenium species present

$$[Ru]_t = [[RuCl_3(H_2O)_3]] + [[RuCl_2(H_2O)_4]^+] + [[RuCl(H_2O)_5]^{2+}]$$

Equation D-6

It follows from substitution from the equilibrium constant equation (equation D-4) and total ruthenium concentration (equation D-5):
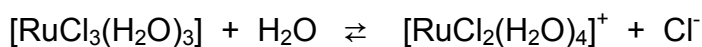
$$[Ru]_t = K_3[[RuCl_2(H_2O)_4]^+][Cl^-] + K_2[[RuCl(H_2O)_5]^{2+}][Cl^-] + [[RuCl(H_2O)_5]^{2+}]$$
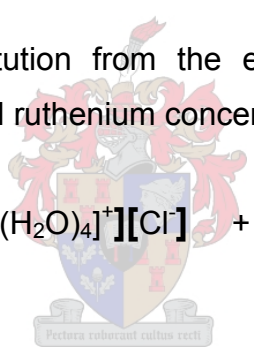
$$[Ru]_t = K_3K_2[[RuCl(H_2O)_5]^{2+}][Cl^-]^2 + K_2[[RuCl(H_2O)_5]^{2+}][Cl^-] + [[RuCl(H_2O)_5]^{2+}]$$

$$[Ru]_t = [[RuCl(H_2O)_5]^{2+}] (K_3K_2[Cl^-]^2 + K_2[Cl^-] + 1)$$

Equation D-7

This can be done for all the species in the $[RuCl_{6-n}(H_2O)_n]^{n-3}$ series. The final equation for the determination of $[RuCl(H_2O)_5]^{2+}$ species will be:

$$\left[[RuCl(H_2O)_5]^{2+}\right] =$$

$$\frac{[Ru]_t}{K_6K_5K_4K_3K_2[Cl^-]^5 + K_5K_4K_3K_2[Cl^-]^4 + K_4K_3K_2[Cl^-]^3 + K_3K_2[Cl^-]^2 + K_2[Cl^-] + 1}$$

Equation D-8

Using equation D-7, the data in the following tables was calculated and the distribution diagram constructed.

K_1														
K_2	2.80	2.78	2.78	2.78	2.78	2.78	2.78	2.78	2.78	2.78	2.78	2.78	2.78	2.78
K_3	2.63	2.63	2.63	2.63	2.63	2.63	2.63	2.63	2.63	2.63	2.63	2.63	2.63	2.63
K_4	0.9597	0.9564	0.8999	0.841	0.786	0.7345	0.6864	0.6415	0.5995	0.5603	0.5236	0.4893	0.4573	0.4274
K_5	0.0379	0.0384	0.0496	0.0658	0.0874	0.116	0.1541	0.2046	0.2716	0.3606	0.4787	0.6356	0.8439	1.1205
K_6	0.0151	0.003	0.0301	0.0602	0.0903	0.1204	0.1505	0.1806	0.2107	0.2408	0.2709	0.301	0.3311	0.3612
[Cl⁻] (M)	**0.05**	**0.1**	**1**	**2**	**3**	**4**	**5**	**6**	**7**	**8**	**9**	**10**	**11**	**12**
$[RuCl(H_2O)_5]^{2+}$	86.26	73.63	5.55	1.08	0.35	0.14	0.06	0.03	0.01	0	0	0	0	0
$[RuCl_2(H_2O)_4]^+$	12.08	20.47	15.44	6.03	2.96	1.57	0.83	0.43	0.22	0.11	0.06	0.03	0.02	0.01
$[RuCl_3(H_2O)_3]$	1.59	5.38	40.60	31.70	23.33	16.50	10.93	6.78	4.00	2.31	1.32	0.77	0.45	0.27
$[RuCl_4(H_2O)_2]^-$	0.08	0.51	36.54	53.32	55.02	48.47	37.52	26.08	16.79	10.34	6.24	3.75	2.26	1.37
$[RuCl_5(H_2O)_2]^{2-}$	0	0	1.81	7.02	14.43	22.50	28.90	32.01	31.91	29.81	26.87	23.81	20.96	18.44
$[RuCl_6]^{3-}$	0	0	0.05	0.85	3.91	10.83	21.75	34.68	47.07	57.43	65.51	71.65	76.32	79.92
Total Ru(III)	100	100	100	100	100	100	100	100	100	100	100	100	100	100

Table D-19: Calculated data for the distribution diagram using Fine[24] and this study.

K_1														
K_2	30	30	30	30	30	30	30	30	30	30	30	30	30	30
K_3	2.7	2.7	2.7	2.7	2.7	2.7	2.7	2.7	2.7	2.7	2.7	2.7	2.7	2.7
K_4	0.8	0.8	0.8	0.8	0.8	0.8	0.8	0.8	0.8	0.8	0.8	0.8	0.8	0.8
K_5	0.14	0.14	0.14	0.14	0.14	0.14	0.14	0.14	0.14	0.14	0.14	0.14	0.14	0.14
K_6	0.0151	0.003	0.0301	0.0602	0.0903	0.1204	0.1505	0.1806	0.2107	0.2408	0.2709	0.301	0.3311	0.3612
[Cl⁻] (M)	**0.05**	**0.1**	**1**	**2**	**3**	**4**	**5**	**6**	**7**	**8**	**9**	**10**	**11**	**12**
$[RuCl(H_2O)_5]^{2+}$	36.89	20.51	0.54	0.09	0.03	0.01	0	0	0	0	0	0	0	0
$[RuCl_2(H_2O)_4]^+$	55.34	61.53	16.12	5.63	2.57	1.33	0.74	0.43	0.26	0.16	0.10	0.07	0.05	0.03
$[RuCl_3(H_2O)_3]$	7.47	16.61	43.51	30.39	20.81	14.39	10.02	7.01	4.94	3.52	2.54	1.85	1.37	1.03
$[RuCl_4(H_2O)_2]^-$	0.30	1.33	34.81	48.63	49.94	46.05	40.07	33.65	27.67	22.52	18.26	14.83	12.01	9.93
$[RuCl_5(H_2O)_2]^{2-}$	0.00	0.02	4.87	13.62	20.97	25.79	28.05	28.27	27.12	25.22	23.01	20.76	18.63	16.68
$[RuCl_6]^{3-}$	0.00	0.00	0.15	1.64	5.68	12.42	21.11	30.63	40.00	48.58	56.09	62.49	67.85	72.32
Total Ru(III)	100	100	100	100	100	100	100	100	100	100	100	100	100	100

Table D-20: Calculated data for the distribution diagram using Connick[21] and this study.